

MONTHLY NOTICES
OF THE
ROYAL ASTRONOMICAL SOCIETY

Volume 120 No. 4 1960

Published and Sold by the

ROYAL ASTRONOMICAL SOCIETY
BURLINGTON HOUSE
LONDON, W.1

Price £1 4s. od.; in U.S.A. \$3.50

Subscription for volume: £6; in U.S.A. \$18

The Geophysical Journal

OF THE

ROYAL ASTRONOMICAL SOCIETY

Editors

A. H. COOK
M.A., Ph.D., F.R.A.S., F.G.S.
National Physical Laboratory
Teddington

T. F. GASKELL
M.A., Ph.D., F.R.A.S.
British Petroleum Company
London

Price £1 per number; in U.S.A. \$3. Annual Subscription £3; in U.S.A. \$9

Volume 3 No. 1 March 1960

CONTENTS

D. S. PARASNIS, The compaction of sediments and its bearing on some geophysical problems.
P. N. S. O'BRIEN, Seismic energy from explosions.
MOHAMMED APTAB KHAN, The remanent magnetization of the basic Tertiary igneous rocks of Skye, Inverness-shire.
M. H. P. BOTT, The use of rapid digital computing methods for direct gravity interpretation of sedimentary basins.
LEON KNOPOFF and GORDON J. F. MACDONALD, An equation of state for the core of the Earth.
J. E. JACKSON, Pendulum observations at Teddington, Singapore, Darwin and Melbourne in 1959.

Notes on Progress in Geophysics

BRIG. G. BOMFORD, The figure of the Earth—its departure from an exact spheroid.
E. IRVING, Palaeomagnetic pole positions, Part I. Pole numbers 1/1 to 1/144.
A. DECAE, On some movements of the ground in Geneva.

Reports of Meetings

Meeting of the International Gravity Commission, Paris, 1959 September 15-19.
Geophysical Discussion of the Royal Astronomical Society, 1959 November 27.
First International Space Science Symposium, Nice, 1960 January 11-16.

Orders should be addressed to :

THE ASSISTANT SECRETARY

ROYAL ASTRONOMICAL SOCIETY, BURLINGTON HOUSE, LONDON, W.1

MONTHLY NOTICES
OF THE
ROYAL ASTRONOMICAL SOCIETY

Vol. 120 No. 4

PHOTOELECTRIC MEASUREMENTS OF THE $\lambda 4200\text{A}$ CN BAND
AND THE G BAND IN G8-K5 SPECTRA

R. F. Griffin and R. O. Redman

(Received 1959 October 2)

Summary

A description is given of a rapid method of using a spectrometer to give reproducible photoelectric measures of integrated intensities over significant features of stellar spectra, without the necessity for a sky of photometric quality. The accuracy achieved is 1 per cent. The $\lambda 4200\text{A}$ CN band has been measured in 712 late-type stars and the G band in 212 of these.

Absolute magnitudes derived from CN intensities have mean errors of at least $1^m.5$. There is only a weak correlation of weak CN with high space velocity. "Weak-line" stars have no anomaly in their CN absorption; "strong-line" stars have slightly enhanced CN.

For G to K₁ stars the spectral type deduced from G band intensities has a mean deviation of 0.15 class from the MK type. There is a small absolute magnitude effect, the G band strengthening with intrinsic luminosity. High-velocity stars have completely normal G band intensities. "Weak-line" stars show the G band very slightly stronger, "strong-line" stars show it slightly weaker than the mean, but the individual scatter is fairly large and the difference between the two groups is scarcely significant statistically.

1. *Introduction.*—Ordinary stellar photometry follows an empirical procedure in which the light from a star is measured successively in three or more broad bands of wave-length, of the order of 1000A wide. These bands are isolated by the combined transmission characteristics of interstellar space, the Earth's atmosphere, the telescope, and a colour filter, and the photometric response characteristic of a particular light receiver. Some of the properties of the Earth's atmosphere, and usually of the apparatus also, are generally unknown and irreproducible, so that each observer measures in his own "system" (and indeed in a succession of different "systems" as he changes his apparatus). For the same reasons, the stars are measured relative to one another and not to a terrestrial source, and the results are not readily linked to the ordinary physical units. A measure of the star's apparent brightness is obtained, but the procedure is not such as to provide the maximum amount of other information about the stars; at best one can sometimes get a rough idea of absolute magnitude, and sometimes an estimate of interstellar absorption. Fundamentally, the method is a modernized version of one devised by the ancient Greeks and it has a number of disadvantages; an important one for us is that the accuracy of modern photometers cannot be exploited without a very good sky, which in Cambridge is experienced scarcely ten times per year.

At the other extreme, one may make a detailed spectrophotometry, usually photographically. In its most elaborate form this requires a large reflector, a good spectrograph, photographic exposures sometimes running into hours, the production of microdensitometer records, and a reduction time which can run

into months. In a less ambitious form, the telescope can be smaller, the spectrograph more modest and examination of the spectrogram confined to a quick visual inspection for estimates of spectral type and luminosity class. The more sophisticated procedures of this kind are expensive in telescope time and man-hours; and although the resulting information can be very detailed, a good deal of care is required to keep errors down to a few per cent. However, the method has the outstanding advantage that the sky quality need not be particularly good.

As a kind of middle course between these two extremes, Strömgren and his pupils have measured stars photoelectrically through interference filters transmitting fairly narrow bands centred near selected features of the spectrum. The results of measurements through two or more different filters can give estimates of spectral type and intrinsic luminosity with a high degree of internal consistency.

2. *Method.*—We seek a quick way of obtaining quantitative information about stellar spectra which can be related, as an ultimate goal, to such parameters as absolute luminosities, chemical abundances, and stellar population characteristics, and hence to stellar evolution. At Cambridge during the past two years a method has been tried which combines some of the virtues of the other methods outlined above. The principle is to isolate some significant feature of the spectrum by means of a spectrometer, using a wave-length band usually 30–50 Å wide, and to measure the total light within this band photoelectrically. Measurements are also made simultaneously upon two comparison bands, approximately symmetrically placed on either side of the principal band. If the light intensities in the three bands are represented by a , b , and c , the ratio $(a+c)/b$ is a measure of the intensity of the spectral feature situated within the middle band, and varies from 2 upwards as the intensity of the (absorption) feature varies from zero upwards. In principle, a considerable number of features could be measured at one time in the same way, as indeed is done in laboratory spectra for rapid analysis of industrial products, where up to about thirty channels have been used.

The transmission of a spectrometer, and (usually) that of the Earth's atmosphere, does not vary greatly over a 50 Å bandwidth, nor does the response of a photomultiplier cathode. Using a spectrometer, therefore, one measures over a fairly flat-topped band with a fairly sharp cut-off at either end. The gradient at the cut-off depends upon the spectrometer slit width and the seeing, or if the latter is very good upon the telescope focusing and guiding as well, but in every case it covers only a small fraction of the whole band. The fraction of light which is transmitted by the spectrometer may be less than that given by a very good interference filter at its peak, but the spectrometer has many advantages; amongst these we may note that the transmission is practically constant over the whole width of the chosen band, the cut-off at each end can be positioned at will, and the wave-lengths accurately specified so that the measurements can, if desired, be repeated by others. Most interference filters have a transmission curve whose peak varies appreciably in wave-length from point to point (and their properties sometimes vary with the passage of time). It is difficult to make an interference filter to a tight specification, so that exact repetition of filter measurements by others is impracticable. A further important advantage of the spectrometer is that the comparison bands can be measured simultaneously with the central band, so that changing sky transparency has no more effect than it does in photographic spectrophotometry. The chief disadvantage in comparison with the

photographic method is that the measured feature is to some extent diluted with other unwanted features.

3. *Apparatus and procedure.*—The spectrometer used in the work described here is a modification of one designed by R. V. Willstrop for three-colour photometry in bands a few hundred angströms wide; however, it has served for the experimental work on relatively narrow bands. It uses the first order of a Wood grating in an Ebert mounting of focal length 36 inches and gives a dispersion of 18.4 \AA/mm . The spectrometer is used at the $f/18$ coudé focus of the 36-inch reflector; the image scale is $12.5/\text{mm}$, and the image of the slit projected into the spectrum is therefore 1.5 \AA wide per second of arc in the star field. The usual width of the slit has been about $2''$; in average seeing the diameter of the star image is of the same order, and a large fraction of the light in it is passed into the spectrometer. This fraction is sufficiently nearly the same for each of the three adjacent bands measured simultaneously. The slit length is 12 seconds of arc.

The spectrometer has no thermostat, and there are appreciable wave-length shifts with changing dome temperature. It is sufficient to correct these at intervals of 20 minutes upwards, according to external conditions. The wave-length adjustment is monitored by bringing a line in another part of the spectrum into coincidence with a crosswire in the focal plane of an eyepiece, using a gas discharge tube as source. The tolerated error is about 1 \AA .

The light from each of the three bands of the spectrum transmitted by the diaphragm in the focal plane of the spectrometer is fed to an unrefrigerated EMI photomultiplier, the output being recorded by pulse-counting (1). After amplification, the output pulses from the photomultiplier pass to a discriminator which rejects those of less than a given amplitude and permits the acceptably large pulses to be counted, the result being displayed on a panel of dekatrons. Potentially, pulse-counting gives the maximum useful response from any photomultiplier, but in fact (since programmes have been restricted to stars brighter than $7^m.5$) there has usually been more than enough light, and no attempt has been made to get maximum electronic efficiency; indeed, neutral filters have been used to reduce the light from the brighter stars in order to avoid the effects of possible non-linearity of the count at high counting rates.

The light response of a photomultiplier varies, sometimes grossly, with position on the photocathode. We have used Fabry lenses imaging the spectrometer collimator aperture, and therefore also the telescope aperture, as 4 mm diameter circular patches on the cathodes. Each patch naturally has a central shadow due to the Cassegrain secondary mirror of the telescope. Moreover, scintillation causes a variation in the distribution of light intensity over the illuminated area of each cathode, as part of the light in the star image formed by the telescope spills onto the jaws of the spectrometer entrance slit; and in addition, poor focusing of the star image upon the slit may cause further irregularity of illumination of the patch.

Despite the fact that the instantaneous pattern of illumination is practically identical upon the several cathodes, it seems possible that in unfavourable circumstances—in particular, if there are extreme variations in sensitivity within the illuminated area of one or more cathodes—errors of a few per cent might arise from these causes. Difficulties recently encountered after further modifications to the spectrometer, involving the use of larger Fabry images

upon the cathodes, have been tentatively ascribed to such origins. (This work is still in progress and is not reported here.) Until these modifications were made, however, no evidence was found, in spite of various tests, that the effects described were of any significance. Although for various reasons the photomultipliers have been moved and readjusted quite a number of times, and the telescope mirrors (irregularity in whose reflectivities would imply corresponding irregularities in illumination of the Fabry images) have been twice realuminized, no suspicion of systematic change has been found in measurements made over periods of up to one year.

In early trials the three wavebands were measured with one photomultiplier; a chopping device gave a $4\frac{1}{2}$ -second "exposure" on each in turn. Thirty exposures (ten on each channel) constituted one observation, the total count being distributed appropriately among the three outputs. This arrangement had the advantage that any change in the photomultiplier sensitivity affected all three channels equally. Nevertheless it was inefficient because, quite apart from observations requiring three times as long as if the counts ran simultaneously, the frequent switching occasioned some additional noise and errors were introduced by changing sky transparency and, worse, by movements of the star image on the slit. By altering the position and shape of the image, seeing causes the fraction of star light which passes the slit to vary, and in the circumstances described this variation cannot be relied on to average out sufficiently accurately between the channels.

When a change was made to three separate photomultipliers, working simultaneously, both speed and accuracy improved; but the relative sensitivities of the three channels may now alter with, say, temperature or mains voltage. These changes might be minimized by using exactly similar photomultipliers and electronic circuits in each channel; but owing to the manner in which the work developed this was not done. In any event, the relative sensitivities of the channels must be checked sufficiently often; in our case checks are made at intervals of 10-15 minutes.

For this purpose a tungsten-filament lamp is used; it is adjusted to have about the same colour temperature as the stars under observation. Our practice has been to reduce observations of stars using lamp counts interpolated to the time at which any given star observation was made. If the star counts on the three channels (after subtraction of dark counts) are A , B , and C , and the interpolated lamp counts A_L , B_L , C_L , then the intensity ratio we require is

$$\left(\frac{A}{A_L} + \frac{C}{C_L} \right) / \frac{B}{B_L}.$$

In effect one is forming the ratio $(a+c)/b$, referred to previously, using not the absolute light intensity of the star in each waveband but its intensity relative to the lamp. As well as taking care of drifts in the relative sensitivities of the three channels, this procedure has the advantage that the two comparison bands are equally weighted in the ratio. Suppose, for instance, that the chosen bands are in a region of steep spectrophotometric gradient, or that the comparison bands are of greatly unequal width: then, although the amount of light in one comparison band will be much greater than in the other for the star, the same will be true for the lamp and the quotients A/A_L and C/C_L will be approximately equal. This condition is desirable since, when it is fulfilled, any change in the

colour of either lamp or star has only a second-order effect upon the intensity ratio; for if, owing to a colour change of the lamp or star, A/A_L rises relatively to B/B_L , then to a first approximation C/C_L is reduced by a corresponding amount and the intensity ratio stands unchanged. (In the special case in which the amount of light in the comparison bands is approximately equal, a worthwhile simplification can be effected by receiving the light from both comparison bands upon a single photomultiplier.) Changes in the apparent colour of the star may be caused by differential absorption and also, in the case of our particular spectrometer, by differential refraction in the Earth's atmosphere. The spectrometer slit is horizontal so that in observations near the meridian atmospheric dispersion lies across it, and movement of the star image on the slit is tantamount to altering somewhat the effective colour of the star. For the same reason, when observing bands in the violet it is appropriate to set the visual image of the star off to one side of the slit by a suitable amount; the effects of dispersion do not however become appreciable until zenith distances of 40° are reached.

Changes in the general brightness of the star or lamp do not affect the intensity ratio. The lamp therefore does not need to be controlled at all accurately and we have in fact used ordinary torch bulbs, behind two spaced diffusers of flashed opal, run from a $4\frac{1}{2}$ -volt dry battery. The original battery is still in use. The spectrometer is diaphragmed so that the lamp uses as far as possible the same optical path as the star; the patch which the lamp illuminates upon the photomultiplier cathodes does not have a central shadow as does the star-lit patch, although even this could be duplicated by placing a central stop on the collimator mirror if it were deemed worth while.

Experience has confirmed the most optimistic expectation in that gross changes in sky transparency do not affect the intensity ratio detectably. Satisfactory results are obtained through passing cloud and on extremely hazy nights with a zenith extinction as great as $2^m.5$. On such occasions there is sometimes pronounced reddening, the absorption in regions only 150 \AA apart differing by (exceptionally) 20 per cent. Observations were once successfully made through a fog which reduced horizontal visibility at the telescope to less than thirty yards. Changes in the telescope transmission are equally without effect: realuminizing the mirrors resulted in a light gain of $1^m.3$ but there was no sign of a systematic change in the measured ratios.

Owing to the small area of sky covered by the slit, and the fairly small bandwidths employed, the contribution of the sky background to the noise count is usually quite negligible; only in strong twilight or near a full moon has it been necessary to distinguish between "sky" and "dark", and observations are practicable almost up to the limb of the Moon. This convenient state of affairs is chiefly a result of programmes so far having been confined to fairly bright stars. If the method is pursued to much fainter stars, as it certainly can be (by using selected photomultipliers, improving the counting circuits and possibly increasing the counting time) more attention to sky brightness will become necessary.

4. *Observations.*—The routine finally adopted is as follows. Each count or "exposure" lasts the same time, about one minute, and is terminated automatically. Two such exposures are made successively on each star before the telescope is moved to the next. After every group of three stars a lamp count

is taken; sometimes this is repeated using a neutral filter in front of the lamp as a rough and ready check on the linearity of the photometric response. At longer intervals, as experience suggests, the spectrometer wave-length setting is checked and if necessary adjusted, and dark counts (and, in a bright sky, sky counts as well) are taken. Normally 12-16 stars are observed per hour; on a number of occasions over 100 stars have been measured in a night.

Each star is usually observed on at least three different nights, i.e. at least six times. Where the results on a particular star have appeared less than usually consistent further observations on subsequent nights have been added, although from a statistical standpoint such a procedure is perhaps not to be recommended. Very few individual observations have been rejected; but whole nights have occasionally been rejected following unsatisfactory readjustments of the apparatus.

The present paper deals with measurements of the $\lambda 4200\text{ \AA}$ CN band in over 700 stars and of the G band in over 200 stars. Other work will be reported elsewhere: it includes measurements of the magnesium b lines in 539 of the same stars by T. J. Deeming, and short programmes on the sodium D lines by Deeming and on the $\lambda 3800\text{ \AA}$ CN band by G. A. H. Walker.

5. *The $\lambda 4200\text{ \AA}$ CN band.*—The first programme carried out by the method outlined above was the measurement of the intensity of the $\lambda 4200\text{ \AA}$ CN band in late-type stars, principally those of types G8-K5. All the stars lie between declinations 0° and $+73^\circ$, the upper limit being imposed by the presence of the spectrometer at the coudé focus to the north of the telescope.

An attempt was made to include all stars, within these ranges of spectral type and declination, brighter than $5^m\cdot5$; most of these have been listed by Roman (2). To these were added dwarfs, subgiants, supergiants and high velocity stars collected from various sources, to a limiting magnitude of $7^m\cdot5$. Later a number of F stars, especially supergiants, were added to the programme after it had been found that high-luminosity stars show appreciable CN absorption as early as F5, although it has been stated that this absorption is undetectable in MK types earlier than G0 (3). In the magnitude range $5^m\cdot5$ - $7^m\cdot5$, preference was given to those stars for which MK spectral types were available.

The purpose of the programme was to elucidate quantitatively the relationship between CN strength on the one hand and spectral type and luminosity on the other; and to investigate the divergences of individual stars from the mean for their type and luminosity, particularly with regard to the supposed weakening of CN in high-velocity stars.

The wave-lengths of the three observed bands were

A 4097-4149 \AA ,

B 4164-4214 \AA ,

C 4230-4283 \AA .

These bands were chosen to avoid the strongly luminosity-sensitive Sr II lines at $\lambda\lambda 4077$, 4216 \AA , the intense Ca I line at $\lambda 4227\text{ \AA}$ and the G band at about $\lambda\lambda 4285$ -4315 \AA . The *A* channel certainly includes a good deal of the weaker structure of the CN band, and also covers H8, but this seemed unavoidable. It is inevitable, too, that owing to the complexity of a late type spectrum a large number of other more or less strong lines, including many of Fe I, are included in each of the three bands, and it should be made clear that the measurements

must to some extent be affected by this. Our observations simply define the degree in which the total absorption in the waveband $\lambda\lambda 4164-4214$ A exceeds that in the specified adjacent regions; and we shall call the results CN intensities, because, although this term may be open to semantic objection, for most of the stars on the present programme the principal cause of the increased absorption around $\lambda 4200$ A is nevertheless CN.

The slit width used throughout the programme was 0.161 mm = 2.0 seconds of arc = 3.0 A width projected in the spectrum.

A total of 5,032 observations was made on 67 nights in 1958 and one night in 1959, the number of stars observed being 712. The mean CN intensity ratio derived for each of these stars is given in Table I.

The number of observations rejected was 65. The deviations of the remainder from their respective means form an accurately Gaussian distribution with a root-mean-square value of 0.0425 . Owing to the derivation of the means for all the stars from the same observations and the consequent reduction of the number of degrees of freedom by 712, the r.m.s. error of a single observation is slightly greater, 0.046 . Since the average of the CN intensity ratios for all the stars measured is about 2.2, this error corresponds to 2.1 per cent; the theoretical value to be expected from the finite number of photoelectrons counted is about half this. The error of the mean CN ratio for one star, which in most cases depends on six observations, made in pairs so that only three are entirely independent, may be estimated at 1.0 per cent. The intrinsic scatter in CN strength among stars of the same spectral type and luminosity is found to be much greater than this, so that the errors of measurement can be ignored in what follows.

TABLE I

No.	Name or H.R.	H.D.	Type	CN ratio	G band ratio	Notes
1	8	166	dG8	2.08		
2		371	G3 II	2.11		
3	19	417	K0 III	2.21		
4		443	dG9	2.11		
5	22 And	571	F2 II \dagger	1.97		
6		613	K4 III	2.28		
7		725	F5 Ib-II	1.98		
8		936	G8 II	2.27		
9		1400	dK5	2.13		
10		1778	F3 II	1.95		
11		2170	G5 III	2.10		
	124	2774	K2 III	2.30		
		2901	K2 III	2.17		
		2925	K0 III	2.10		
		3147	K2 Ib-II	2.36		
152		3346	K5 III	2.16		
161		3457	K4 III	2.19		
		3489	K3 Ib-II	2.38		
ϵ And		3546	G8 IIIp	2.08		
8 And		3627	K3 III \dagger	2.33		sc

TABLE I (continued)

No.	Name or H.R.	H.D.	Type	CN ratio	G band ratio	Notes
21	54 Psc α Cas	3651 3712 3765	Ko V† Ko II-III K2 V	2.11 2.45 2.09		d
	32 And	3817	G8 III	2.19		d
	177	3856	G9 III-IV	2.20		
		3989	K5 III	2.14		
	207	4362	Go Ib†	2.15		
	ζ And	4502	K1 II	2.25		
	212	4440	sgKo	2.21		
	222	4628	K2 V	2.01		
31	δ Psc	4656	K5 III	2.16		
	η Cas	4614	Go V†	1.96 :		
	237	4817	K3 Ia	2.18		
	υ ¹ Cas	5234	K2 III	2.27		
	36 And	5286	sgK ₁	2.26		
	υ ² Cas	5395	G8 III-IV	2.12		e
	η And	5516	G8 III-IV	2.26		d
		5916	G8 III-IV	2.10		
	ε Psc	6186	Ko III	2.20		e
		6474	Go Ia	2.22 :		
41	316	6497	K2 III	2.25		a
	μ Cas	6582	G5 VI	1.98		
		6833	K1 III	2.03		a
	χ Psc	7087	Ko III	2.31		d
	τ Psc	7106	Ko III-IV	2.36		d
	ϕ Psc	7318	Ko III	2.37		d
	ϕ Cas	7927	Fo Ia†	2.05		
	ξ And	8207	Ko III-IV	2.29		d
	396	8375	G8 IV	2.11		a
	ψ Cas	8491	Ko III	2.27		b
51		8701	K2 pII	2.41		
	ω And	8799	F5 III	1.97 :		
		8906	F3 Ib	2.02		
	49 And	9057	Ko III	2.31		b
	μ Psc	9138	K4 III	2.18		a
	η Psc	9270	G8 III†	2.28		d
		9166	K3 III	2.38		a
		9250	Go Ib	2.13		
	439	9352	cK ₁	2.15		
	χ Cas	9408	G8 III	2.20		e
61	452	9712	K1 III	2.30		a
	40 Cas	9774	G8 II-III	2.24		e
		9973	F5 Ib	2.03		
	51 And	9927	K3 III†	2.36		
	χ And	10072	G8 III	2.18	2.72 :	e
	483	10307	G2 V†	2.00		d
	ν Psc	10380	K3 III	2.22		
	107 Psc	10476	K1 V	2.07		
	495	10486	sgK2	2.31		
		10494	F5 Ia†	2.08		

TABLE I (continued)

No.	Name or H.R.	H.D.	Type	CN ratio	G band ratio	Notes
71	o Psc	10761	G8 III	2.25		
	511	10780	Ko V	2.03		
	521	10975	Ko III	2.20		
		11092	K5 Iab-Ib	2.22		
	α Tri	11443	F6 IV	1.97:		
	ξ Psc	11559	Ko III	2.25		
		11544	G2 Ib	2.23		
	56 And	11749	Ko III	2.28		
	ι Ari	11909	K1 p	2.25		
		12399	G5 Ia	2.22		
81	γ^1 And	12533	K3 II	2.40		
	α Ari	12929	K2 III \dagger	2.32		
	60 And	13520	K4 III	2.16		
	ξ^1 Cet	13611	G8 II	2.21		
	645	13530	Ko III	2.33		ab
		13686	K3 Ib	2.34		
		13725	K4 II	2.17		
	δ Tri	13974	Go V	1.97:		
	690	14662	F7 Ib \dagger	2.06		
	64 And	14770	G8 III	2.26		d
91	65 And	14872	K4 III	2.14		
	27 Ari	15596	G5 III-IV	2.01		
	737	15694	K3 III	2.22:		
	14 Tri	15656	K5 III	2.15		
	ν Cet	16161	G8 III	2.15		
	753	16160	K3 V	2.00		
	743	15920	G8 III	2.11:		
	747	16024	cK5	2.20		
	14 Per	16901	Go Ib	2.12		
	39 Ari	17361	K1 III	2.27		d
101	825	17378	A5 Ia \dagger	1.98:		
	η Per	17506	K3 Ib \dagger	2.36		
	17 Per	17709	K5 III	2.08		
		17971	F5 Ia \dagger	2.06:		
	861	17958	K3 Ib	2.32		
	24 Per	18449	K2 III	2.26		
		18391	Go Ia \dagger	2.16		
	885	18474	Gp	2.08		
	918	18970	Ko II-III	2.24		
	ι Per	19373	Go V	1.97:		
111	κ Per	19476	Ko III	2.30		
	ω Per	19656	K1 III	2.31		d
	δ Ari	19787	K2 III	2.26		
	949	19735	K5 III	2.18		
	969	20123	G5 II	2.24		
	978	20277	sgG8	2.19		
	991	20468	K2 II	2.41		
	κ Cet	20630	G5 V \dagger	1.99:		
	59 Ari	20618	sgG5	2.11		
	999	20644	K4 III	2.21		

TABLE I (continued)

No.	Name or H.R.	H.D.	Type	CN ratio	G Band ratio	Notes
121	63 Ari	20893	K3 III	2.26		
	α Per	20902	F5 Ib†	2.04		
	σ Tau	21120	G8 III†	2.24		d
	σ Per	21552	K3 III	2.19		
	5 Tau	21754	Ko II-III	2.34		d
	36 Per	21770	F4 III†	1.97:		
	1085	22072	dG7	2.07		
	14 Tau	23183	Ko III	2.20		a
	ν Per	23230	F5 II†	2.03		
		23841	K2 III	2.16		a
131		25056	Go Ib	2.13		
	1242	25291	Fo II†	1.97:		
	37 Tau	25604	Ko III	2.34		d
	1255	25602	Ko III-IV	2.17		
		25893	dK2	2.04		
	49 Per	25975	K1 III	2.22		a
	1270	25877	G8 II	2.30		
	1286	26311	cK5	2.35		
	μ Per	26630	Go Ib†	2.13		
	1327	27022	G5 III†	2.07		e
141	γ Tau	27371	Ko III†	2.37		d
			dK5	2.17		f
	54 Per	27348	G8 III	2.25		b
	ϕ Tau	27382	K1 III	2.22		e
	8 Tau	27697	Ko III†	2.34		d
	1390	27971	K1 III	2.27		e
	π Tau	28100	G8 III	2.26		d
	75 Tau	28292	K2 III	2.28		
	ϵ Tau	28305	Ko III†	2.35		e
	θ^1 Tau	28307	Ko III†	2.24		d
151	α Tau	29139	K5 III†	2.14		
	58 Per	29094	G8 II	2.28		g
	3 Cam	29317	Ko III	2.23		d
	1533	30504	K4 II	2.11		
	2 Aur	30834	K3 III	2.20		
	σ^3 Ori	31421	K2 III	2.27		
	ι Aur	31398	K3 II	2.36		
	π^6 Ori	31767	K2 II	2.39		
		31782	Ko IV	1.93:		a
	ϵ Aur	31964	Fo Iap	2.03:		
161	β Cam	31910	Go Ib	2.13		
	104 Tau	32923	G4 V	1.95		d
		33209	K1 Ib	2.48		
	1684	33554	K5 III	2.14		
	ρ Ori	33856	K3 III	2.36		h
	16 Aur	34334	K3 III	2.14		
	λ Aur	34411	G2 IV-V	1.97:		
	1720	34255	cK4	2.32		
	109 Tau	34559	G8 III	2.24		
	21 Ori	34658	F5 II	1.95:		e

TABLE I (continued)

No.	Name or H.R.	H.D.	Type	CN ratio	G band ratio	Notes
171		34575	dG6	2.04		
	σ Aur	35186	K4 III	2.28		
	ϕ Aur	35620	K3 p	2.41		
	1884	36891	G3 Ib	2.20	:	
	ϕ^2 Ori	37160	G8 IIIp	2.03		ac
	1908	37171	K5 III	2.03		a
	1925	37394	dK1	2.00		
	24 Cam	37601	sgG9	2.12		
	51 Ori	37984	Ko III	2.15		ae
		37981	sgK1	2.18		
181		38247	G8 Iab	2.44	:	
		38230	dK1	2.06		
	τ Aur	38656	G8 III	2.14		e
	132 Tau	38751	G8 III	2.21		b
	ν Aur	39003	Ko III	2.32		d
	56 Ori	39400	K2 II \dagger	2.35		
	χ^1 Ori	39587	Go V	1.98		d
	2048	39632	G9 II	2.37		
	δ Aur	40035	Ko III \dagger	2.16		e
		40460	K1 III	2.22		a
191	38 Aur	40801	Ko III	2.11		a
	2153	41636	Ko III	2.17		
	37 Cam	41597	G8 III	2.17		e
	36 Cam	41927	K2 II-III	2.31		
	κ Aur	43039	G8 III	2.16		ae
	43 Aur	43380	K2 III	2.33		a
	ψ^1 Aur	44537	Mo Iab \dagger	2.19		
	T Mon	44990	G5 Ip	2.34		
	BL Ori	44984	C	2.79	:	
	5 Lyn	44708	K4 III	2.13		
201		45088	dK3	1.97		
	77 Ori	45416	K1 II \dagger	2.47		
	6 Lyn	45410	sgG8	2.11		
		45829	Ko Iab	2.56		
	UU Aur	46687	C5	2.26	:	
	8 Lyn	46480	sgG7	1.96		
	ψ^2 Aur	47174	K3 III	2.31		
	25 Gem	47731	G5 Ib \dagger	2.30		
	ψ^4 Aur	47914	K5 III	2.16		
	ϵ Gem	48329	G8 Ib \dagger	2.62		
211	30 Gem	48433	K1 III	2.26		d
	ξ Gem	48737	F5 III	1.94	:	
	13 Lyn	48432	Ko III-IV	2.11		e
	56 Aur	48682	Go V	1.96		d
	ψ^4 Aur	48781	K1 III	2.34		d
	17 Mon	49161	K4 III	2.22		
	18 Mon	49293	Ko III	2.36		d
	ψ^7 Aur	49520	K3 III	2.32		a
	62 Aur	51440	K2 III	2.14		
	41 Gem	52005	cK4	2.22		

TABLE I (continued)

No.	Name or H.R.	H.D.	Type	CN ratio	G band ratio	Notes
221		52071	K2 III	2.13		
	ω Gem	52497	G5 II \dagger	2.22		
	2649	52960	K3 III	2.29		
		54371	dG6	2.01		
	2692	54563	dG7	2.02		
	τ Gem	54719	K2 III	2.38		
	63 Aur	54716	K4 II-III	2.19		
	18 Lyn	55280	K2 III	2.20	2.77:	a
		56224	K1 III	2.30		a
	65 Aur	57264	G8 III	2.16		e
231	57 Gem	57727	G8 III	2.12		e
	66 Aur	57669	Ko III	2.41		b
	ι Gem	58207	Ko III	2.22		e
	ϵ CMi	58367	G8 III	2.27		d
	γ CMi	58972	K3 III	2.16		
	65 Gem	59148	K2 III	2.35		
	6 CMi	59294	K2 III	2.35		
	2896	60318	Ko III	2.27		e
	ν Gem	60522	Mo III \dagger	2.07		
	σ Gem	62044	K1 III	2.23		d
241	76 Gem	62285	K5 III	2.14		
	κ Gem	62345	G8 III \dagger	2.21		d
	β Gem	62509	Ko III \dagger	2.25		e
		61994	dG5	1.95	2.56:	
	81 Gem	62721	K5 III	2.08		a
		63410	G8 III	2.10		a
	14 CMi	65345	Ko III	2.21		ae
		65583	G8 V	1.95		
	3145	66141	K2 III	2.18		a
	χ Gem	66216	K2 III	2.24		
251	μ Cnc	67228	G2 IV	2.01:		
	55 Cam	67447	G8 II	2.23	2.74:	
	β Cnc	69267	K4 III \dagger	2.18		
	31 Lyn	70272	K5 III	2.08		
	3306	71115	G8 II	2.20		
		71597	K2 III	2.19		a
	o UMa	71369	G5 II	2.13:		
		71952	sgKo	2.11		
	3360	72184	K2 III	2.31		a
	η Cnc	72292	K3 III	2.29		
261	v^3 Cnc	72324	G9 III	2.32		a
	σ Hya	73471	K2 III	2.37:		
	π^3 UMa	73108	K2 III	2.14	2.75:	
	34 Lyn	73593	G8 IV	2.15		
	δ Cnc	74442	Ko III	2.28		e
	ι Cnc	74739	G8 II	2.24		
	ϵ Hya	74874	Go III	2.03:		
	35 Lyn	75506	Ko III	2.14		e
	55 Cnc	75732	dKo	2.15		
	ρ^3 Cnc	76219	G8 II-III	2.29		d

TABLE I (continued)

No.	Name or H.R.	H.D.	Type	CN ratio	G band ratio	Notes
271	ζ Hya	76294	Ko II-III	2.28		
	3545	76291	K1 IV	2.19		
	ω Hya	77996	K2 II-III	2.29	2.82 :	
	3612	77912	G8 Ib-II	2.27	2.77 :	
	σ^1 UMa	77800	K5 III	2.06	2.80	
	τ Cnc	78235	G8 III	2.13	2.69 :	e
		78249	K1 IV	2.16	2.68 :	
		78479	K3 III	2.41		a
	ξ Cnc	78515	Ko III	2.29	2.65	d
	81 Cnc	79096	dG7	1.98		
281	17 UMa	79354	K5 III	2.05	2.80	
	3664	79452	G6 III	2.02		a
		79969	dK4	1.97		
	κ Leo	81146	K2 III	2.27	2.81	
		81192	G8 III	2.01		a
	λ Leo	82308	K5 III	2.10	2.76 :	
	ξ Leo	82395	Ko III	2.25	2.76	e
	6 Leo	82381	K3 III	2.22	2.75 :	
		82394	cG7	2.39		
	θ UMa	82328	F6 IV	1.99 :		
291		82443	dG9	2.06 :		
	24 UMa	82210	G5 IV	1.99	2.59	d
	10 LMi	82635	G8 III	2.15	2.65 :	d
	3809	82741	Ko III	2.16	2.78 :	e
	11 LMi	82885	G8 IV-V	2.09	2.66 :	
	10 Leo	83240	K1 III	2.33	2.71 :	e
	3834	83425	K3 III	2.17	2.82 :	a
	27 UMa	83506	Ko III	2.33 :	2.77	d
	43 Lyn	83805	G8 III	2.24	2.68	e
	ϵ Leo	84441	G0 II \dagger	2.17		
301	14 LMi	84453	Ko IV	2.16		
		84406	sgKo	2.11	2.81	
	3881	84737	G2 V	2.02 :		
	μ Leo	85503	K2 III	2.41	2.82 :	
	31 Leo	87837	K4 III	2.16	2.77 :	
		89269	dG5	1.98		
	γ^1 Leo	89484	Ko III	2.16	2.78 :	b
	29 LMi	90250	K1 III	2.29		a
		90572	sgKo	2.17		
	β LMi	90537	G8 III-IV	2.18	2.57 :	d
311	31 Sex	91011	sgKo	2.19		
	48 Leo	91612	G8 II-III	2.15	2.69 :	e
	37 LMi	92125	G2 II	2.12 :		
	4165	92095	K3 III	2.30		a
	38 UMa	92424	K2 III	2.37	2.88	
	4181	92523	K3 III	2.17	2.80	
	4242	94084	K2 III	2.27		
	4243	94132	dG9	2.19	2.82	
	46 LMi	94264	Ko III-IV	2.19	2.71 :	e
	44 UMa	94247	K3 III	2.21	2.78 :	

TABLE I (continued)

No.	Name or H.R.	H.D.	Type	CN ratio	G band ratio	Notes
321	46 UMa	94600	K ₁ III	2.21	2.75 :	
		94549	dG8	2.13	2.75	
	4264	94669	K ₂ III	2.20		
	47 UMa	95128	G ₀ V	1.99 :		
	58 Leo	95345	K ₁ III	2.21		e
	α UMa	95689	K ₀ III†	2.25 :	2.66	d
	65 Leo	96436	sgG ₇	2.08		
	ψ UMa	96833	K ₁ III	2.22	2.78 :	e
		97561	G ₇ IV	2.04		
	73 Leo	97907	K ₃ III	2.19		
331	ξ UMa	98230	G ₀ V	1.98 :		
	ν UMa	98262	K ₃ III	2.18	2.80 :	
		98824	K ₁ III-IV	2.21		
	56 UMa	98839	G ₈ II†	2.30 :		
	4404	99196	K ₄ III	2.27		a
	83 Leo	99491	dK ₀	2.11		
	7 Leo	99648	G ₈ II-III	2.31		d
	4452	100470	K ₀ III	2.25		a
	2 Dra	100696	K ₀ III	2.19	2.78	e
	92 Leo	101484	K ₀ III	2.22	2.70 :	e
341	61 UMa	101501	G ₈ V	2.01		
	3 Dra	101673	K ₃ III	2.30	2.84	
	χ UMa	102224	K ₀ III	2.18	2.81 :	e
	4521	102328	K ₃ III	2.30	2.90 :	
	4550	103095	G ₈ VI	1.94		
		104556	G ₈ V	1.98	2.68	
	ο Vir	104979	G ₈ III	2.15	2.73	e
	4610	105043	K ₂ III	2.18	2.86	
		105475	dG ₉	2.25	2.77	
		105631	dK ₁	2.05	2.64	
351		105963	dK ₂	1.98	2.67	
	7 Com	106714	K ₀ III	2.14	2.73	e
	4668	106760	K ₁ III	2.23	2.85	d
	16 Vir	107328	K ₀ III	2.25	2.82	ac
	11 Com	107383	G ₈ III	2.17	2.71	e
		107469	dK ₀	2.09	2.69	
	5 CVn	107950	G ₇ III	2.14	2.62	d
	6 CVn	108225	G ₈ III-IV	2.20	2.67	e
	15 Com	108381	K ₁ III-IV	2.40	2.79	b
	18 Com	108722	F ₅ III	1.98 :		
361	4783	109317	K ₀ III	2.23	2.81	e
	β CVn	109358	Go V†	1.97 :		
		110833	dK ₀	2.03	2.77 :	
	γ CVn	110914	C ₅	2.23 :		
	33 Vir	111028	K ₁ IV	2.13 :	2.69	
	27 Com	111067	K ₃ III	2.22	2.82	
	31 Com	111812	Go III†	2.01 :		
	35 Com	112033	G ₈ III	2.23	2.59	d
	37 Com	112989	K ₁ p	2.27	2.62	
	9 Dra	113092	G ₈ III	2.15	2.81	c

TABLE I (continued)

No.	Name or H.R.	H.D.	Type	CN ratio	G band ratio	Notes
371	ε Vir	113226	G9 II-III	2.26	2.68	d
	41 Com	113996	K5 III	2.18	2.83	
		114960	K5 III	2.28	2.91	
	4997	115004	Ko III	2.34	2.80	d
		115404	dK3	2.02	2.72	h
	59 Vir	115383	Go V	1.98		
	5013	115478	K3 III	2.21	2.86	
		115539	G8 III-IV	2.12	2.76	
	70 Vir	117176	G5 V	2.03	2.59	
	5102	117876	Ko III	2.15	2.69	a
381		118643	cK3	2.23	2.89	
	84 Vir	119425	K2 III	2.33	2.87	ah
	v Boo	120477	K5 III	2.16	2.80	
	6 Boo	120539	K4 III	2.19	2.82	
	5227	121146	sgK2	2.21	2.85	
	η Boo	121370	Go IV†	1.99		
	9 Boo	121710	K3 III	2.25	2.84	
	5273	122742	G8 V	2.00		
	5302	123977	Ko III	2.22	2.83	a
	15 Boo	124679	Ko III	2.23	2.72	e
391	α Boo	124897	K2 IIIp	2.19	2.85	
	A Boo	125351	K1 III	2.23	2.81	d
	20 Boo	125560	K3 III	2.36	2.88	
	ρ Boo	127665	K3 III†	2.29	2.90	
		128165	K3 V†	1.99	2.75	
	5462	128750	sgK2	2.20	2.86	
	5464	128902	K4 III	2.13	2.75	a
	31 Boo	129312	G8 III	2.31	2.73	e
	32 Boo	129336	G8 III	2.25	2.74	a
		129580	dKo	2.18	2.82	
401	ο Boo	129972	Ko III	2.27	2.73	d
	5541	131111	Ko III-IV	2.16	2.81	e
	ξ Boo	131156	G8 V†	2.03	2.59	
		131507	K4 III	2.21	2.87	a
	5553	131511	dK1	2.08	2.69	
	ι Ser	132132	sgK1	2.32	2.83	
	ω Boo	133124	K4 III	2.19	2.83	
	β Boo	133208	G8 II-III	2.27	2.73	d
	110 Vir	133165	Ko III	2.22	2.79	d
	ψ Boo	133582	K2 III	2.30	2.85	
411	5635	134190	G8 III	2.19	2.75	e
	δ Boo	135722	G8 III†	2.15	2.75	e
	11 UMi	136726	K4 III	2.26	2.87	
	ο CrB	136512	Ko III	2.20	2.85	
	6 Ser	136514	K3 III	2.26	2.81	
	η CrB	137107	Go V	2.00		
	ι Dra	137759	K2 III†	2.30	2.87	
	5741	137704	K4 III	2.13	2.83	a
	ν ¹ Boo	138481	K5 III	2.11	2.71	
	16 Ser	139195	Ko p	2.25	2.70	

TABLE I (continued)

No.	Name or H.R.	H.D.	Type	CN ratio	G band ratio	Notes
421		139341	dK4	2.15	2.80	
	φ Boo	139641	G8 IV	2.08	2.70	d
	ψ Ser	140538	dG5	1.97	2.55	
	α Ser	140573	K2 III	2.43	2.89	
	λ Ser	141004	Go V	1.98		
	δ CrB	141714	G5 III-IV	2.09	2.60	e
	ω Ser	141680	G8 III	2.17	2.81	e
	ρ Ser	141992	K5 III	2.15	2.80	
	κ CrB	142091	Ko III-IV	2.22	2.78	d
	5924	142574	K4 III	2.06	2.78	a
431	φ Ser	142980	K1 IV	2.24	2.86	
	ε CrB	143107	K3 III	2.29	2.82	
	5 Her	143666	Ko III	2.21	2.80	e
	ρ CrB	143761	G2 V	1.98	2.50	e
	ν Her	144046	F2 II	1.92		
		144287	G8 V	1.99	2.78	
		144579	dG8	1.98	2.71	
	κ ¹ Her	145001	G8 III	2.16	2.62	d
	κ ² Her	145000		2.36	2.80	
	6014	145148	Ko IV	2.11	2.80	
441	τ CrB	145328	Ko III†	2.21	2.82	e
	14 Her	145675	dK1	2.16	2.75	
	49 Ser A	145958	dKo	2.02	2.67	
	49 Ser B		dKo	2.02	2.63	
	ξ CrB	147677	Ko III	2.26	2.80	d
	ν ² CrB	147767	K5 III	2.12	2.77	
	6126	148293	K2 III	2.36	2.80	
	η Dra	148387	G8 III†	2.20	2.70	d
	6136	148513	K4 IIIp	2.26	2.92	b
		148653	dK2	2.00	2.75	
451	β Her	148856	G8 III†	2.23	2.71	d
	6152	148897	G8 p	2.06	2.66	c
	29 Her	149161	K5 III	2.09	2.79	a
	6199	150449	K1 III	2.23	2.79	d
	ζ Her	150680	Go IV	2.03		
	18 Dra	151101	K1 p	2.22	2.68	c
	η Her	150997	G8 III-IV	2.16	2.75	d
	43 Her	151217	K5 III	2.14	2.80	
	48 Her	151937	K1 II-III	2.10	2.83	
	51 Her	152326	K2 II-III	2.38	2.91	
461		152391	G6 V	2.00	2.63	
	6286	152812	K2 III	2.21	2.85	
	6287	152815	G8 III	2.21	2.77	e
	54 Her	152879	K4 III	2.23	2.86	
	6301	153226	Ko IV	2.11		
	κ Oph	153210	K2 III†	2.36	2.93	
		154345	dKo	2.02	2.68	
	6342	154278	K1 III	2.15	2.74	
	6364	154733	K4 III	2.25	2.86	a
	6388	155410	K3 III	2.27	2.90	

TABLE I (continued)

No.	Name or H.R.	H.D.	Type	CN ratio	G band ratio	Notes
47 ¹	π Her	156283	K3 II [†]	2.31	2.92	
	6433	156681	K4 II-III	2.18	2.80	
	72 Her	157214	G2 V	2.01 :		
	σ Oph	157999	K3 II	2.33	2.90	
	6518	158633	dK ₁	2.00		
	λ Her	158899	K4 III	2.28	2.88	
	β Dra	159181	G2 Ib	2.16		
	27 Dra	159966	Ko III	2.22		ac
		160346	dK ₃	2.00	2.74	
	83 Her	161074	K4 III	2.14	2.84	
48 ¹	β Oph	161096	K2 III [†]	2.36	2.91	
		161198	dG8	2.02	2.68	
		161796	F3 Ib	2.08 :		
	μ Her	161797	G5 IV [†]	2.08	2.65	
	6638	162076	sgG ₅	2.24	2.76	
	87 Her	162211	K2 III	2.33	2.85	
	90 Her	163217	K3 III	2.25	2.78	h
	ξ Dra	163588	K2 III [†]	2.27	2.83	
	89 Her	163506	F2 Ia [†]	2.05		
	θ Her	163770	K1 II [†]	2.58	2.92	
49 ¹	γ Dra	164058	K5 III [†]	2.18	2.87	
	ξ Her	163993	Ko III	2.27	2.71	d
	93 Her	164349	Ko II-III	2.41	2.89	b
		164922	Ko V	2.04	2.61	
	70 Oph A	165341	Ko V [†]	2.05	2.68	
	70 Oph B		K7 V	1.88 :	2.69	
	71 Oph	165760	G8 III-IV	2.25	2.76	d
	6791	166208	Ko p	2.21	2.53	c
	6793	166229	K2 III	2.35	2.88	
	6806	166620	K2 V	2.02	2.75 :	
50 ¹	6817	167042	K1 III	2.19	2.78 :	a
	6820	167193	K4 III	2.20	2.81	
	6853	168322	Ko III	2.13	2.83	a
	105 Her	168532	K4 II	2.28	2.87	
	κ Lyr	168775	K2 III	2.38	2.91	
	74 Oph	168656	G8 III	2.21	2.75	d
	108 Her	168913	F9 Ib	1.85 :		
	6885	169191	K3 III	2.23	2.83 :	
	109 Her	169414	K2 III	2.24	2.85 :	
	42 Dra	170693	K2 III	2.22		
51 ¹	6950	170829	G8 IV	2.06		
	45 Dra	171635	F7 Ib [†]	2.07 :		
	6983	171779	Ko III	2.34	2.79 :	d
	6995	171994	G8 IV	2.12		
	7008	172365	F8 Ib-II	2.09 :		
	7064	173780	K3 III	2.25	2.83 :	
	σ Dra	175306	Ko II-III	2.18		c
	7123	175225	dG8	2.13	2.66 :	
	7137	175535	G8 III	2.19	2.60 :	d
	ν Dra	176524	Ko III	2.23		e

TABLE I (continued)

No.	Name or H.R.	H.D.	Type	CN ratio	G band ratio	Notes
521	ε Aql	176411	K2 III	2.41	2.82 :	
	7181	176527	K2 III	2.20	2.85 :	
	λ Lyr	176670	K3 II	2.37	2.92 :	
	7275	179094	K1 IV	2.18	2.72 :	
	53 Dra	180006	G8 III	2.33		b
		179784	G5 Ib	2.40		
		179785	K3 II-III	2.34		
	δ Dra	180711	G9 III	2.20		e
		180028	F6 Ib	2.09		
	54 Dra	180610	K2 III	2.26		
531	7308	180583	F6 II	2.10		
	θ Lyr	180809	Ko II†	2.38	2.89 :	
	κ Cyg	181276	Ko III†	2.28	2.74 :	d
	23 Aql	180972	K2 II-III	2.34		
	7345	181655	G8 V	2.02		
		182293	K3 III	2.21	2.89 :	a
		182296	G3 Ib	2.33		
	7368	182488	Ko V	2.09	2.72 :	
	31 Aql	182572	G8 IV	2.14		b
	4 Vul	182762	Ko III	2.20		e
541	7421	184010	sgG8	2.15		
	7428	184398	K2 II-III	2.15	2.55 :	g
		184467	K1 V	2.01		
	μ Aql	184406	K3 III	2.29		a
	σ Dra	185144	Ko V†	2.02		
	ε Sge	185194	G8 III	2.33		d
	7468	185351	Ko III	2.22	2.75 :	e
	7475	185622	cK5	2.26		
		185662	dK4	2.19		
	φ Cyg	185734	G8 III-IV	2.24	2.77 :	d
551	α Sge	185758	Go II†	2.15		
	β Sge	185958	G8 II†	2.35		
		186120	sgKo	2.37		
	10 Vul	186486	G8 III	2.22		e
	15 Cyg	186675	G8 III	2.25	2.73 :	d
	γ Aql	186791	K3 II†	2.30		
	7542	187203	Go Ib	2.17		
		187299	G5 Iab-Ib	2.39		
	ε Dra	188119	G8 III†	2.07 :		e
	20 Cyg	188056	K3 III	2.41	2.91 :	
561	7573	187982	A2 Ia	1.95 :		
	ξ Aql	188310	Ko III	2.23		e
		188507	K4 II-III	2.18		
	β Aql	188512	G8 IV†	2.05		e
		188753	dKo	2.12 :		
	η Cyg	188947	Ko III	2.29		e
	7633	189276	K5 II-III	2.17		
	γ Sge	189319	K5 III	2.15		
		189671	G8 II	2.42		
	26 Cyg	190147	K1 II-III	2.38	2.82 :	b

TABLE I (continued)

No.	Name or H.R.	H.D.	Type	CN ratio	G band ratio	Notes
571	16 Vul	190004 331777	F5 II F8 Ia	2.01 2.17:		
	7670	190360 190403 190404	G6 IV G5 Ib-II K1 V	2.10 2.34 1.99		
	ρ Dra	190940	K3 III	2.32		
	η Sge	190608	K2 III	2.27:		
	27 Cyg	191026	Ko IV	2.15		
	66 Dra	191277 191046	K3 III Ko III	2.28 2.14		a
581		191785	K1 V	2.04		
	19 Vul	192004	K3 II-III	2.43		
	α^1 Cyg	192577	K2 II	2.10	2.47:	g
	22 Vul	192713	G2 Ib†	2.28		
	23 Vul	192806	K3 III	2.17		
	α^2 Cyg	192909	K3 Ib-II	2.11	2.59:	g
	24 Vul	192944	G8 III	2.24		
	7759	193092	K4 II	2.22		
	7762	193217	K4 II	2.29		
	35 Cyg	193370	F5 Ib†	2.10		
591		193469	K5 Ib	2.23		
	7795	194069	G2 II	2.29		
	γ Cyg	194093	F8 Ib†	2.11		
	7794	194013	G8 III-IV	2.27		e
	39 Cyg	194317	K3 III	2.25		
	7810	194526	K5 III	2.16		
		195100	G5 III	2.18		
		195338	G7 II	2.30		
	41 Cyg	195295	F5 II†	2.01		
	7841	195506	K2 III	2.17	2.81:	a
601	44 Cyg	195593	F5 Iab†	2.05		
		195987	G9 V	1.99		
	47 Cyg	196093	K2 Ib	2.14		g
	θ Del	196725	K3 Ib	2.38		
	κ Del	196755	G5 IV	2.04		
	1 Aqr	196758	K1 III	2.29		e
	α Cyg	197345	A2 Ia†	1.93:		
	30 Vul	197752	K2 III	2.33		
	52 Cyg	197912	Ko III	2.25		e
		197913	dG9	2.05		
611	η Cep	198149	Ko IV†	2.14		c
	ϵ Cyg	197989	Ko III	2.22		d
	γ Del A	197964	sgK1	2.26		
	7956	198134	K3 III	2.29		
	7972	198387	dKo	2.06		
	31 Vul	198809 199191	G8 III G8 III	2.18 2.05		d
	32 Vul	199169	K4 III	2.25		a
	17 Del	199253	Ko III	2.30		e
	8026	199612	G8 II-III	2.33		

TABLE I (continued)

No.	Name or H.R.	H.D.	Type	CN ratio	G band ratio	Notes
621		199580	K ₁ IV	2.15		
		200102	G ₁ Ib	2.22		
	ξ Cyg	200905	K ₅ Ib†	2.19		
	8082	201051	sgK ₁	2.21		
	61 Cyg A	201091	K ₅ V†	1.89		
	61 Cyg B	201092	K ₇ V†	1.81		
	63 Cyg	201251	K ₄ II	2.28		
	ζ Cyg	202109	G ₈ II	2.39		
		203358	G ₈ IV-V	2.08		
	8165	203344	K ₀ III-IV	2.28		
631	1 Peg	203504	K ₁ III	2.30		ae
	71 Cyg	204771	K ₀ III	2.28		e
	8248	205349	K ₁ Ib	2.44		
	ρ Cyg	205435	G ₈ III	2.17		c
	72 Cyg	205512	K ₁ III	2.35		ab
		206078	G ₈ III	2.06		a
		205941	dG ₈	2.08		
		206121	G ₅ II	2.10		
	25 Aqr	206067	K ₀ III	2.23		e
		206312	K ₁ II	2.43		
641		206374	G ₈ V	2.03		
	8304	206731	G ₈ II	2.30		
	11 Cep	206952	K ₀ III	2.41		e
	ε Peg	206778	K ₂ Ib†	2.42		
	μ Cep	206936	M ₂ Ia†	2.11 :		
	9 Peg	206859	G ₅ Ib†	2.40		
	8324	207130	K ₁ III	2.36		b
		207119	K ₅ Ib	2.37		
	12 Peg	207089	K ₀ Ib	2.36		
	ν Cep	207260	A ₂ Ia†	2.01 :		
651	8325	207134	K ₃ III	2.26		a
		207991	K ₅ Ib	2.19		
	8374	208066	G ₈ Ib†	2.48		
	ν Peg	209747	K ₄ III	2.29		a
	20 Cep	209960	K ₄ III	2.24		
	8424	209945	K ₅ III	2.15		
	8442	210220	G ₆ III	2.20		
	π Peg	210459	F ₅ II-III	1.99 :		
	24 Cep	210807	G ₈ III	2.18		d
	ζ Cep	210745	K ₁ Ib†	2.49		
661	8475	210889	K ₂ III	2.27		
	8485	211073	K ₃ III	2.25		
		211076	K ₄ III	2.23		
	1 Lac	211388	K ₃ II-III	2.38		
	RW Cep	212466	? Ia	2.53		
	β Lac	212496	G ₉ III	2.15		e
	35 Peg	212943	K ₀ III-IV	2.14		ae
	5 Lac	213310	M ₀ Iab	2.08		
		213893	K ₅ III	2.12		
	11 Lac	214868	K ₃ III	2.24		a

TABLE I (continued)

No.	Name or H.R.	H.D.	Type	CN ratio	G band ratio	Notes
671	η Peg	215182	G2 II-III	2.12		
	13 Lac	215373	Ko III	2.30		e
		215549	K1 III-IV	2.10		
	λ Peg	215665	G8 II-III	2.39		d
	μ Peg	216131	Ko III	2.21		d
	ι Cep	216228	K1 III	2.25		d
	8692	216266	G4 Ib†	2.28		
	8726	216946	K5 Ib†	2.15		
	8752	217476	Go Ia†	2.17		
	8761	217673	K2 II	2.36		
681	8779	218029	K3 III	2.40		
	3 And	218031	Ko III	2.24		e
	8784	218101	G8 IV	2.14		
	56 Peg	218356	Ko IIp	2.27		
	4 And	218452	K5 III	2.22		
	60 Peg	218395	Ko IV	2.14		
	8832	219134	K3 V†	2.08		
	γ Psc	219615	G7 III	2.15		ac
	8857	219668	sgKo	2.32		
	α Cep	219916	Ko III	2.16		e
691	11 And	219945	Ko III	2.22		e
		219978	K5 Ib	2.19		
	8875	219962	K2 III	2.34		a
	7 Psc	220009	K2 III	2.11		
	66 Peg	220363	K3 III	2.34		
	ν Peg	220657	F8 IV	1.97		
	θ Psc	220954	K1 III	2.33		b
	70 Peg	221115	G8 III	2.23		e
	14 And	221345	Ko III	2.20		ac
		221354	Ko V	2.10		
701		221585	G8 IV	2.05		
		221639	sgG9	2.17		
	72 Peg	221673	K4 III	2.24		
	8952	221861	Ko Ib	2.42		
	λ And	222107	G8 III-IV	2.09		c
	78 Peg	222842	Ko III	2.25		e
	ψ And	223047	G5 Ib	2.31		
	19 Psc	223075	C6	2.58		
	9010	223173	K3 II	2.34		
	τ Cas	223165	K1 III	2.28		e
711	ρ Cas	224014	? Ia	2.26	2.71	
	ω Psc	224617	F4 III	1.96		

Notes to Table I

(1) The order is that of R.A. for epoch 1960.

(2) No observations of the following northern G5-K5 stars brighter than $5^m.5$ were secured: HR 1205, 47 Tau, μ UMa, 6 Dra, 24 Com A, ϵ^1 Boo, 3 Ser, 95 Her B or β^1 Cyg; or upon the following, which are in declination $> +73^\circ$: HR 285, 49 Cas, HR 1523, HR 2527, HR 3751, HR 4126, 4 UMi, 5 UMi, β UMi, θ UMi, ϵ UMi, HR 7117, τ Dra, HR 8702, HR 8748, π Cep, γ Cep.

(3) Meaning of symbols:

- : Mean of observations made on fewer than three nights.
- † MK standard spectrum.
- a Dynamical space velocity greater than 80 km/sec.
- b "4150".
- c "Weak-CN".
- d "Strong-line".
- e "Weak-line".
- f B.D. +42° 939.
- g Composite spectrum, early-type companion.
- h Double, companion star only partly excluded by slit.

In the cases of all other double stars, where the angular separation is less than 2" the two stars have been measured together, and where the separation is more than 2" the brighter component alone has been observed.

(4) The CN anomaly of a class III star may be obtained by subtracting the following quantity from its CN ratio: G8 2.19, K0 2.23, K1 2.25, K2 2.28, K3 2.27, K4 2.21, K5 2.13. The G band anomaly may likewise be obtained by subtraction of: G8 2.71, K0 2.76, K1 2.80, K2 2.84, K3 2.85, K4 2.83, K5 2.80.

The CN ratios given in Table I are compared in Fig. 1 with results published for some of the same stars by Lindblad (4), Öhman (5), Iwanowska (6), Keenan (7), Plassard (8), and Gyldenkerne (9).

Although Lindblad used the method of exposure-ratios on objective-prism spectra, modestly remarking (4), "It is, of course, freely admitted that the method of exposure-ratios is a fairly crude spectrophotometric method in the case of bright stars", his observations show the best correlation with ours.

The earlier measurements just cited and used in constructing Fig. 1 are not exactly comparable with each other or with ours. Most of them are on a logarithmic or magnitude scale and most are based on slitless or objective prism spectra, although Gyldenkerne used interference filters. There are differences in the wave-length bands used and for instrumental reasons there is much variation in the sharpness with which these bands are defined. The rather large scatter seen in Fig. 1 is therefore not unexpected. The tail of the distribution in the cases of Plassard and Gyldenkerne is due to stars of spectral types K₄ and K₅.

5.1. *Variation of CN intensity with spectral type and luminosity.*—For most of the programme stars an MK spectral classification is available. An attempt was made to assemble more accurate absolute magnitude data, from the various published catalogues of spectroscopic parallaxes or luminosities, but this effort only served to convince us that the most reliable and homogeneous collection of these data lay in the MK classifications themselves, so that these have been used wherever they exist.

The CN intensity ratios were first plotted against spectral type at each whole luminosity class. The mean curves are shown in Fig. 2. It is important to notice that these curves simply summarize the average results for all stars; individual stars show quite large deviations from the appropriate curve, the r.m.s. deviation being about 0.07, i.e. over 3 per cent. The deviations for luminosity class V, where there is very little CN absorption at any spectral type, are rather less; and rather remarkably those of the supergiants of luminosity class Ib are also smaller than the average. Since a scatter of 0.07 is over three times the error of measurement, it must be due either to an intrinsic scatter in

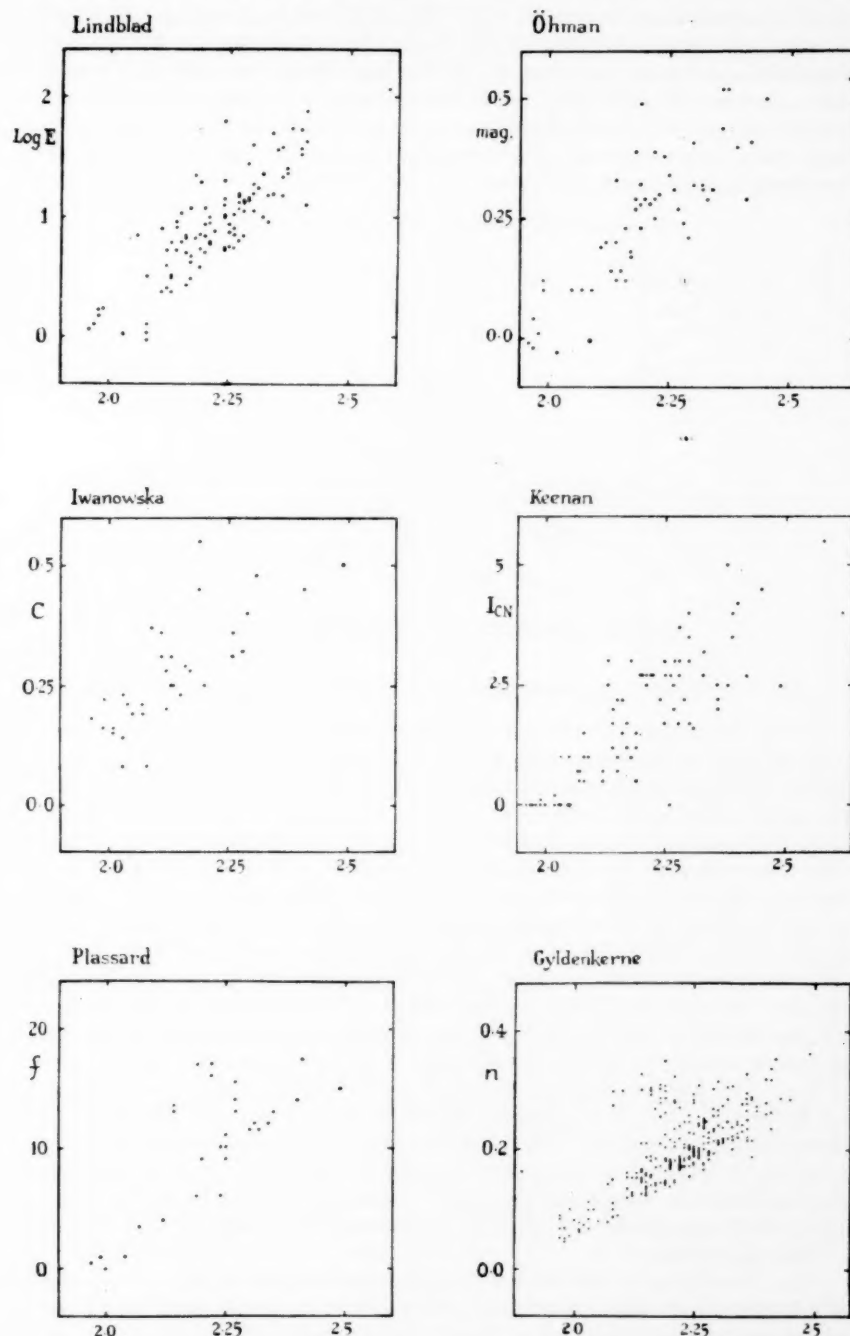


FIG. 1.—CN ratios (abscissae) compared with intensities derived by previous authors.

the CN intensities or to errors in the MK types and luminosities. However, our measurements of the G band (see Section 6) suggest that the MK spectral classification errors are not normally greater than about one-tenth of a spectral class; they would need to be three times as great to explain the CN scatter. Alternatively, mean errors of a whole luminosity class would be needed. We think that such an explanation is untenable and that the major part of the CN deviations represents a real scatter.

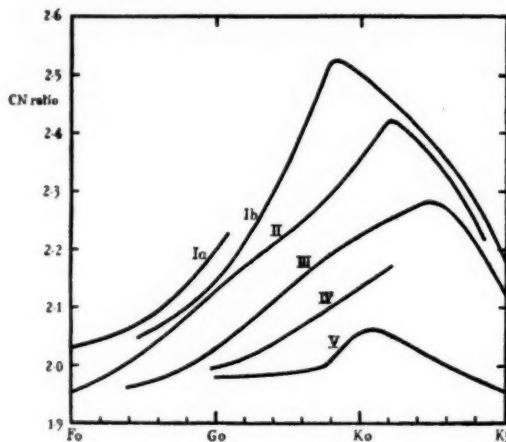


FIG. 2.—Mean curves of CN ratio as a function of spectral type for each luminosity class.

Owing to this large scatter it is not possible accurately to deduce the absolute magnitude of a given star from its CN ratio, even if the spectral type is accurately known. If one attempts to derive what we might call "CN absolute magnitudes", the r.m.s. difference of these from the MK luminosity is of the order of $1^m.5$ even in the range of spectral type G8–K1 where the sensitivity of the *average* CN ratio to luminosity is particularly favourable. The CN luminosity is not rarely greatly at variance with the value reliably determined by other methods, or in direct conflict with the trigonometrical parallax. In quoting examples we do not need to fall back upon well-known peculiar stars such as ϕ^2 Orionis. The CN absolute magnitude for ϵ Dra (G8 III), for instance, is $4^m.4$, which would require a parallax of $0''.120$ compared with the value of $0''.001 \pm 0''.006$ observed trigonometrically. Again, the consensus of opinion of several authors prevents us from accepting the absolute magnitudes of about -2 predicted for γ , δ , ϵ and π Tau. The high accuracies ($0^m.5$ or even $0^m.3$) claimed by previous authors (4, 8) for CN absolute magnitudes appear to be fictitious and due in part to observational selection of a rather homogeneous group of stars—which we have intentionally avoided as far as possible—and in part to the lack of alternative luminosity data for comparison purposes. For instance, comparison of Lindblad's (4) derived magnitudes with the MK data reveals a standard error not far short of two magnitudes.

5.2. *Correlation of CN intensity with space velocity.*—In order to correlate CN intensity with space velocity it is desirable first to remove the grosser effects of spectral type and luminosity. This is readily performed by subtracting from

the measured CN ratio for each star the mean value for all observed stars of the same spectral type and luminosity: the difference we shall call the CN anomaly. Space velocity data are available (2, 10, 11) for almost all of the 342 luminosity class III stars on the programme but are lacking for many of the others, so that the present discussion will be restricted to normal giants. It is difficult to say just how accurate these data are, but in so far as the velocities depend upon proper motions and upon absolute magnitudes estimated spectroscopically, mean errors of perhaps 25 per cent or more can be expected.

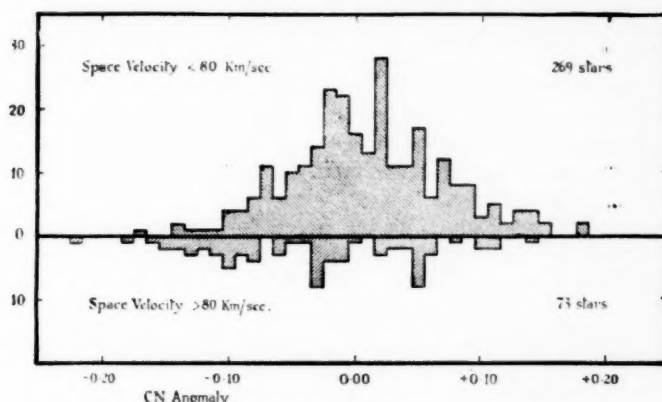


FIG. 3.—Frequency distribution of CN anomalies for luminosity class III stars.

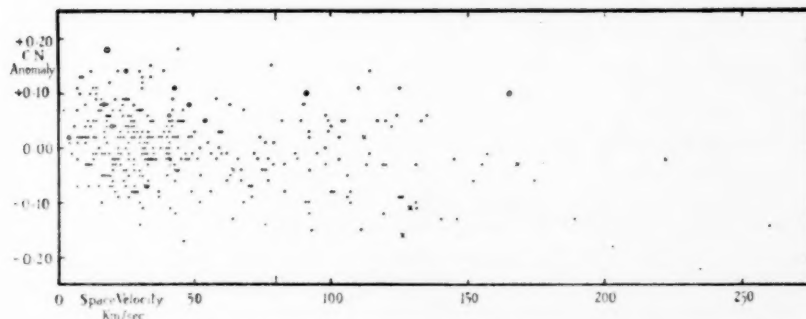


FIG. 4.—CN anomalies as a function of space velocity for class III stars. Crosses distinguish "weak-CN" stars, circles "4150" stars.

The frequency distribution of CN anomalies for all observed giant stars is shown in Fig. 3. High-velocity stars are plotted below the horizontal axis, low-velocity stars above; the dividing velocity is taken as 80 km/sec. In Fig. 4, CN anomalies are plotted against space velocities directly.

It is quite clear that there is nothing like a one-to-one correspondence between high velocity and weak CN absorption. Some high-velocity stars do have weak

CN, but in many others the CN ratio is abnormally high. Many low-velocity stars, on the other hand, have weak CN. There is indeed a small statistical difference in the CN ratio between the two groups of stars shown in Fig. 3, viz. 0.042 ± 0.010 (s.e.), which is little more than half the random scatter within either group.

These conclusions are surprisingly at variance with what may have become established as a supposed fact. It was early found (12) that certain objects which displayed spectral peculiarities, sometimes including a weakening of the CN absorption, had high velocities, and it perhaps came to be supposed that such peculiarities were a quite general characteristic of high-velocity stars (11, 13); and objects in whose spectra these characteristics were detected have sometimes been labelled "high-velocity" irrespective of their space motions (14). To apply this term to stars merely on the basis of spectroscopic peculiarities and not on a measured velocity appears to us most undesirable. Especially is this the case when the peculiarity concerned is so weakly correlated with velocity as is CN. We emphasize that not all weak-CN stars have high velocities and not all high-velocity stars have weak CN.

It is worth pointing out that if for any reason the intrinsic luminosity of a star is overestimated or its parallax underestimated, its computed space velocity will be too high and also the CN intensity will be weaker than expected. One might in this way obtain a spurious correlation between high velocities and weak CN. It is not, of course, suggested that this is the whole story, since many stars have radial velocities which are themselves sufficient to warrant inclusion of these bodies in the high-velocity group; but it is an effect that will tend systematically towards a weak correlation of the observed sign.

5.3. *Weak- and strong-line, weak- and strong-CN stars.*—Miss Roman (2) and others (11) have classified stellar spectra on the MK system and have noted in particular cases an abnormal weakness or strength of the CN band. Miss Roman has in addition detected spectroscopic differences leading to her well-known classes of "weak-line" and "strong-line" stars. These classes have aroused interest because they have been associated with the velocity characteristics of their members and hence with their membership of Populations I or II, or at least of distinguishable population groups. The spectroscopic characteristics are supposed to reflect variations of chemical composition and these may be related to stellar age or the stage of evolution reached.

Owing to a certain amount of confusion we must quote briefly what Miss Roman (2) means when she classifies G8-K1 stars into "weak-line" and "strong-line" groups. She says that 85 per cent of all G8 to K1 stars can be assigned to one of two groups typified respectively by HR 4126 and 2 Draconis. The HR 4126 stars have $\lambda 4227\text{A}$ CaI and the G band both *weaker* than average, but their velocity distribution is similar to that of the "strong-line" stars of late F and early G types. She describes the HR 4126 group as "strong-line" by this analogy, "although the name is no longer descriptive". Conversely, the 2 Dra stars have strong $\lambda 4227\text{A}$ CaI and G band but are associated in velocity characteristics with the weak-line stars of earlier type and are described as "weak-line" stars. The remaining 15 per cent of the G8-K1 stars share the spectroscopic characteristics of the latter group but also have the $\lambda 4200\text{A}$ CN band either unusually weak, being then called "weak-CN" stars, or unusually strong, in which case they are designated "4150" stars. This last name has

received objection as 'rather ambiguous, for some objects designated as "4150 stars" in the literature (e.g. γ Cep) actually do not have very strong CN bands' (14).

The nomenclature in this subject seems to us to be greatly in need of improvement.

Our own measurements show that "4150" stars in fact have positive CN anomalies, and that all but two of the "weak CN" stars have negative anomalies, the exceptions being 16 Vir and η Cep. However, many stars with equally or even more anomalous intensities have passed without comment.

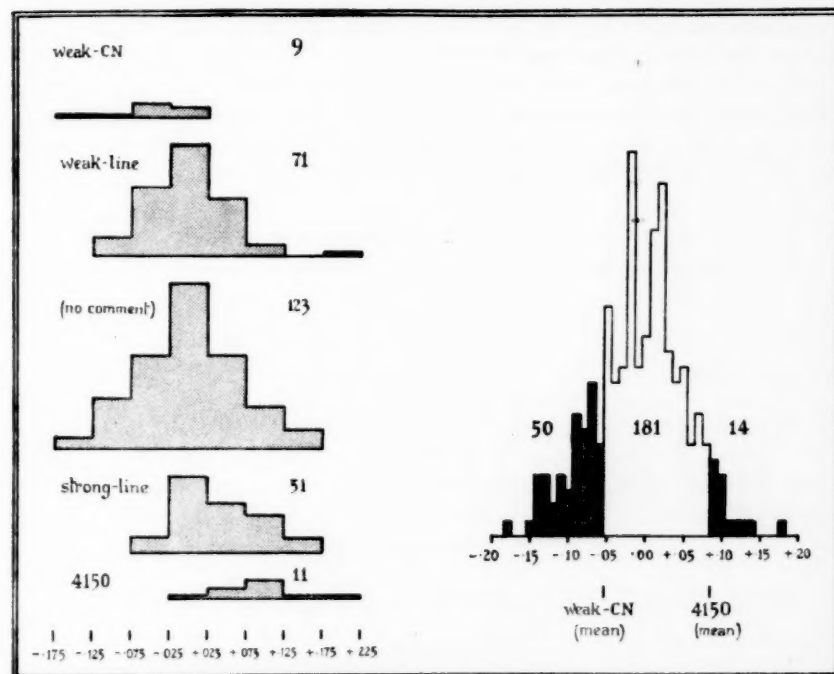


FIG. 5.

Of the giant stars observed by us, 265 are in Miss Roman's catalogue (2). Nine are noted by her as "weak-CN" stars and their average anomaly is -0.051 ± 0.018 (s.e.). Only three of the nine have anomalies more negative than this, but in our own measures as many as fifty stars altogether, 19 per cent of the total, have such anomalies, while in 14 of these the anomaly exceeds twice the quantity just cited. The mean anomaly of the eleven "4150" stars is $+0.087 \pm 0.014$; five of these have greater anomalies, but so have nine other stars whose excessive CN intensity apparently has passed unnoticed.

The "weak-line" stars show no systematic anomaly, but the "strong-line" stars have slightly enhanced CN absorption, their mean CN anomaly being

$+0.039 \pm 0.007$. The anomalies of the individual stars are shown in histogram form in Fig. 5.

6. *The G band*.—During an intermission in the CN programme in 1958 April–June some measurements were made on the G band, using the same method and apparatus and observing some of the same stars. The wave-length regions used were

$$\begin{aligned} A & 4230-4270 \text{ Å}, \\ B & 4285-4315 \text{ Å}, \\ C & 4342-4380 \text{ Å}. \end{aligned}$$

The slit width was $0.121 \text{ mm} = 1''.5 = 2.2 \text{ Å}$. Since the consistency of the early measurements was rather lower than expected, all observations made in the period 1958 April 8–23 were rejected *en bloc*. The total number of later observations was 1259, made on 23 nights, on 212 stars. Two only of these observations were discordant and were rejected. The rest fit a Gaussian error curve very well; the r.m.s. width is 0.047, implying a root-mean-square error per observation of 0.052, or slightly better than 2.0 per cent.

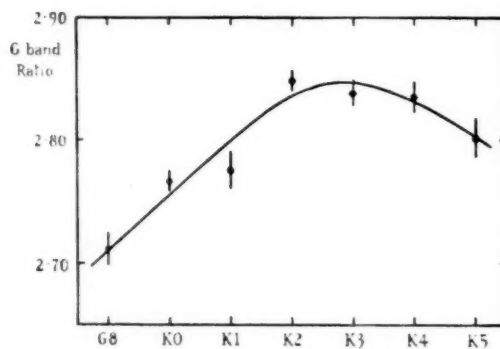


FIG. 6.—Mean curve of G band ratio as a function of spectral type for luminosity class III.

The mean G band ratio for each of the observed stars is shown in Table I. 125 of these stars are normal giants; the variation of G band ratio with spectral type at this luminosity is shown in Fig. 6. Since the ratio reaches a maximum in the K types, it is not by itself a good criterion of type there. Up to K1, however, the spectral type predicted from the G band has a mean deviation of 0.15 class from the MK type; this is satisfactory but not unexpected, as the MK types rely heavily on the G band in the range G8–K1. Assuming the accuracy of the MK types, the r.m.s. deviation per star in G band ratio from the mean line drawn in Fig. 6 is 0.05. It is very unlikely that this scatter is due wholly to errors of measurement; nor can it be due to errors in MK type since it persists at the same value throughout the range of types studied, including the mid-K's where the G band ratio reaches a rather flat maximum and type errors are unimportant. At least part of the scatter must therefore be regarded as intrinsic, as in the case of CN; but it is small enough to make the type corresponding to the G band

intensity a useful first approximation to the MK type for G stars and, it may well prove, in the F's as well.

The mean "G band anomaly" for fifteen high-velocity stars of luminosity class III is 0.000 ± 0.013 (s.e.); seven of these stars have positive anomalies, seven negative, and one zero. The G band anomaly is plotted as a function of space velocity in Fig. 7. It seems clear that, contrary to what has been supposed (11), there is no general systematic dependence of the intensity of this band upon stellar velocity. The mean anomaly of the 23 "weak-line" stars is $+0.006 \pm 0.010$, and that of the 22 "strong-line" stars is -0.023 ± 0.012 . The difference between the two groups is therefore 0.029 ± 0.016 , which is hardly of statistical significance. The scatter within the groups is much greater than the difference between them.

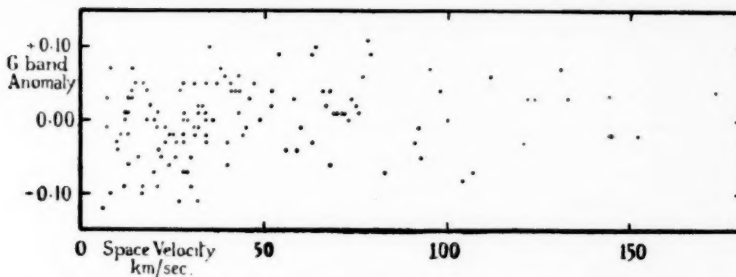


FIG. 7.—*G band anomalies as a function of space velocity for class III stars.*

There are too few stars of luminosity classes other than III and whose G bands have been measured to permit any detailed conclusions to be drawn from them. So far as the data go, they show a weak dependence of G band ratio upon luminosity, the higher ratios corresponding to the higher luminosities; the dependence upon spectral type at each luminosity is indistinguishable in form from the curve shown in Fig. 6 for luminosity class III. The mean vertical

TABLE II

Luminosity class	Displacement	No. of stars
II	$+0.07 \pm 0.015$	7
II-III	$+0.015 \pm 0.02$	9
III-IV	0.00 ± 0.02	11
IV	-0.035 ± 0.025	8
V	-0.07 ± 0.015	12

distance through which this curve should be displaced to represent the G band intensities at other luminosities is shown in Table II. At the season when the observations were made, practically no apparently bright stars of class Ib were in the easily accessible part of the sky.

7. *Acknowledgments.*—We wish to express our thanks to Mr D. W. Beggs, who designed, made and maintained most of the electronic equipment used for this work. The investigation followed exploratory measurements made by one of us (R.O.R.) on spectrograms at the Dominion Astrophysical Observatory, Victoria, B.C., and thanks are also due to Dr R. M. Petrie and his staff.

*The Observatories,
Madingley Road, Cambridge:*

1959 October 1.

References

- (1) G. G. Yates, *M.N.*, **108**, 476, 1948.
- (2) N. G. Roman, *Ap. J.*, **116**, 122, 1952.
- (3) W. W. Morgan, P. C. Keenan and E. Kellman, *An Atlas of Stellar Spectra*, Chicago, 1943.
- (4) B. Lindblad, *Ups. Medd.*, **28**, 1927.
- (5) Y. Öhrman, *Ups. Medd.*, **33**, 1927.
- (6) W. Iwanowska, *Stock. Ann.*, **12**, 5, 1936.
- (7) P. C. Keenan, *Ap. J.*, **93**, 475, 1941.
- (8) J. Plassard, *Ann. d'Astr.*, **13**, 1, 1950.
- (9) K. Gyldenkerne, *Ann. d'Astr.*, **21**, 26, 1958.
- (10) P. C. Keenan and G. Keller, *Ap. J.*, **117**, 241, 1953.
- (11) N. G. Roman, *Ap. J. Supplement*, **2**, 198, 1955.
- (12) B. Lindblad, *Ap. J.*, **55**, 85, 1922.
- (13) P. C. Keenan, W. W. Morgan, and G. Münch, *A.J.*, **53**, 194, 1948.
- (14) P. C. Keenan, *Handbuch der Physik*, **50**, 93, Berlin, 1958.

PRELIMINARY LIST OF RADIAL VELOCITIES FOR 33 STARS NEARER THAN 20 PARSECS

B. R. Leaton and B. E. J. Pagel

(Communicated by the Astronomer Royal)

(Received 1959 September 22)

Summary

To extend the available data on space motions of stars within 20 pc, 140 spectra of standard velocity stars and stars from Gliese's catalogue were taken with the 80 A/mm Xf spectrograph camera of the Mt Wilson 60-inch telescope by the Astronomer Royal during 1958 February–March. Using effective wave-lengths from 12 plates of 5 stars with quality "a" velocities in R. E. Wilson's catalogue, radial velocities have been determined for 33 stars with no previous determinations and for 17 stars with previous determinations of quality poorer than "a". The scatter among individual plates is sometimes as large as 10 km/sec, but the mean from 3 or more plates should be accurate to ± 4 km/sec within the wave-length system employed. A further series of observations of this type is planned.

1. *Introduction.*—A large amount of observational material exists for the small region of the galaxy in the immediate vicinity of the Sun, but there are a number of deficiencies. For instance, in the best available collection of data for nearby stars, Gliese's *Katalog der Sterne näher als 20 Parsek für 1950.0* (Gliese 1957), of 1094 stars listed whose parallax is supposed to be $0^{\circ}050$ or greater, over 300 stars have, as yet, had no determination made of their radial velocity, even allowing for binary stars which may be presumed to have a common motion. Hence, although there are observations of the proper motions of these stars, it is impossible to deduce their space motions. It is obvious that any conclusions drawn from analyses of such motions (e.g. Woolley 1958) would be greatly strengthened if such deficiencies were made good.

Most of the stars in Gliese's catalogue for which there are, as yet, no measures of radial velocity are late-type dwarfs or sub-dwarfs, whose relative faintness has made such observations over-tedious or impracticable with even moderate-sized telescopes. Advantage has been taken of an opportunity to use the X-spectrograph on the 60-inch telescope at Mt Wilson to make the data on nearby stars more complete*. The comparatively large aperture of the 60-inch coupled with the speed of the four-inch X-spectrograph camera ($f/1$) renders possible the production of a usable spectrogram, dispersion 80A/mm, in a reasonably short observing time, e.g. a tenth-magnitude Mo in about one hour.

This paper gives the results of measurements of spectrograms taken by Dr R. v. d. R. Woolley in 1958 February and March. It is intended to make a further series of observations of this type in the near future.

* I am very much indebted to the Carnegie Institution of Washington for appointing me a Research Associate in 1958 and to Dr I. S. Bowen for making the 60-inch telescope available to me for securing these spectra.

R. v. d. R. Woolley.

2. *Summary of measurements.*—The plates have been measured by Woolley (RW), Leaton (RL), Pagel (BP), and Alexander (JA) as shown. The whole series of measurements was analysed by Leaton, with some help from Pagel, using adopted wave-lengths (Table I) derived from measurements of stars of velocities having quality "a" in Wilson's catalogue (Wilson 1953), which are given in Table II. Results for other stars with published radial velocities are given in Table III, and new velocities for 33 stars with no previous measurements available are shown in Table IV.

TABLE I

Adopted wave-lengths, A.	Wave-lengths recommended by PAM*	Original Victoria system†
4455.03		4454.91
4435.28		35.23
4415.26	4415.20	15.15
4404.75	4404.74	04.75
4383.82		4383.56
4352.08 (G—K ₃)		51.85
51.74 (K ₄ —M)		
4325.32 (G—K ₃)		25.64
4308.05		07.93
4290.00		
4271.69		4271.56
4260.52	4260.60	60.48
4254.71 (G—K ₃)		54.35
4.54 (K ₄ —M)		
4250.30		50.47
4226.81	4226.85	26.74
4191.37		4191.56
4187.37		
4143.60		43.72
4101.66 (G—K ₃)	4101.74	01.75
4071.83	4071.70	4071.74
4063.52 (G—K ₃)		63.62
4063.82 (K ₄ —M)		
4045.72	4045.76	45.82
4030.67	4030.70	30.77
4005.38	4005.30	05.26

* Petrie, Andrews and McDonald (1958)

† Harper (1938)

Taking means from Table I, we find

$$\begin{aligned} \text{adopted minus Victoria} &= +0.014 \text{ A} \pm 0.02 \text{ (p.e.)} \\ \text{adopted minus PAM} &= +0.001 \text{ A} \pm 0.014 \text{ (p.e.)} \end{aligned}$$

Thus the present system agrees with that of Petrie, Andrews and McDonald within 0.1 km/sec, which is very satisfactory.

Wave-lengths derived by averaging *all* stars of "known" velocity (i.e. Wilson "a", "b" and "c" and some measured by Dyer (1954)) gave a system of wave-lengths that are low on PAM by

$$0.036 \text{ A} \pm 0.014 \text{ (p.e.)},$$

i.e. these give velocities that are 2.5 km/sec greater.

Of the 140 plates,

- 12 are of 5 stars with "a" velocities in Wilson;
- 34 are of 17 stars with some sort of measurements available ("b", "c", and Dyer);
- 73 are of 33 stars with no previous measurements available;
- 19 were not measured because of overexposure, underexposure, lack of focus, or double Fe lines;
- 1 appears to be the wrong star;
- 1 remains unidentified.

The measures for the first three categories appear in Tables II, III, and IV respectively.

TABLE II
Stars with "a" velocities in Wilson

Star	m_r	Wilson No.	Wilson velocity	Gliese No.	Plate Xf	Exp. time	Measured velocities	Mean R.G.O.
η Cas A (G0V)	3.4	447	+9.4 a	34A	3437	1 ^m	+11 (RL)	
					3438	1 ^m	-7 (RL)	+2 ± 3 (p.e.)
					3460	3 ^m	+3 (RL)	
κ Cet (G5V)	4.8	1838	+19.3 a	137	3440	1 ^m	+15 (RL)	+15
119 Tau (cM2)	4.7	3354	+22.5 a		3332	1 ^m	+21 (RL)	+18 ± 1 (p.e.)
					3336	2 ^m	+21 (RL)	+16 (RW)
36 Com (gMo)	5.0	7746	-1.6 a		3342	3 ^m	+2 (RL)	-1 (BP)
					3347	7 ^m	+4 (RL)	+2 (BP)
					3357	4 ^m	+7 (RL)	+6 (BP)
ξ Boo A (G8V)	4.7	8634	+3.9 a	566 A	3456	1 ^m	+5 (RL)	
					3457	40 ^s	+8 (RL)	+5 ± 1 (p.e.)
					3491	1 ^m	+3 (RL)	

Mean Wilson "a"—RL (km/sec): +0.5 ± 1.3 (p.e.)

3. *Quality of the results.*—The best indication of the accuracy of the results is given by an inspection of Table II. Different plates of one star occasionally give startlingly large discrepancies, perhaps owing to the increased effect of asymmetrical guiding on the wide slits employed in modern spectrographs. The effect is worst of all among the stars used as standards, since the exposures on these were very short; experience with other spectrographs suggests that 5 minutes is the minimum exposure time for adequate guiding, while the brightest standards used here were exposed for 1 minute only. However, discrepancies of the order of 10 km/sec still exist between plates of one star that were exposed for longer than 5 minutes, e.g. for η Cas B (Table III).

Thus the average of three plates should be correct with the probable error stated in Table IV *within the present system of wave-lengths*. Further observations with the Xf spectrograph are, however, needed to check the system itself. Values obtained from single plates may be out by as much as 10 or even 15 km/sec.

TABLE III
Other stars for which previous velocity measurements exist

Star	m_v	Gliese No.	Source	Published velocity	Plate No.	Exp. time (mins.)	Measured velocities	Mean R.G.O.
η Cas B (dM0)	7.2	34 B	W 448	+12.8 b	3419 3439	10 7	+15(BP) +7(BP)	..
+47° 977 (dK8)	9.1	168	Dyer	-72	3405 3421	30 37	-83(RL) -80(RL) -85(BP)	-73(BP) -79(RW) -81(RW)
-3° 1061 (K3V)	7.5	200 A	W 3169	+85.2 b	3389	13	+86(RL)	+88(RW)
+37° 1312 (dK2)	7.3	217	W 3571	-30.9 b	3333	11	-40(RL)	-46(JA)
-4° 2490 (dK3)	5.9	327	W 5857	+26 c	3395	3	+37(RL)	-42(RW)
+50° 1725 (dM0)	6.6	380	W 6436	-27 c	3396 3399 3424 3425 3426	5 12 8 10 20	-29(RL) -31(RL) -37(RL) -32(RL) -32(RL)	-32(BP) -31(BP) -34(BP) -31(BP) -27(RW)
+56° 1458 (K7V)	8.7	394	W 6586	+12 d	3496 3506	33 32	-37(RL) -6(RL)	-36(JA) -41(RW)
+36° 2147 (M2V)	7.5	411	W 6818	-86.5 b	3340 3341 3356	13 9 15	-88(RL) -89(RL) -85(RL)	-87(RW) -65(RW) -83(RW)
+31° 2249 (dK8)	9.0	439	Dyer	+35	3412 3447	46 30	+24(RL) +23(RL)	+22(RW) +20(RW)

+10±7 (p.e.)

..

-80±2

-22±10 Var?

-22±2

-83±2

TABLE III (continued)
Other stars for which previous velocity measurements exist

Star	<i>mv</i>	Gliese No.	Source	Published velocity	Plate Xf	Exp. time (mins)	Measured velocities	Mean R.G.O.
+21° 2486 (dM0)	9.6	499	Dyer	- 9	3450	42	- 11(RL) - 11(BP)	- 11
+68° 771 (dK1)	8.2	W 8320	-	8.1 b	3500	28	- 21(RL)	- 21
+ 1° 2920 (dG3)	6.3	547	W 8401	-17.5 b	3402	16	- 4(RL)	- 4
+53° 1719 (K3V)	7.2	556	W 8489	+14.1 b	3501	21	o(RL) + 1(JA)	o(RW) o
+24° 2786 (dG2)	5.8	564	W 8622	- 1 c	3403 3416 3417 3432 3433 3434 3454	16 10 5 2 3 5 1	- 28(RL) - 10(RL) - 4(RL) + 4(RL) o(RL) - 8(RL) - 9(RL)	- 7 ± 3 S.B.
+64° 1046 (dG5)	8.5	577	W 8744	- 4.3 b	3418 3435	30 20	- 18(RL) - 12(RL)	- 15 ± 2
+67° 935 (MoV)	8.6	617 A	W 9393	-14 c	3483	20	+ 1(RL)	+ 1
- 4° 3873 (K6)	9.7	583	Dyer	-26	3455	38	- 10(RL)	- 10

N.B.—In fixing probable errors, each plate was given unit weight independent of the number of times it was measured.

Mean Wilson "b" — RL (km/sec): +4.5 ± 1.8 (p.e.)
Mean remainder — RL (km/sec): +6.0 ± 2.0 (p.e.)

Differences between measures by RL and others are insignificant.

* The system based on non- "a" velocities is thus 5 km/sec high on that from "a" velocities, but the latter seems preferable as it agrees with PAM.

TABLE IV
R.G.O. measures of Xf plates of Gliese and other stars with no previous measures available

Star	Gliese No.	Spec. type	App. vis. magnitude	Plate Xf	RW	RL	BP	Mean R.G.O. (unweighted)
20° 802	174	K ₃ V	8.0	3334 3348 3420	+17 ± 6.1 (p.e.) + 6 6.6 - 6 3.2	+20 ± 3.8 (p.e.) +17 5.7	+18 ± 1.5	
+11° 878	208	dMo	8.8	3349 3390	+17 5.7	-14 2.0	-17 ± 1.4	
+20° 1018	209	G ₄ IV-V	7.6	3350 3391 3502	-17 2.7	-17 3.3	-13 ± 3.0	
+53° 935	212	M ₁	9.7	3351 3441	-19 2.7	-17 3.3	-13 ± 3.0	
-15° 1126	214	G ₅	8.0	3406 3472	-17 2.0	+71 2.0	+62 ± 6.0	
+2° 1085	223	K ₃	8.8	3392 3471 3508	-27 2.6	-36 1.8	-32 ± 1.8	
+18° 1214	233	K ₃	6.7	3344 3352 3504	-32 4.2	+40 1.3	-8 ± 2.0 Var?	
+52° 1088	235	dMo	9.6	3353 3492	-32 4.2	-3 2.4	-1 ± 1.4	
+60° 1003	247	dMop	8.6	3345 3393 3423	-58 1.8	-57 3.1	-57 ± 0.4	
-9° 1858	267	dK8	8.5	3407 3484	-57 1.6	+26 2.2	+21 ± 3.5	
+14° 1684	276	dK8	8.9	3335 3337 3509	+63 2.6	+69 2.3	+64 ± 1.5	

TABLE IV (continued)
R.G.O. measures of Xf plates of Gliese and other stars with no previous measures available

Star	Gliese No.	Spec. type	App. vis. magnitude	RW	Plate Xf	RI	BP	Mean R.G.O. (unweighted)
+ 2° 1729	281	dMo	9.8	3474 3485 3510	- 5 ± 6.3 - 2 4.1 + 3 5.7	- 1 ± 1.6		
+ 2° 1766	287	dMo	10.2	3475 3494	- 27 3.1 - 26 5.6	- 26 ± 1.0		
+ 56° 1320?		dF6	10.1	3443	- 46 3.2	- 46		
- 12° 2618	313	dK8	9.1	3468	+ 27 3.3	+ 27		
+ 25° 1981*		A	9.7	3394 3354	+ 51 7.7 + 49 7.1	+ 50 ± 1.0		
+ 66° 582	322	dMo	9.1	3444 3463 3493	- 20 5.3 - 28 2.2 - 30 2.0	- 26 ± 2.1		
- 10° 2857	335	Ko	7.5	3338 3410 3476	+ 12 1.3 + 19 3.3 - 4 3.1	+ 9 ± 3.6		
+ 3° 2279	371	dMep	9.2	3346 3477 3505	+ 22 3.1 + 8 3.0 0 3.7	+ 10 ± 4.3 Var?		
+ 48° 1829	378	dM2	9.4	3339 3355 3397	- 5 2.2 - 7 2.2 - 15 4.7	- 9 ± 2.1		
+ 85° 161	396	Ko	7.2	3411 3445 3446	- 10 2.4	- 3 ± 2.0 - 11 2.6 - 2 2.1	- 6 ± 1.6	
+ 16° 2216	413	dMop	9.2	3495	+ 100 3.1	+ 100		
+ 5° 2463	418	dK8	8.8	3449 3464	+ 14 1.7 + 17 2.7	+ 15 ± 1.2		

* A star placed on the programme as a suspected subdwarf; laboratory wave-lengths used.

TABLE IV (continued)
R.G.O. measures of Xf plates of Gliese and other stars with no previous measures available

Star	Gliese No.	Spec. type	App. vis. magnitude	Plate Xf	RW	RL.	BP	Mean R.G.O. (unweighted)
+72° 545	441	dK8	9.2	3398 3413 3427		-29 ± 1.7	-26 ± 1.7 -33 2.3	-29 ± 1.3
+59° 1428	457	dM0	10.0	3428 3478 3497		-1.2 3.7 -26 2.5 -23 3.0		-20 ± 2.9
+55° 1536		K0	7.8	3451		-10 4.1		-10
+16° 2404	481	dK8	8.4	3401	+22 ± 2.0	+18 1.9		+20
+50° 1979	498	dK8	8.7	3414 3410		-14 1.8 -9 3.1		-12 ± 2.0
+50° 2030	532	dM0p	8.2	3415		-48 1.9		-48
+23° 2640	535	dM0p	9.1	3466 3479		-53 2.3 -55 2.0		-54 ± 1.0
+27° 2411	561	G5	9.5	3452 3480		-80 2.7 -74 1.9		-77 ± 2.0
+16° 2722	573	dK8	8.7	3433 3481		+6 2.0 -10 3.1		-2 ± 5.5
+7° 3180	626	dK8	8.8	3482		-36 2.6		-36

We are grateful to the Astronomer Royal for securing the observational material on which this paper is based and to the Director of the Mt Wilson and Palomar Observatories for making the 60-inch telescope available for this purpose.

*Royal Greenwich Observatory,
Herstmonceux Castle,
Hailsham, Sussex:
1959 September 21.*

References

Dyer, E. R. Jr., 1954, *A.J.*, **59**, 218.
Gliese, W., 1957, *Ast. Rech. Inst. Heidelberg, Mitt A.* No. 8.
Harper, W. E., 1938, *Pub. D.A.O. Victoria*, **6**, 297.
Petrie, R. M., Andrews, D. H., McDonald, J. K., 1958, *Pub. D.A.O. Victoria*, **10**, No. 22.
Wilson, R. E., 1953, *General Catalogue of Stellar Radial Velocities*.
Woolley, R. v. d. R., 1958, *M.N.*, **118**, 45.

H_I, He_I AND He_{II} INTENSITIES IN PLANETARY NEBULAE

M. J. Seaton

(Received 1959 September 15)

Summary

Recombination spectra have been calculated for H_I, He_{II} and the 2p-nd series of He_I. Expressions are given for the calculation of He⁺²/H⁺ and He⁺/H⁺ abundance ratios. It is shown that the ionized region of a nebula will contain a negligible amount of neutral helium if

$$I(\text{He II}, \lambda 4686)/I(\text{He I}, \lambda 5876)$$

exceeds 1.2.

For NGC 7662 and 2392 the measured relative intensities within each spectrum are in good agreement with theory but for NGC 7027 the agreement is poor for the weak lines and for the infra-red. The suggestion that the intensity anomalies for NGC 7027 may be due to collisional processes is found to be difficult to accept. The possibility is considered that there may be systematic errors in the intensity measurements.

The He/H abundance ratios, by numbers of atoms, are found to be 0.20 for NGC 7662, 0.16 for NGC 2392 and 0.19 for NGC 7027.

1. Introduction.—It is usually assumed that the H_I, He_I and He_{II} spectra in gaseous nebulae are excited by radiative recombination. The aim of the present paper is to check the theory by comparing observed and calculated relative intensities within each spectrum, and if these checks prove satisfactory, to obtain improved estimates of the He/H abundance ratios. We consider three planetary nebulae for which detailed spectrophotometric observations have been made. For NGC 7662 and 2392 the measurements by Minkowski and Aller (1) are found to be in good agreement with theory but for NGC 7027 the measurements by Aller, Bowen and Minkowski (2) are found to be in disagreement with theory for the weak lines and for the infra-red. We can find no satisfactory explanation in terms of physical processes in the nebula and therefore consider the possibility of systematic errors in the observations.

2. Theory

(a) H_I and He_{II}.—In earlier calculations (3) it was assumed that the *nl* states were populated in proportion to the statistical weights $(2l+1)$:

$$N_{nl} = \frac{(2l+1)}{n^2} N_n. \quad (1)$$

Calculations by Burgess (4) and by Searle (5) show that (1) is not true but that calculations made assuming (1) nevertheless give quite good results for the observed intensities,

$$I(n, n') = \sum_{ll'} I(nl, n'l'). \quad (2)$$

We make the usual distinction between Case A (optically thin in Lyman lines) and Case B (optically thick in Lyman lines). In Case B transitions to the ground

state are not taken into account, it being assumed that these are counterbalanced by absorptions from the ground state. It has been shown (6) that, in calculations assuming (1), the errors are greater for Case A than for Case B, the reason being that in reality transitions to the ground state take place only from the np states and that the importance of such transitions is exaggerated when (1) is assumed. For bright planetaries we may expect Case B to apply and calculations based on (1) to give good results for the H I and He II lines. In the present paper only Case B is considered.

For the $n \rightarrow n'$ line the absolute quantum emission rate (quahta $\text{cm}^{-3} \text{sec}^{-1}$) is denoted by $\mathcal{Q}_{n,n'}$. For a recombination line of the ion X^{+m} we have

$$\mathcal{Q}_{n,n'}(X^{+m}) = N_e N(X^{+m+1}) \alpha_{n,n'}(X^{+m}) \quad (3)$$

where N_e is the electron density, $N(X^{+m+1})$ the density of recombining ions and $\alpha_{n,n'}(X^{+m})$ is the *effective recombination coefficient* for the $n \rightarrow n'$ line. From formulae given by Seaton (6),

$$\alpha_{n,n'} = 2 \mathcal{D} Z \lambda^{3/2} b_n e^{x_n} \frac{g_{n,n'}}{n n' (n^2 - n'^2)} \quad (4)$$

where Z is the ion charge before recombination,

$$\mathcal{D} = \frac{2^6 \pi^{1/2} \alpha^4 c a_0^2}{3^{3/2}} = 5.197 \times 10^{-14} \text{ cm}^3 \text{ sec}^{-1} \quad (5)$$

(α being the fine structure constant, c the speed of light and a_0 the Bohr radius),

$$\lambda = \frac{\hbar R c Z^2}{kT} = 157890 \left(\frac{Z^2}{T} \right) (T \text{ in } {}^\circ\text{K}) \quad (6)$$

and $x_n = \lambda/n^2$. The factors $b_n(\lambda) e^{x_n}$ are tabulated by Seaton (6) and the $g_{n,n'}$ by Baker and Menzel (3).

Table I gives coefficients for recombination to the hydrogenic ions H⁰ and He⁺; this includes ground-state recombination coefficients α_1 , coefficients α_B defined by

$$\alpha_B = \sum_{n=2}^{\infty} \alpha_n \quad (7)$$

and effective recombination coefficients $\alpha_{4,2}(\text{H}^0)$, $\alpha_{3d,2p}(\text{H}^0)$ and $\alpha_{4,3}(\text{He}^+)$. Values of $\alpha_{4,2}(\text{H}^0)$ and $\alpha_{3d,2p}(\text{H}^0)$ are obtained from the work of Burgess (4), allowing for l -degeneracy; all other coefficients are obtained from the work of Seaton (6, 7).

The relative intensities in each spectrum are insensitive to the electron temperature. In subsequent discussions we consider only Case B and

$$T_e = 1.5 \times 10^4 {}^\circ\text{K}.$$

The results of Burgess are used for the H α /H β ratio and the results of Seaton for all other H I and He II ratios.

(b) He I.—For He⁰ orbital degeneracy is removed and it becomes essential to take proper account of the individual nl levels. Since (1) is not true calculations made assuming (1) will give incorrect intensities for the $nl \rightarrow n'l'$ lines. Such calculations will also be over-sensitive to transitions to the ground state, and the $2s$ metastable states. This explains the poor agreement, noted by Aller and Menzel (8), between observed singlet to triplet intensity ratios and those calculated by

TABLE I

Recombination coefficients in units $\text{cm}^3 \text{sec}^{-1}$

	$T_e = 1 \times 10^4$	$T_e = 2 \times 10^4$
$10^{14}\alpha_1(\text{H}^0)$	15.5	10.5
$10^{14}\alpha_B(\text{H}^0)$	25.8	14.3
$10^{14}\alpha_{4,2}(\text{H}^0)$	2.99	1.59
$10^{14}\alpha_{3d,2p}(\text{H}^0)$	5.27	2.38
$10^{14}\alpha_1(\text{He}^+)$	63.6	44.5
$10^{14}\alpha_B(\text{He}^+)$	154.0	90.1
$10^{14}\alpha_{4,2}(\text{He}^+)$	20.8	11.8

Goldberg (9) assuming (1) for $n > 2$. Further evidence that Goldberg's calculations are inexact was obtained by Wurm (10), who noted that the deduced He/H chemical abundance ratios depended systematically on the $\text{He}^+/\text{He}^{+2}$ ratios.

Greatly improved He I calculations have been made by Mathis (11). These give singlet to triplet ratios in satisfactory agreement with observation and ratios He/H showing no systematic dependence on $\text{He}^+/\text{He}^{+2}$ but the calculations still do not make full allowance for all of the individual nl levels.

Most of the observed He I lines are of the type $ns \rightarrow 2p$ and $nd \rightarrow 2p$. We consider only the $nd \rightarrow 2p$ transitions. The d states, and all states with $l > 2$, are nearly hydrogenic. The rate of population of a level nd is determined almost entirely by capture on nd and by capture on states with $l > 2$ followed by cascade to nd . Allowing for statistical weight factors, a good approximation should be

$$\left. \begin{aligned} \alpha_{n,1D,2^1P}(\text{He}^0) &= \frac{1}{4} \alpha_{nd,2p}(\text{H}^0) \\ \alpha_{n,1D,2^3P}(\text{He}^0) &= \frac{3}{4} \alpha_{nd,2p}(\text{H}^0) \end{aligned} \right\} \quad (8)$$

Some error will result from the fact that the ratios

$$A_{nd,2p} / \sum_{n'} A_{nd,n'p} \quad (9)$$

will be different for He^0 and H^0 but this error is negligible for $3d \rightarrow 2p$ and is probably small for the higher states. We use values of $\alpha_{nd,2p}(\text{H}^0)$ obtained from the calculations of Burgess (4); these will be accurate for small n but less accurate for large n . Finally it may be noted that the $\alpha_{nd,2p}(\text{H}^0)$ are insensitive to transitions to the ground state (Cases A and B giving results which never differ by more than two per cent) and that we may expect $\alpha_{n,1D,2^1P}$ to be insensitive to transitions to or from 1^1S and 2^1S and $\alpha_{n,1D,2^3P}$ to be insensitive to transitions to or from 2^3S .

(c) He/H abundance ratios.—For abundance determinations we consider the lines: $\text{H}\beta, 4 \rightarrow 2, \lambda 4861$; $\text{He I}, 3^3D \rightarrow 2^3P, \lambda 5876$; $\text{He II}, 4 \rightarrow 3, \lambda 4686$.

The relative quantum emission rates are

$$\frac{q(4686)}{q(4861)} = \frac{\int \alpha_{4,3}(\text{He}^+) N_e N(\text{He}^{+2}) dV}{\int \alpha_{4,2}(\text{H}^0) N_e N(\text{H}^+) dV} \quad (10)$$

$$\frac{q(5876)}{q(4861)} = \frac{\int \alpha_{3,1D,2^3P}(\text{He}^0) N_e N(\text{He}^+) dV}{\int \alpha_{4,2}(\text{H}^0) N_e N(\text{H}^+) dV} \quad (11)$$

where the integrals are over the nebular volume. The ratios of recombination coefficients are insensitive to T_e . For constant temperatures and densities we obtain the abundance ratios in terms of intensity ratios:

$$\frac{N(\text{He}^{+2})}{N(\text{He}^+)} = 0.134 \frac{I(4686)}{I(4861)} \quad (12)$$

$$\frac{N(\text{He}^+)}{N(\text{H}^+)} = 1.00 \frac{I(5876)}{I(4861)} \quad (13)$$

where the numerical factors are calculated for $T_e = 1.5 \times 10^4$ K. The chemical abundance ratio is given by

$$\frac{N(\text{He})}{N(\text{H})} = \frac{N(\text{He}^{+2}) + N(\text{He}^+)}{N(\text{H}^+)} \quad (14)$$

if there is a negligible amount of He^0 in the ionized region. We now show that He^0 will have a negligible abundance if

$$\frac{I(4686)}{I(5876)} \geq 1.2. \quad (15)$$

Consider the case of a pure He nebula, assume complete absorption of all stellar quanta capable of ionizing He^0 and let $\mathcal{N}(\text{He}^0)$ be the number of stellar quanta capable of ionizing He^0 and $\mathcal{N}(\text{He}^+)$ the number capable of ionizing He^+ . The number of He^+ ionizations due to quanta produced in the nebula is equal to the number of recombinations to the He^+ ground state and the number of ionizations due to stellar quanta is therefore equal to the number of recombinations on excited states; hence

$$\mathcal{N}(\text{He}^+) = \int \alpha_B(\text{He}^+) N_e N(\text{He}^{+2}) dV \quad (16)$$

with α_B defined by (7). In the same way one obtains

$$\mathcal{N}(\text{He}^0) = \int \alpha_B(\text{He}^0) N_e N(\text{He}^+) dV \quad (17)$$

noting that nearly all recombinations to He^+ produce one quantum capable of ionizing He^0 . The integrals in (16) and (17) are proportional to observed quantum emission rates. Using the approximation $\alpha_B(\text{He}^0) = \alpha_B(\text{H}^0)$ we obtain*

$$\frac{I(4686)}{I(5876)} = 1.2 \frac{\mathcal{N}(\text{He}^+)}{\mathcal{N}(\text{He}^0)} \quad (18)$$

and hence $I(4686)/I(5876) \leq 1.2$. If the ratio is greater than 1.2 we may conclude that absorption by He^0 is incomplete and for typical dimensions and densities of planetary nebulae this implies a negligible amount of He^0 .

For the pure He nebula a ratio exceeding 1.2 implies a limit on the amount of gas available to be ionized. For a real nebula, containing a mixture of H and He, this is no longer true but a ratio greater than 1.2 still implies a negligible amount of He^0 in the ionized region. Fig. 1 illustrates two possible situations. In Fig. 1(a) the He^+ region is limited by He^0 absorption and the intensity ratio must be less than 1.2 while in Fig. 1(b), which shows the position for higher star temperatures (13), the extent of the He^+ region is limited by H^0 absorption and the intensity ratio may exceed 1.2.

If the ratio $I(4686)/I(5876)$ is less than 1.2 the position may be that of Fig. 1(a) and in this case a reliable estimate of the He/H abundance ratio can be made only by examining the sizes of monochromatic images of the nebula in $\text{H} I$ and

* A similar relation for $I(4686)/I(4861)$ has been discussed by Wurm and Singer (12).

† But some of these quanta may ionize H^0 .

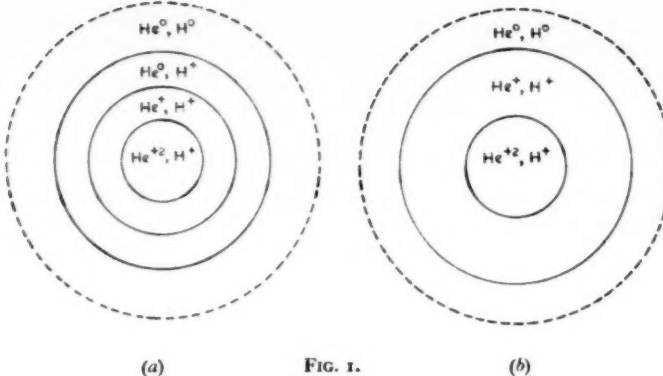


FIG. 1.

(b)

He I radiations. Mathis (11) finds that a number of nebulae have similar sizes in H I and He I. It would be interesting to know if this is the case for objects having very small values of the intensity ratio.

3. *Relative intensities for NGC 7662 and 2392.*—We consider the intensities measured by Minkowski and Aller (1) and ignore all lines for which the intensities may be uncertain due to blending. Let $I_o(\lambda)$ denote the observed intensities and $I_e(\lambda)$ the intensities which would be observed if there were no interstellar reddening; then

$$\log I_e(\lambda) = \log I_o(\lambda) + cf(\lambda) \quad (19)$$

where $f(\lambda)$ is a known function (4) and c a constant which determines the amount of reddening. The function $f(\lambda)$ is chosen to be such that 10^c is the factor by which the absolute H β intensity must be multiplied in order to correct for extinction. Let $I_r(\lambda)$ denote the calculated recombination intensities. Our procedure is to determine c on comparing I_o and I_r for the stronger Balmer lines and then to compare I_e and I_r for all of the H I, He I and He II lines. Table II gives values of c and Table III gives values of I_o , I_e and I_r for NGC 7662 and 2392. The values of I_e and I_r are made to agree for H I $\lambda 4861$, He I $\lambda 5876$ and He II $\lambda 4686$; intensities for these lines are given in italic type.

TABLE II
Values of the reddening constant

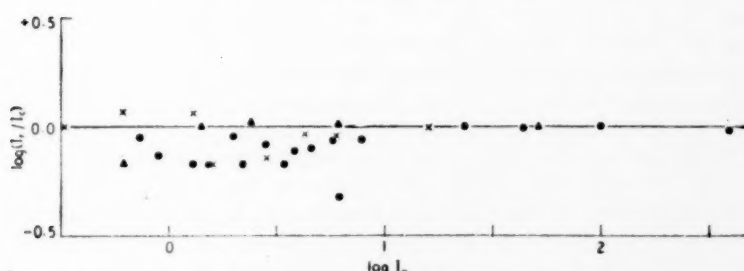
NGC	<i>c</i>
7662	0.46
2392	0.32
7027	1.22

The agreement between theory and observation is seen to be good and it is doubtful if there are any differences greater than probable errors of measurement. To see if there is any suggestion of systematic errors, in Fig. 2 we plot $\log (I_r/I_e)$ against $\log I_o$ and in Fig. 3 we plot $\log (I_r/I_e)$ against λ , in both cases for NGC 7662. With the single exception of the Paschen line furthest in the red ($\lambda 8863$) the values of $\log (I_r/I_e)$ are never greater than 0.06 or less than -0.18. Fig. 3 suggests that the values of $\log I_o$ may be overestimated by about 0.15 for $\lambda \leq 4000$ but in this region all lines considered have small value of I_o and will be difficult to measure accurately.

TABLE III

Intensities for NGC 7662 and 2392

Series	λ	n	NGC 7662			NGC 2392		
			I_o	I_e	I_r	I_o	I_e	I_r
H I	8863	11	6.2	3.2	1.53	—	—	—
$n \rightarrow 3$	8751	12	2.8	1.5	1.22	—	—	—
	8665	13	2.0	1.1	0.98	—	—	—
H I	6563	3	390	269	257	380	294	257
$n \rightarrow 2$	4861	4	100	100	100	100	100	100
	4340	5	44	51	49.8	44.1	48.5	49.8
	4102	6	23.2	28.7	29.0	28	32.5	29.0
	3835	9	7.7	10.3	9.0	7.7	9.5	9.0
	3798	10	5.7	7.8	6.7	5.6	6.9	6.7
	3771	11	4.6	6.3	5.0	4.8	6.0	5.0
	3750	12	3.8	5.2	4.0	2.9	3.6	4.0
	3734	13	3.4	4.7	3.2	2.1	2.6	3.2
	3712	15	2.2	3.1	2.1	1.5	1.9	2.1
	3704	16	—	—	—	1.4	1.8	1.7
	3697	17	1.5	2.1	1.4	—	—	—
	3692	18	1.3	1.8	1.2	—	—	—
	3687	19	0.9	1.3	1.0	—	—	—
	3683	20	0.73	1.0	0.9	—	—	—
He I	5876	3	16	12.6	12.6	9.9	8.3	8.3
$n^3D \rightarrow 2^3P$	4471	4	4.3	5.5	5.1	2.7	2.9	3.4
	4026	5	2.8	3.6	2.6	1.7	2.0	1.7
	3820	6	1.6	2.2	1.5	—	—	—
He I	6678	3	5.9	4.0	3.7	3.3	2.5	2.4
$n^1D \rightarrow 2^1P$	4922	4	1.3	1.3	1.5	—	—	—
	4388	5	0.6	0.7	0.8	—	—	—
	4144	6	0.33	0.4	0.4	1.0	1.2	0.3
He II	4686	4	51	53	53	57	59	59
$n \rightarrow 3$	5412	7	6.0	5.2	5.2	5.4	4.9	5.8
$n \rightarrow 4$	4542	9	2.4	2.6	2.8	2.7	2.9	3.1
	4200	11	1.4	1.7	1.6	1.5	1.7	1.8
	3858	17	0.62	0.8	0.5	—	—	—

FIG. 2.— $\log (I_r/I_e)$ against $\log I_o$ for NGC 7662.
(H I: ●, He I: ×, He II: ▲.)

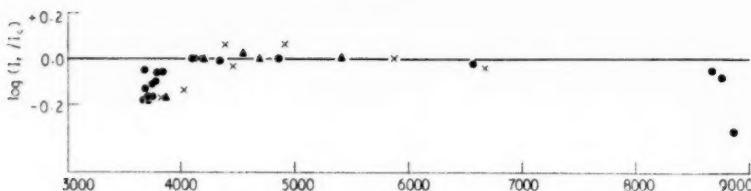


FIG. 3.— $\log (I_r/I_c)$ against λ for NGC 7662.
(H I: ●, He I: ✕, He II: ▲)

4. *Relative intensities for NGC 7027.*—We consider the intensities I_o measured by Aller, Bowen and Minkowski (2) and ignore lines for which the intensities may be uncertain due to blending or are marked as uncertain for any other reason. Table II gives the value of c obtained from the stronger Balmer lines and Table IV gives values of I_o , I_c and I_r . It is seen that there is fair agreement between I_c and I_r for the stronger lines but that the overall agreement between I_r and I_c is far from satisfactory. The general trend of the discrepancies is such that the measured intensities are too strong for small I_o and too weak in the infra-red.

We are faced with two possibilities: either (a) that the observed intensities are correct but that the recombination theory is insufficient or (b) that the discrepancies are due to errors in the observations. The first of these possibilities has been discussed, for the case of the H I and He II lines, by Aller, Bowen and Minkowski (2) and by Aller and Minkowski (14).

(a) *Collisional effects.*—If the recombination theory is suspect another method of determining reddening must be sought. Aller and Minkowski (14) considered the ratios of Paschen to Balmer intensities for lines having the same upper state, these ratios being calculated assuming the condition (1) to be satisfied. This method gives a much smaller reddening constant, $c \approx 0.6$ compared with $c = 1.22$ from the stronger Balmer lines assuming recombination theory. With $c \approx 0.6$ the corrected decrement for the stronger Balmer lines is much steeper than the recombination decrement. Aller and Minkowski suggested that this was due to collisional excitation from the ground state and showed that this requires $N_1 \sim \frac{1}{2}N_e$ where N_1 is the density of H I atoms. This very large concentration* of neutral hydrogen is difficult to reconcile with the high degree of ionization for other elements (14) and it is also difficult to see how the condition $N_1 \sim \frac{1}{2}N_e$ could be maintained; with $N_e \sim 10^4 \text{ cm}^{-3}$, linear dimensions of order $2 \times 10^{17} \text{ cm}$ and an absorption cross section of order 10^{-17} cm the optical depth would be of order 10^4 for the Lyman continuum and ionizing radiation could not penetrate. One cannot overcome these difficulties by supposing (14) T_e to be much greater than the accepted value ($\approx 1.5 \times 10^4 \text{ }^\circ\text{K}$) since this would give a Balmer discontinuity much smaller than that observed.

Whether or not one assumes some collisional excitation intensity, anomalies remain for the weak lines and for the continuum (1). It has been suggested that the anomalies for the weak lines may be due to collisional redistribution effects (1, 14). Approximate calculations by Aub and Seaton (to be published) suggest that, with $N_e \sim 10^4 \text{ cm}^{-3}$ and $T_e \sim 10^4 \text{ }^\circ\text{K}$, such effects will be important

* Due to the use of Born collision cross sections the required value of N_1 will be underestimated.

in H for $n \sim 100$. It seems very improbable that they will be important for $n \sim 15$ as required to explain the intensity anomalies. The idea of collisional redistribution may also be criticized on more empirical grounds. Such processes would tend to make the usual b_n factors (3) tend to unity, corresponding to conditions of thermodynamic equilibrium. With any reasonable b_n values for the lower levels the observed intensities for H I and He II give b_n which, for large n , are greater than unity and are increasing rapidly with n .

(b) *Possible errors in the observed intensities.*—We assume that the recombination theory gives correct relative intensities and that the measured intensities are correct for the strong lines; we then have $c = 1.22$. Assuming that there are calibration errors for the weak lines and in the infra-red we may deduce a correcting factor $\xi = (I_r/I_c)$. We consider the possibility of putting

$$\xi = \xi_1(I_o)\xi_2(\lambda). \quad (20)$$

In Fig. 4 we plot $\log(I_r/I_c)$ against $\log I_o$ for all lines of Table IV having $\lambda < 8000$ (that is, we exclude the Paschen lines and He II $\lambda 8237$). For $I_o \leq 5$ we see that, as I_o decreases, (I_r/I_c) decreases systematically and shows an increasing amount of scatter. The fact that similar results are obtained from the various series of H I, He I and He II would be expected if calibration errors depend systematically on I_o but would not be expected if the anomalies were due to the recombination theory being inapplicable. We take it that the dashed curve of Fig. 4 gives us the function $\log \xi_1(I_o)$. Intensities corrected for systematic errors which depend only on I_o will then be given by $\xi_1(I_o)I_c$.

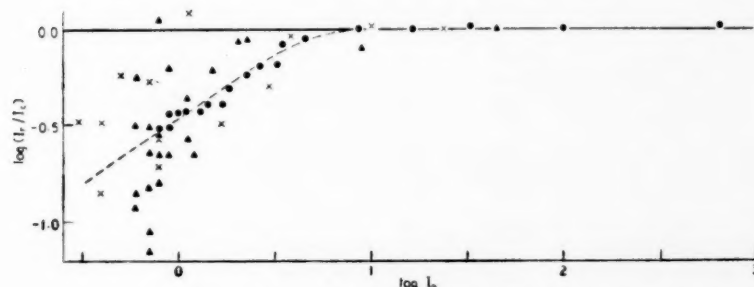


FIG. 4.— $\log(I_r/I_c)$ against $\log I_o$ for NGC 7027
(H I: ●, He I: ✕, He II: ▲.)

To examine the position in the infra-red, in Fig. 5 we plot $\log(I_r/\xi_1 I_c)$ against λ . To reduce scatter we exclude the weakest lines ($I_o < 1.5$). We include points obtained from continuum intensities. In the spectral region of Fig. 5 a good first approximation is to take the continuum intensities I_r , per unit frequency, proportional to $\exp(-hv/kT_e)$. We use the Mt Wilson continuum intensities of Minkowski and Aller (1). The intensities measured per unit wavelength are converted to intensities per unit frequency and corrected for reddening with $c = 1.22$. For the continuum we take $\xi_1(I_o) = 1$ and take $(I_r/I_c) = 1$ in the 5000 Å region.

TABLE IV

Intensities for NGC 7027

Series	λ	n	I_o	I_e	I_r
H I $n \rightarrow 3$	9015	10	5.5	0.94	2.04
	8863	11	3.5	0.62	1.53
	8750	12	3.1	0.55	1.22
	8665	13	2.7	0.49	0.98
H I $n \rightarrow 2$	6563	3	659	242	257
	4861	4	100	100	100
	4340	5	33	48	49.8
	4102	6	16.3	29.0	29.0
	3889	8	8.8	18.5	18.5
	3835	9	4.6	10.1	9.0
	3798	10	3.5	7.9	6.7
	3771	11	3.3	7.6	5.0
	3750	12	2.7	6.3	4.0
	3734	13	2.3	5.5	3.2
	3712	15	1.8	4.3	2.1
	3704	16	1.7	4.1	1.7
	3697	17	1.4	3.4	1.4
	3692	18	1.3	3.2	1.2
	3687	19	1.1	2.7	1.0
	3683	20	1.0	2.5	0.9
	3679	21	0.9	2.2	0.8
	3676	22	0.9	2.2	0.7
	3674	23	0.8	2.0	0.6
He I $n^3D \rightarrow 2^3P$	5876	3	24	12.7	12.7
	4472	4	3.9	5.2	5.1
	3820	6	1.1	2.4	1.5
	3705	7	0.7	1.7	0.9
	3634	8	0.8	2.0	0.6
	3587	9	0.8	2.1	0.4
	3554	10	0.3	0.8	0.3
He I $n^1D \rightarrow 2^1P$	6678	3	10	3.5	3.7
	4922	4	3.1	3.0	1.6
	4388	5	1.7	2.4	0.8
	4144	6	0.5	0.9	0.4
	4009	7	0.4	0.8	0.3
	3927	8	0.4	0.8	0.2
He II $n \rightarrow 5$	8237	9	5.2	1.05	1.31
	6891	12	2.1	0.72	0.63
	6407	15	0.8	0.32	0.35
	6234	17	0.9	0.40	0.25
	6171	18	1.1	0.50	0.22
	6037	21	1.1	0.53	0.14
	6005	22	1.2	0.59	0.13
	5977	23	0.7	0.35	0.11
	5953	24	0.9	0.45	0.10
	5932	25	0.8	0.41	0.09

TABLE IV—(continued)

Intensities for NGC 7027

Series	λ	n	I_o	I_e	I_r
He II	4686	4	45	50	50
$n \rightarrow 3$					
He II	5412	7	9	6.2	4.9
$n \rightarrow 4$	4542	9	2.3	2.9	2.6
	4200	11	1.5	2.5	1.5
	3924	15	0.6	1.2	0.68
	3858	17	0.8	1.7	0.49
	3834	18	0.6	1.3	0.42
	3814	19	0.7	1.6	0.36
	3782	21	0.8	1.8	0.28
	3769	22	0.7	1.6	0.24
	3749	24	0.6	1.4	0.19
	3740	25	0.6	1.4	0.17
	3733	26	0.7	1.7	0.16
	3715	29	0.7	1.7	0.12

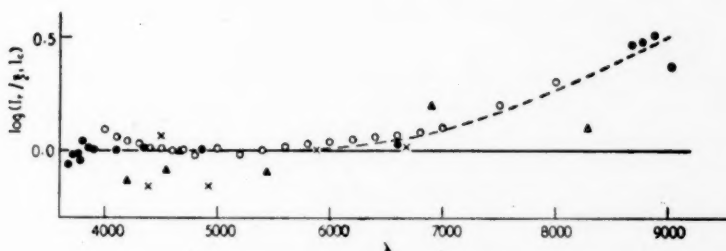


FIG. 5.— $\log (I_r/\xi_1 I_e)$ against λ for NGC 7027
(H I: ●, He I: ×, He II: ▲, continuum: ○).

Fig. 5 suggests that, for $\lambda > 6000 \text{ \AA}$, all measured intensities are underestimated by a factor which decreases with increasing λ . We take it that the dashed curve of Fig. 5 gives us the function $\log \xi_2(\lambda)$. Aller and Minkowski (14) consider it possible that the Paschen intensities may have been underestimated due to the continuum having been drawn too high; we consider it more probable that all intensities have been underestimated in the infra-red.

(c) *Further discussion of the continuum intensities.*—In Fig. 6 logarithms of continuum intensities, per unit frequency, are plotted against $\sigma = 10^4/\lambda$. The full line curve is calculated (13) allowing for: H I and He II recombination and free-free continua using asymptotic expansions for the Gaunt factors; the He I recombination and free-free continuum, assumed hydrogenic; the H I two-quantum continuum. The calculations are made for $T_e = 1.7 \times 10^4 \text{ }^\circ\text{K}$ and $N_e = 2.2 \times 10^4 \text{ cm}^{-3}$, which are the best estimates obtained (13) from forbidden line data and H β brightness. The intensities measured by Minkowski and Aller (1) are corrected for reddening with $c = 1.22$ and, in the infra-red, multiplied

by the correction factor $\xi_2(\lambda)$ of Fig. 5. The measurements are in arbitrary units and we therefore have one adjustable scale parameter when comparing theory and observation. Fig. 6 shows that this may be chosen so as to obtain very good agreement both for long wave-lengths and for the short wave side of the Balmer limit but that the measured intensities then show a depression to the long wave side of the Balmer limit. Referring to Table IV we see that it is in this region to the long wave side of the Balmer limit that there are the

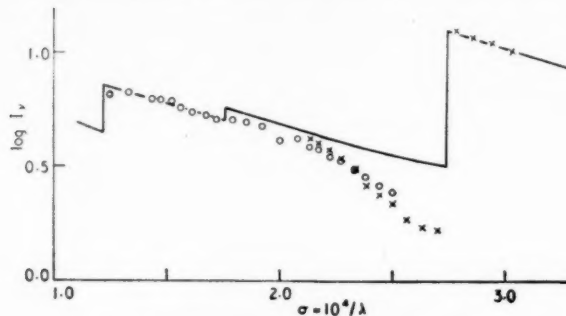


FIG. 6.—Continuum intensities for NGC 7027.
(Mount Wilson observations \circ , McDonald observations \times).

biggest discrepancies between I_e and I , for the very weak lines, particularly those of He II. We suggest that, from about 4500 Å to the Balmer limit at 3647 Å, the continuum may have been drawn too low and that in consequence the intensities of very weak lines may have been overestimated.

(d) *Conclusions on NGC 7027.*—The intensity list of Aller, Bowen and Minkowski (2) for NGC 7027 contains many weak lines which have not been measured in other nebulae. NGC 7027 is therefore of particular interest for theoretical work such as that involved in the determination of chemical compositions but in such work one cannot simply ignore the intensity anomalies for the weak lines of H I, He I and He II. We cannot find any satisfactory explanation of these anomalies in terms of physical processes in the nebula but we have been able to show that the general trend is consistent with the suggestion of calibration errors depending on the observed quantities I_e and λ . If this suggestion is correct the true relative emission intensities are given approximately by ξI_e where $\xi = \xi_1(I_e) \xi_2(\lambda)$.

This whole question can, of course, be settled only by further observational work.

5. *Helium abundances.*—The condition (15) is satisfied for the three nebulae considered and we may therefore neglect He⁰ in determining He/H abundance ratios. Results are given in Table V.

TABLE V
Helium abundances

NGC	$\frac{N(\text{He}^{+2})}{N(\text{H}^+)}$	$\frac{N(\text{He}^+)}{N(\text{H}^+)}$	$\frac{N(\text{He})}{N(\text{H})}$
7662	0.071	0.126	0.197
2392	0.079	0.083	0.162
7027	0.067	0.127	0.194

6. *Acknowledgments.*—I would like to thank Dr L. H. Aller and Dr R. Minkowski for discussions of the work of the present paper.

Department of Physics,
University College London:
1959 September.

References

- (1) R. Minkowski and L. H. Aller, *Ap. J.*, **124**, 93, 1956.
- (2) L. H. Aller, I. S. Bowen and R. Minkowski, *Ap. J.*, **122**, 62, 1955.
- (3) J. G. Baker and D. H. Menzel, *Ap. J.*, **88**, 52, 1938.
- (4) A. Burgess, *M.N.*, **118**, 477, 1958.
- (5) L. Searle, *Ap. J.*, **128**, 489, 1958.
- (6) M. J. Seaton, *M.N.*, **119**, 90, 1959.
- (7) M. J. Seaton, *M.N.*, **119**, 81, 1959.
- (8) L. H. Aller and D. H. Menzel, *Ap. J.*, **102**, 239, 1945.
- (9) L. Goldberg, *Ap. J.*, **93**, 244, 1941.
- (10) K. Wurm, *Mém. Soc. Roy. Sci. Liège*, **14**, 387, 1954.
- (11) J. S. Mathis, *Ap. J.*, **125**, 318 and 328 and **126**, 493, 1957.
- (12) K. Wurm and O. Singer, *Z. Astrophys.*, **30**, 387, 1952.
- (13) M. J. Seaton, *Rep. Progr. Phys.*, **23**, 313, 1960.
- (14) L. H. Aller and R. Minkowski, *Ap. J.*, **124**, 110, 1956.

RADIO-SOURCE PROBLEMS

F. Hoyle

(Received 1959 July 29)

Summary

The present paper is based on the theory first proposed by Ginzburg and Shklovsky that all non-thermal, non-stellar, cosmic radio emission arises from synchrotron radiation by electrons. The electrons will be regarded as secondaries from nuclear collisions of cosmic rays with ambient gas. Evidence for this point of view can be adduced from the observed radio frequency spectra. The consequences of cosmic rays existing (i) in galaxies, (ii) in clusters of galaxies, (iii) in space generally, are examined, on the assumption that the cosmic-ray energy density is always $\sim 1 \text{ eV cm}^{-3}$.

Apart from the introduction, the paper is divided into three parts :

- I. Weak emission from galaxies, clusters, and intergalactic space.
- II. Strong emission from extragalactic sources.
- III. Strong emission from galactic sources.

Halo emission from spiral galaxies—from M31 and the Galaxy in particular—is considered in I. The cases of Cygnus A and NGC 1275 are investigated in II—a new class of optically non-visible source being also proposed in this part. The cases of the Crab Nebula, Cassiopeia A, and IC 443 are discussed in III.

So far as strong sources are concerned, the argument depends in an important way on the conditions that develop at the shock front of a cloud expanding at great speed into an ambient medium. The present situation differs in a curious way from ordinary gas dynamics, in that the momentum and energy terms of the Rankine-Hugoniot relations are carried by quite different components of the assembly—the momentum by the material of the gas cloud and the ambient medium, and the energy by a reservoir of relativistic particles and by a magnetic field. To overcome the difficulty that the detailed physical processes that take place within the shock front itself are not well understood, a rule is proposed that receives strong empirical support from a wide range of observed phenomena, including such diverse cases as the radio emission of Cygnus A and the optical emission of the Crab Nebula.

When the magnetic field dominates in the energy terms, the rule yields results that differ markedly from those given by the de Hoffman-Teller equations. The field does not preserve a uniform structure at the front, as in the de Hoffman-Teller case, but develops a highly wrapped, contorted structure—such as is suggested by the observed optical filaments of Cassiopeia A.

If the rule were also applicable to cases where the energy and momentum were carried by different components, the momentum by a comparatively high-density, low-temperature gas and the energy by a low-density, high-temperature non-relativistic gas (the gas considered in the present paper is relativistic) a new process would be available for producing very high temperatures.

Introduction.—The total energy e of an electron or positron may be written

$$e = \gamma mc^2, \quad \gamma = (1 - v^2/c^2)^{-1/2}, \quad (1)$$

where m is the mass and v the velocity of the electron, and c is the velocity of light. If H_\perp is the magnitude of the component of the magnetic field perpendicular to v ,

then for a highly relativistic positron or electron ($\gamma \gg 1$) the rate of energy loss $P(\gamma)$ through synchrotron radiation is given by (1)

$$P(\gamma) = 1.58 \times 10^{-15} H_{\perp}^2 \gamma^2 \text{ erg sec}^{-1}, \quad (2)$$

where H_{\perp} is in gauss. The energy is always radiated in a spectrum of the same form, provided a scale factor proportional to $H_{\perp} \gamma^2$ is used in the frequency unit.

In the following work, electron distributions of the form $d\gamma/\gamma^r$ often arise. For such distributions the radio emission can be estimated to a satisfactory accuracy by calculating as if each electron emitted the whole of its radiation at a single frequency ν given by

$$\nu = 4.19 \times 10^6 H_{\perp} \gamma^2 \text{ c/s.} \quad (3)$$

This simple procedure is particularly accurate when the exponent r is close to 3, as it will be in many of the cases examined below.

It may be noted that for an electron distribution confined within a range $\gamma_1 < \gamma < \gamma_2$ this method of calculation becomes inaccurate near its end points; i.e. for $\nu < \sim 2\nu_1$ or $\nu > \sim 0.5\nu_2$, where ν_1, ν_2 are given by substituting γ_1, γ_2 in (3). Likewise the method is inaccurate near the join of two distributions $d\gamma/\gamma^r, \gamma < \gamma_3$; $d\gamma/\gamma^s, \gamma \geq \gamma_3$; i.e. for $\nu < \sim 2\nu_3$ or $\nu > \sim 0.5\nu_3$, where ν_3 is given by substituting γ_3 in (3).

The present point of view is that all non-thermal, non-stellar, radio emission arises from synchrotron radiation by electrons produced in the nuclear collisions of cosmic rays with ambient gas (2). For simplicity, both the cosmic rays and the ambient nuclei will be taken to be protons. The number of cosmic rays per unit volume $Q(E)$ with kinetic energies between E and $E+dE$ is given by

$$Q(E) dE \approx 5 \times 10^{-10} \frac{dE}{(1+E)^{5/2}}, \quad (4)$$

where E is in BeV. Experimental evidence (3) suggests that (4) remains valid down to about 0.5 BeV. The mean kinetic energy over the whole distribution is easily shown to be ~ 3.5 BeV. At very high energies, $E > 10^6$ BeV, a distribution somewhat steeper than (4) must be used. There will be no occasion in the following work, however, to consider electrons derived from such very energetic protons.

The multiplicity s of electrons and positrons appearing in a nuclear collision is somewhat uncertain, but theory and observation seem to be tolerably well represented by

$$s \approx 2E^{1/4}. \quad (5)$$

The total energy of the electron-positron secondaries may be taken as a constant fraction ~ 0.1 of the proton kinetic energy (cf. 4), so that

$$s \approx 10^2 E^{3/4}, \quad (6)$$

with E in BeV

The probability of a nuclear collision of a cosmic ray per unit time $\sim cN\sigma(E)$, where N is the number density of hydrogen atoms in the ambient medium and $\sigma(E)$ is the collision cross-section. In the following, a further simplification will be effected by taking σ to be $2 \times 10^{-26} \text{ cm}^{-2}$ independent of E (5). (A slight error at this stage would influence later work by distorting the calculated radio spectra in some small degree.)

The probability of a collision is thus $6 \times 10^{-16} N \text{ sec}^{-1}$. With $N \sim 10^{-5}$ atom cm^{-3} in intergalactic space, the probability of collision is very small over the

cosmological time scale $\sim 10^{17}$ sec. This is even true for heavy nuclei among the cosmic rays. Within the Galaxy and its halo, where N probably averages about 10^{-2} atom cm^{-3} , the chance that a proton will survive for a time $\sim 10^{17}$ sec is still appreciable.

The rate at which electrons and positrons are produced by cosmic rays between E and $E+dE$ is

$$6 \times 10^{-16} s N Q(E) dE \quad \text{cm}^{-3} \text{sec}^{-1},$$

a factor s being introduced to take account of the multiplicity. Substituting for $Q(E)$ and s from (4), (5), and expressing E, dE in terms of $\gamma, d\gamma$ with the aid of (6), the electron-positron production rate per cm^3 becomes

$$\sim 1.5 \times 10^{-21} N \frac{\gamma^{-8/3} d\gamma}{[1 + (10^2/\gamma)^{4/3}]^{5/2}}. \quad (7)$$

Since we shall not normally be concerned with values of γ as low as 10^2 , it will usually be sufficient to approximate (7) by

$$\sim 1.5 \times 10^{-21} N d\gamma / \gamma^{8/3}. \quad (8)$$

For any electron energy it is possible to define a radiation time scale t_r by

$$t_r P(\gamma) = \gamma m c^2. \quad (9)$$

Evidently t_r is the order of the time required for synchrotron radiation to produce an appreciable degradation in the electron energy. Using (2) for $P(\gamma)$, and writing the total magnetic intensity H in place of H_\perp (this will not affect order of magnitude estimates), the condition (9) for t_r is readily found to be

$$t_r \approx 5 \times 10^8 \gamma^{-1} H^{-2} \text{sec}. \quad (10)$$

Eliminating γ between (3), (10) gives

$$t_r \approx 10^{12} \nu^{-1/2} H^{-3/2} \text{sec}, \quad (11)$$

H_\perp being also written as H in (3).

PART I

WEAK EMISSION FROM GALAXIES, CLUSTERS, AND INTERGALACTIC SPACE

1. *The radio emission of the Galaxy.*—The following considerations support the somewhat startling conclusion that the majority of cosmic ray protons have traversed 30 grams or more of hydrogen. The implication of this conclusion in its relation to the cosmic ray abundances of lithium, beryllium, and boron is discussed in a separate paper.

Throughout the following work it will be assumed that secondary electrons and positrons do not escape from the Galaxy, and that secondaries produced in the disk of the Galaxy can pass freely into the halo.

It is reasonable to take the halo as a spheroidal region with polar diameter ~ 30 kpc and equatorial diameter ~ 50 kpc, the volume being $\sim 10^{69} \text{cm}^3$. The present day total mass of neutral atomic hydrogen lying in the disk of the Galaxy $\sim 1.5 \times 10^9 \odot \approx 3 \times 10^{42} \text{gm}$. Such a mass distributed uniformly throughout the halo would yield a mean density of $\sim 3 \times 10^{-27} \text{gm cm}^{-3}$. Assuming the cosmic ray protons to move freely to and fro between the disk of the Galaxy and the halo, this gives a lower limit to the mean density of the matter through which the protons

move; for it ignores both the contribution of molecular hydrogen in the disk and the contribution of ionized hydrogen in the halo. These might well double the mean density. Moreover in the past the total mass of gas in the Galaxy must almost certainly have been greater than the present day value, so that any calculation made over a time interval $\sim 10^{17}$ sec must take account of the higher density that presumably was operative in the past. All in all, a mean density $\sim 10^{-26}$ gm cm $^{-3}$ is as good an estimate as it seems possible to make, averaging being both spatial and temporal. That is to say, the mean density N of the ambient medium should be set at $\sim 10^{-2}$ atom cm $^{-3}$ in applying (8) to the case of the Galaxy.

A relativistic proton travels $\sim 3 \times 10^{27}$ cm in time $\sim 10^{17}$ sec. At a mean density $\sim 10^{-26}$ gm cm $^{-3}$ it therefore moves through ~ 30 gm of material. Remembering that the cross-section for a nuclear collision $\sim 2 \times 10^{-26}$ cm $^{-2}$, it is clear that an appreciable fraction of the cosmic ray protons within the Galaxy have experienced such a collision.

To obtain the secondary electron distribution, consider three time scales t_c, t_r, t_a , where $t_c \sim 10^{17}$ sec is a cosmological time scale of the order of (but less than) the age of the Galaxy, t_r is the synchrotron life-time given by (10), and t_a is the lifetime of an electron against serious energy loss by atomic collisions. The latter time scale is given by (6)

$$t_a \approx 2 \times 10^{12} \gamma N^{-1} \text{ sec.} \quad (12)$$

Then the electron distribution is determined to a satisfactory approximation by multiplying (8) by $\min(t_c, t_r, t_a)$,

$$\sim 1.5 \times 10^{-21} N \frac{d\gamma}{\gamma^{8/3}} \min(10^{17}, 2 \times 10^{12} \gamma N^{-1}, 5 \times 10^8 H^{-2} \gamma^{-1}). \quad (13)$$

This simple procedure ignores the detailed effects of energy degradation. As an electron loses energy, either by atomic collisions or by synchrotron radiation, it augments the distribution at a lower value of γ . This augmentation is not important, however, because of the steep dependence of the $d\gamma/\gamma^{8/3}$ factor in (8). This steep dependence means that the electron distribution cannot be appreciably changed by electrons falling from higher values of γ .

With $N = 10^{-2}$ atom cm $^{-3}$, $H = 10^{-6}$ gauss, the distribution is

$$\sim 3 \times 10^{-9} \gamma^{-5/3} d\gamma, \quad 10^2 < \gamma < 5 \times 10^2, \quad (14)$$

$$\sim 1.5 \times 10^{-6} \gamma^{-8/3} d\gamma, \quad 5 \times 10^2 < \gamma < 5 \times 10^3, \quad (15)$$

$$\sim 7.5 \times 10^{-3} \gamma^{-11/3} d\gamma, \quad \gamma \geq 5 \times 10^3. \quad (16)$$

The main contribution to the total electron energy density comes from (14) and (15), and amounts to $\sim 10^{-13}$ erg cm $^{-3}$. This is about 0.1 of the energy of the protons, reflecting the fraction of the proton energy that passes into electron secondaries in a nuclear collision.

According to (16), the total number of electrons with energies > 5 BeV is $\sim 6 \times 10^{-14}$ cm $^{-3}$. The corresponding value for protons $\sim 2 \times 10^{-11}$ cm $^{-3}$ showing an electron concentration of about 1/3 per cent of the protons. At lower energies the proportion of electrons increases, rising to about 5 per cent at a kinetic energy of 0.5 BeV.

With $H = 10^{-6}$ gauss, and $\nu > 10^7$ c/s, (14) is not required, since the γ values appropriate to such frequencies lie appreciably above 500. The emissivity is

given by multiplying by $P(\gamma)$ and by replacing $\gamma, d\gamma$ by $\nu, d\nu$. Thus (15) gives

$$\sim 10^{-33} \frac{d\nu}{\nu^{5/6}} \text{ erg cm}^{-3} \text{ sec}^{-1}, \quad \nu < 10^8 \text{ c/s}, \quad (17)$$

and (16) gives

$$\sim 10^{-29} \frac{d\nu}{\nu^{4/3}} \text{ erg cm}^{-3} \text{ sec}^{-1}, \quad \nu \geq 10^8 \text{ c/s}. \quad (18)$$

The discontinuity of slope of the emissivity at the join of (17), (18) evidently arises from the method of calculation, which becomes inaccurate at the join of the distributions (15), (16). An accurate procedure would obviously give a smooth transition from the slope 5/6 to the slope 4/3.

Measures by Baldwin (7) at $\nu = 8 \times 10^7 \text{ c/s}$ indicate an emissivity of 1.8×10^8 watts per pc^3 per steradian per cycle per sec—i.e. $7.7 \times 10^{-40} \text{ erg cm}^{-3} \text{ sec}^{-1} (\text{c/s})^{-1}$. At $\nu = 8 \times 10^7 \text{ c/s}$ (17) gives $\sim 2.6 \times 10^{-40} \text{ erg cm}^{-3} \text{ sec}^{-1} (\text{c/s})^{-1}$. The agreement is even better than this comparison would suggest, for Baldwin's value was derived on the assumption of a halo volume smaller than that used above by a factor ~ 5 . The discrepancy largely vanishes when an adjustment is made for this difference.

2. *The steady radio emission from galaxies in general.*—The radio emissivity might be considered to vary from galaxy to galaxy because H, N vary, or because secondary electrons might not be wholly trapped.

To examine the effect of changing the magnetic intensity, consider a corresponding calculation, first for the case

$$H = 10^{-13/2} \text{ gauss}, \quad N = 10^{-2} \text{ atom cm}^{-3}.$$

In place of (15), (16) we have,

$$\sim 1.5 \times 10^{-6} d\gamma/\gamma^{8/3}, \quad 5 \times 10^2 < \gamma < 5 \times 10^4, \quad (19)$$

$$\sim 7.5 \times 10^{-2} d\gamma/\gamma^{11/3}, \quad \gamma \geq 5 \times 10^4. \quad (20)$$

And in place of (17), (18) we now have

$$\sim 10^{-34} \frac{d\nu}{\nu^{5/6}}, \quad \nu < 3 \times 10^9 \text{ c/s}, \quad (21)$$

$$\sim 5 \times 10^{-30} \frac{d\nu}{\nu^{4/3}}, \quad \nu \geq 3 \times 10^9 \text{ c/s}, \quad (22)$$

for the emissivity in $\text{erg cm}^{-3} \text{ sec}^{-1}$.

The effect of decreasing the magnetic intensity is thus to flatten the spectrum in the range $10^8 - 3 \times 10^9 \text{ c/s}$, and to decrease the emissivity, particularly for $\nu \sim 10^8 \text{ c/s}$ where the reduction is by a factor of about 10. The reduction is less at higher frequencies. It is of interest that the emissivity at $\nu = 8 \times 10^7 \text{ c/s}$ is about $3 \times 10^{-41} \text{ erg cm}^{-3} \text{ sec}^{-1} (\text{c/s})^{-1}$, in reasonable agreement with the value $\sim 10^{-40} \text{ erg cm}^{-3} \text{ sec}^{-1} (\text{c/s})^{-1}$ given by Baldwin (7) for the Andromeda Nebula. The observed spectrum of M31 is in tolerable agreement with (21), but appears somewhat less steep—the observations are rather fragmentary, however.

A stronger magnetic intensity increases the emissivity, and for frequencies less than $\sim 10^8 \text{ c/s}$ steepens the spectrum. Thus it can readily be shown that for

$H = 10^{-11/2}$ gauss, $N = 10^{-2}$ atom cm^{-3} , the emissivity is given by

$$\sim 1.5 \times 10^{-29} \frac{dv}{v^{4/3}} \text{ erg cm}^{-3} \text{ sec}^{-1} \quad (23)$$

at all $v > 10^7$ c/s. The emissivity at $v = 8 \times 10^7$ c/s in this case is $\sim 5 \times 10^{-40}$ erg cm^{-3} sec^{-1} (c/s) $^{-1}$.

The total emissivity taken over the frequency range $10^7 \leq v \leq 10^9$ is readily found to be $\sim 1.5 \times 10^{-31}$ erg cm^{-3} sec^{-1} at $H = 10^{-11/2}$ gauss, $\sim 8 \times 10^{-32}$ at $H = 10^{-6}$ gauss, and $\sim 10^{-32}$ at $H = 10^{-13/2}$ gauss. For a halo volume of 10^{69} cm^3 the total emission of a whole galaxy would thus fluctuate from $\sim 10^{37}$ erg sec^{-1} to $\sim 10^{38}$ erg sec^{-1} .

On the basis of these results it seems that the emissivity per unit volume should be about ten times greater in the disk of the Galaxy than it is in the halo. Indeed (23) should be applicable to the disk. Because of the much smaller volume of the disk, 10^{67} cm^3 , it is clear that the major contribution to the total emission must come from the halo, however—the disk should contribute only some 10 per cent of the total.

The next step is to examine the effect of reducing the amount of gas contained within a galaxy. In elliptical galaxies, for example, the value of N might well be as small as 10^{-4} atom cm^{-3} . Consider the case

$$H = 10^{-6} \text{ gauss}, \quad N = 10^{-4} \text{ atom cm}^{-3}.$$

The electron distribution again follows from (13),

$$\sim 1.5 \times 10^{-8} \frac{dy}{y^{8/3}}, \quad 10^2 < y < 5 \times 10^3, \quad (24)$$

$$\sim 7.5 \times 10^{-5} \frac{dy}{y^{11/3}}, \quad y \geq 5 \times 10^3. \quad (25)$$

The emissivity is

$$\sim 10^{-35} \frac{dv}{v^{5/6}}, \quad v < 10^8 \text{ c/s}, \quad (26)$$

$$\sim 10^{-31} \frac{dv}{v^{4/3}}, \quad v \geq 10^8 \text{ c/s}, \quad (27)$$

the distribution being essentially the same as in (17), (18), except that the coefficients are reduced by 10^2 because of the reduction in N . Thus the emissivity of a galaxy is reduced to the extent that the amount of gas within it is reduced.

Two important conclusions follow :

The steady emission from normal elliptical galaxies is very low because such galaxies contain comparatively little gas, and hence the ambient medium is ineffective in exposing the cosmic rays to nuclear collisions.

The argument often used to overcome the lithium, beryllium, and boron paradox—that cosmic ray protons in the Galaxy have traversed only three or four grams of matter—cannot be supported (8). If this were so N would need to be $\sim 10^{-3}$ atom cm^{-3} , and at this value there would be a tenfold discrepancy between the observed radio emission of the Galaxy and its calculated value.

A further reason why galaxies may differ one from another was mentioned above—secondary electrons may not be trapped or may be only partially trapped. In such cases the radio emission will be reduced to the extent that secondaries escape from the system. It is possible that the comparatively low radio emission of the Magellanic Clouds is to be explained in this way.

3. *The correlation between photographic and radio magnitudes.*—A correlation $m_r - m_p = \text{constant}$, between the apparent radio magnitude m_r and the apparent photographic magnitude m_p has been obtained for Sb galaxies and for Sc galaxies by Brown and Hazard (9, 10) and by Mills (11). It is possible that this result can be explained in a simple way.

The major class of galaxy (masses $\sim 10^{11} \odot$) all seem to be of about the same optical size (this statement is valid for ellipticals, although this fact will not be used here). Hence the halo systems may be expected to be of much the same size. The other factors promoting radio-emission—the magnetic intensity, the mean density N —may well also be fairly constant from one galaxy to another. That is to say, the absolute radio magnitudes of the galaxies probably have fairly small dispersion among themselves. Since the absolute photographic magnitudes also have small dispersion it follows immediately that variability in apparent magnitudes—radio or photographic—arises essentially only from variability in distance. This variability obviously is removed when the difference $m_r - m_p$ is taken.

4. *The general emissivity within clusters of galaxies.*—The emissivity within clusters of galaxies will be calculated on the assumptions

- (i) that the cosmic-ray spectrum is given by (4) throughout a cluster,
- (ii) that the ambient gas density $\sim 3 \times 10^{-27} \text{ gm cm}^{-3}$, i.e. $N \approx 1.8 \times 10^{-3} \text{ atom cm}^{-3}$,
- (iii) that the magnetic intensity $\sim 3 \times 10^{-7} \text{ gauss}$,
- (iv) that secondary electrons remain trapped over a time scale $\sim 10^{17} \text{ sec}$.

All these assumptions tend to promote a high emissivity, so that the value calculated below is in the nature of an upper limit.

With $N \approx 1.8 \times 10^{-3} \text{ atom cm}^{-3}$, $H \approx 3 \times 10^{-7} \text{ gauss}$, $t \approx 10^{17} \text{ sec}$, the electron distribution given by (13) is

$$\begin{aligned} &\sim 2.7 \times 10^{-7} d\gamma/\gamma^{8/3}, & 10^2 < \gamma < 5.5 \times 10^4 \\ &\sim 1.5 \times 10^{-2} d\gamma/\gamma^{11/3}, & \gamma \geq 5.5 \times 10^4. \end{aligned} \quad (28)$$

The emissivity is given once again by multiplying (28) by $P(\gamma)$ and by replacing γ , $d\gamma$ by ν , $d\nu$ with the aid of (3). For $H \approx 3 \times 10^{-7} \text{ gauss}$, the result for $5 \times 10^9 > \nu > 10^7 \text{ c/s}$ is

$$\sim 2 \times 10^{-35} \frac{d\nu}{\nu^{5/6}} \text{ erg cm}^{-3} \text{ sec}^{-1}, \quad (29)$$

which is less, at $\nu = 10^8 \text{ c/s}$, than the emissivity in halo of the Galaxy or in M31 by a factor of $\sim 10^2$.

5. *The radio emission by the universe as a whole.*—The present calculation will be based on the extreme assumption that cosmic rays with energy density $\sim 1 \text{ eV cm}^{-3}$ exist everywhere throughout space. It will be shown that the magnetic intensity in space must then be less than 10^{-7} gauss in order that there shall be no conflict with observations.

For convenience, $H < 10^{-7} \text{ gauss}$ will be assumed at the outset. Because the observed radio band is confined to $\nu > 10^7 \text{ c/s}$ it follows immediately from (3) that we are concerned only with values of γ greater than $\sim 5 \times 10^3$. Reference to (11) also shows that t_r is greater than the cosmological time scale, $\sim 10^{17} \text{ sec}$, for all ν up to $\sim 10^{11} \text{ c/s}$. Hence for electrons yielding synchrotron radiation within the normal radio band there is no appreciable degradation of energy, even over the full cosmological time scale, t_c say.

The spatial density of electrons and positrons therefore builds up over time t_e , and is given simply by multiplying (8) by t_e ,

$$\sim 1.5 \times 10^{-21} N t_e d\gamma / \gamma^{5/3} \text{ cm}^{-3}. \quad (30)$$

Build up is of course limited to the time scale t_e , since the expansion of the universe prevents any continued accumulation of the electron-positron reservoir on a time scale longer than this. The general emissivity of space is now obtained by multiplying (30) by $P(\gamma)$, and by replacing γ and $d\gamma$ by ν , $d\nu$ from (3), viz.

$$\sim 10^{-37} t_e N H^{11/6} \frac{d\nu}{\nu^{5/6}} \text{ erg cm}^{-3} \text{ sec}^{-1}. \quad (31)$$

Now the general emission in space is only lost through the expansion of the universe. The radio energy density therefore also builds up for a time t_e . Thus to obtain the energy density, (31) must be multiplied again by t_e . With $t_e \sim 10^{17}$ sec, $N \sim 10^{-5}$ atom cm^{-3} , the energy density is therefore

$$\sim 10^{-8} H^{11/6} \frac{d\nu}{\nu^{5/6}} \text{ erg cm}^{-3}.$$

By equating this expression to the Planck distribution

$$8\pi\nu^2 c^{-3} k T d\nu, \quad h\nu \ll kT,$$

an effective temperature $T(\nu)$ can be defined as a function of the frequency. The observed condition that T does not exceed ~ 300 deg. K at $\nu = 10^8$ c/s requires H to be not greater than $\sim 10^{-7}$ gauss, as stated at the outset.

PART II

STRONG SOURCES OF EXTRAGALACTIC ORIGIN.

1. *Preliminary remarks.*—It is known, or suspected, that in all intense sources of radio waves considerable masses of gas are in rapid dynamical motion. In a series of papers Burbidge has demonstrated a remarkable result (12, 13, 14). Even setting the dynamical energy very high, the energy that must be present as cosmic ray protons is at least as great as the dynamical energy—if secondary electrons are to be produced in situ at a rate adequate to explain the observed radio emission.

For the Cygnus A source, Burbidge finds the necessary proton energy to be $\sim 10^{61}$ erg. For the dynamical energy to be as great as this, say for a motion of 1000 km sec^{-1} , the mass of moving gas would have to be $\sim 10^{12} \odot$. An even more extreme situation seems to exist in the Crab Nebula. The mass of gas in this case can hardly be much greater than the Sun, and the speed of motion is known to be $\sim 1000 \text{ km sec}^{-1}$. The dynamical energy cannot therefore be much in excess of $10^{49} \text{ erg sec}^{-1}$. Yet Burbidge (4) finds the necessary proton energy to be appreciably greater than 10^{50} ergs.

Attempts have been made to argue that in some, if not all, of these intense sources the electrons might be primary. Because no proton concentration would then be necessary the energy requirement could be reduced by a factor $\sim 10^2$, thereby bringing the energy of the reservoir of relativistic particles down to a more plausible level. But this is a council of desperation. Except perhaps in the case of the Crab, the frequency spectra of the intense sources are of just the form to be expected from electrons that are secondary to the normal cosmic ray distributions. To throw away this most striking agreement is to lose the one solid foundation on which a theory of the radio emission should be built.

If the cosmic ray protons are produced *in situ*, the difficulty is to understand how the dynamical energy of mass motion of the gas comes to be converted quickly into relativistic protons with almost 100 per cent efficiency. The problem is made worse by the requirements that must be placed on the magnetic field. To keep the total proton energy at all within bounds it is necessary that the proton energy and the magnetic energy shall be comparable. This implies a field of $10^{-4} - 10^{-5}$ gauss throughout the large extended Cygnus A source and a field of $10^{-2} - 10^{-3}$ gauss in the Crab Nebula. These values are very much above normal, so that the dynamical motion must not only generate cosmic ray pistons with great efficiency but must also be capable of building magnetic fields of large intensity. No such wonder-process is known. The very nature of the gas motion—radial expansion in the case of the Crab Nebula and probably also in the other intense sources—would seem to preclude the building of a magnetic field by turbulence. Polarization measures (15) of the Crab Nebula show indeed that the magnetic field does not possess the detailed, irregular structure that it would have to possess if the lines of force had been lengthened by turbulence.

The attempt by Burbridge (4) to evade these difficulties in the case of the Crab Nebula by supposing that the proton distribution is not derived directly from the gas at all, but was supplied by the initial explosion that gave rise to the expanding gas, fails for two reasons: first, the high magnetic intensity remains unexplained; second, the proton energies would long ago have been degraded. (If there was no gas to hold them back, the protons would stream rapidly into space without loss of energy. But with gas to hold them back, through the agency of a magnetic field, the protons simply lose energy through mechanical work done on the expanding gas.)

The only possible escape from the dilemma along these lines would be to suppose that the relativistic protons are produced *currently* by a supernova remnant, as indeed was suggested by Oort and Walraven (15) for electrons. This suggestion is still unsatisfactory, however, because it leaves the magnetic field problem unsolved. It is also a suggestion that could scarcely be applied to the intense extra-galactic sources, since there are no mysterious remnants to fall back on in such cases.

The present point of view is that all relativistic electrons are produced as secondaries from the normal cosmic ray protons, *and that there is no special concentration of this distribution in any of the intense sources*. The energy problems and difficulties outlined above do not then arise at all.

An essential step is that electrons are not produced concurrently with the episode of intense emission. The electron distribution is built up on a long-time scale, in precisely the manner discussed in the foregoing part of the paper. An intense source comprises a physical condition that allows the electrons of a *pre-existing reservoir* to be used quickly. The physical condition in question is one that operates at the surface of any rapidly expanding cloud of gas. Its nature will now be discussed.

2. *The shock-front condition.*—A discontinuity must exist at the surface of any mass of gas that expands rapidly into an ambient medium. Over a limited portion of the surface the effects of curvature can be neglected. The ambient medium being of essentially uniform density, the front can be taken as moving with the speed V of the expanding gas. According to recent investigations (16, 17) the

thickness of the front is determined by the Debye length calculated for a thermal speed V , not by the mean free path for atomic collisions or by the Larmor radii of particles in a magnetic field. Oscillating electric fields within the front prevent the high-speed penetration of one gas into the other. Since the Debye length is always very small compared with the radius of the expanding surface, the front approximates closely to the concept of a discontinuity.

Material from the ambient medium flows through the front, say from right to left. On the right of the shock the speed of flow relative to the front is V and is supersonic. On the left the flow speed is markedly less than V and is subsonic. A pressure gradient causes the subsonic flow to tend ultimately to zero on the left—i.e. the ambient material, having flowed through the front, ultimately joins the expanding gas cloud.

Write ρ , u , p , U for the mass density, the speed of flow relative to the front, the pressure, and the internal energy per unit mass, and denote values immediately to the right and left of the front by the subscripts 1, 2. The Rankine-Hugoniot relations, expressing the conservation of energy, momentum, and mass for a normal shock, are

$$\begin{aligned} \rho_1 u_1 &= \rho_2 u_2 && \text{(mass)} \\ p_1 + \rho_1 u_1^2 &= p_2 + \rho_2 u_2^2 && \text{(momentum)} \\ U_1 + p_1/\rho_1 + \frac{1}{2}u_1^2 &= U_2 + p_2/\rho_2 + \frac{1}{2}u_2^2 && \text{(energy).} \end{aligned} \quad (32)$$

In all cases with which we shall be concerned the terms in p_1 , U_1 are small. Thus with $u_1 = V$ we have

$$\begin{aligned} \rho_1 V &= \rho_2 u_2, \\ \rho_1 V^2 &= p_2 + \rho_2 u_2^2, \\ V^2 &= 2U_2 + 2p_2/\rho_2 + u_2^2, \end{aligned} \quad (33)$$

which solve to give

$$\rho_2 = \rho_1 \frac{\gamma + 1}{\gamma - 1}, \quad u_2 = V \frac{\gamma - 1}{\gamma + 1}, \quad p_2 = \frac{2\rho_1 V^2}{\gamma + 1}, \quad (34)$$

when the ratio of specific heats γ , defined by

$$\gamma = 1 + p/\rho U, \quad (35)$$

takes the same value at all points behind the front, so that

$$(\gamma - 1)\rho_2 U_2 = p_2. \quad (36)$$

These equations determine the condition of material behind the shock front— γ , V and also the density ρ_1 of the ambient medium being given.

The above equations are very well known. What is new here is that the equations will be used in cases where a reservoir of relativistic particles, or a magnetic field, makes the main contribution to U , not the usual thermal motions of the ordinary ambient medium (this gas still determines ρ_1 , ρ_2 of course).

As they pass through the front the lines of force of the magnetic field become plastered onto the expanding gas cloud. It will be assumed that the field suffers sufficient distortion for the relativistic particles to remain entirely trapped as they pass through the front. The following important assumption will also be made: whichever component—ordinary ambient gas, relativistic particles, or magnetic field—makes the chief contribution to U_1 will also make the chief contribution to U_2 .

The changes across the front of the minor components, whichever they may be, are to be calculated in accordance with an ordinary straightforward compression determined by the ratio ρ_2/ρ_1 .

Consider as an example the case $\rho_1 = 10^{-26} \text{ gm cm}^{-3}$, $H = 10^{-6} \text{ gauss}$, $V = 10^8 \text{ cm sec}^{-1}$. Suppose the contribution of the ordinary thermal energy of the ambient gas to U_1 happens to be less than the contribution of the cosmic rays, viz. $\sim 1.6 \times 10^{-12} \text{ erg cm}^{-3}$. Since $H^2/8\pi$ is also small compared with the latter value, it is clear that the cosmic rays then make the main contribution to U_1 . The above rule therefore requires the relativistic particles to make the main contribution to U_2 .

For isotropic cosmic rays, $\gamma = 4/3$. Equations (34) accordingly give

$$\rho_2 = 7\rho_1, u_2 = \frac{1}{7}V, p_2 = \frac{6}{7}\rho_1 V^2.$$

Also by (36),

$$\rho_2 U_2 = 3p_2 = \frac{18}{7}\rho_1 V^2. \quad (37)$$

Inserting values of ρ_1 , V we obtain $\rho_2 U_2 \approx 2.6 \times 10^{-10} \text{ erg cm}^{-3}$.

The increase of energy density from

$$\sim 1.6 \times 10^{-12} \text{ erg cm}^{-3} \text{ to } \sim 2.6 \times 10^{-10} \text{ erg cm}^{-3}$$

is due in part to the sevenfold rise of the density of the relativistic particles that accompanies the general rise of density from ρ_1 to ρ_2 . *But a further factor ~ 23 must come from a rise in the energy of each particle.*

The increase of the magnetic intensity is calculated from the sevenfold compression through the front. Since this compression is one-dimensional, the magnetic intensity increases proportionately to the density—i.e. sevenfold to $7 \times 10^{-6} \text{ gauss}$.

Gas dynamics is of no help toward understanding what physical process could promote such an increase in the energies of individual cosmic rays. The above rule implies that conditions within the front are controlled in such cases by the relativistic plasma rather than by the ambient gas.

The considerations of the following sections provide strong support for the rule, provided we add the further requirement:

The energy gain of relativistic particles follows a Fermi statistical dependence in which the proportionate gain of energy is the same for all particles.

Two additional issues can be dealt with at the present stage, at any rate partially. First, the propriety arises, when the magnetic vector is not parallel to the expanding surface, of using the Rankine-Hugoniot relations for a normal shock. So long as p_1 , U_1 can be neglected from the equations, and so long as the contribution of the magnetic field to p_2 , U_2 is small—as it is in the above example—the obliquity of the shock is small. Equations (32) then represent a satisfactory approximation.

Even if the magnetic field makes the main contribution to the energy density, the above treatment is still probably substantially correct in cases where the magnetic energy density rises by a very large factor through the front (provided p_1 , U_1 are still negligible). Such cases are not required in the present part of the paper but will arise in Part III. The very large increase of the energy density demands a high degree of wrapping of the lines of force, the wrapping being given by a process occurring within the front, again probably of a statistical type.

With a random wrapping of the field there is no important deviation from the normal condition implied by equations (32).

A second question arises concerning the value $4/3$ chosen for γ in the above example. This is correct only for relativistic particles with isotropy. There is no guarantee, however, that the particles gain speed equally in all directions. Rather would a greater gain normal to the front be expected than in transverse directions. But a reconsideration of the above example shows that no important change occurs even on the extreme hypothesis that the whole energy gain takes place in the normal direction. The magnetic field, plastered on the expanding surface, serves in this case to randomise two components of velocity, yielding the value $\gamma = 3/2$ appropriate for a two-dimensional relativistic gas. The value $\gamma = 3/2$ must accordingly be used in (34) and (36). The rise of the energy density through the front is thereby reduced by $28/45$ to $\rho_2 U_2 = 8\rho_1 V^2/5$. In the above example the rise would therefore be by a factor ~ 100 instead of by ~ 160 . Evidently the process is not appreciably affected, although it is slightly reduced in effectiveness.

Throughout the following work the isotropic case $\gamma = 4/3$ will be used.

3. *The Cygnus A case.*—It will be supposed that as an outcome of a collision between two galaxies a mass of gas M has been set in expansive motion with speed V . The condition that V shall not have been much reduced by an ambient medium of density ρ_1 is

$$\frac{4\pi}{3} R^3 \rho_1 < M, \quad (38)$$

where for convenience the cloud is assumed to be a sphere of radius R .

We suppose further that the collision has occurred in a cluster of galaxies where the density $\rho_1 \sim 10^{-26} \text{ gm cm}^{-3}$. This is a high value, but since we are now concerned with a radio source of very exceptional intensity it is permissible, and even desirable, to take rather abnormal values for all the quantities that affect the determination of the radio emissivity. An important practical advantage of choosing this value is that the particle density becomes close to the value used in Part I, Section 1, viz. $N \sim 10^{-2} \text{ atom cm}^{-3}$. Since moreover the cosmological time scale for building the reservoir of relativistic electrons is $\sim 10^{17} \text{ sec}$, again the same as that used in Part I, Section 1, the electron distributions (14), (15) and (16) can immediately be taken over to the present case. This means that the electron energy density in the ambient medium is $\sim 10^{-13} \text{ erg cm}^{-3}$ —i.e. about 0.1 of the proton energy density.

Each relativistic particle experiences a rise of energy at the shock front (there should be no difference between electrons and protons in this respect). Thus after passing through the front the electron energy contained in unit mass of material rises to $0.1 U_2$, where U_2 is given by (37). Write f for the fraction of the electron energy lost by synchrotron radiation in the time scale R/V determined by the expansion of the gas cloud. Then the total radio emission rate over all frequencies is given simply as a fraction f of the rate at which electron energy is swept up by the expanding gas, viz.

$$0.1 f U_2 (4\pi \rho_1 R^2 V) \approx \frac{1}{2} \rho_1 f R^2 V^3, \quad (39)$$

using (37) for U_2 .

These considerations can be subject to rather stringent tests, on the basis that V, R, f be chosen so that (39) takes its maximum value in the Cygnus A case.

Galaxies in clusters can collide at relative speeds up to about 3000 km sec^{-1} . Write M_1, M_2 for the colliding masses of gas. If no energy were lost by radiation, the combined gas cloud, $M = M_1 + M_2$, would possess sufficient energy to expand outwards from its mass centre at a speed V less than the relative speed at collision by the factor $(M_1 M_2)^{1/2}/M$. It follows that V must always be set less than half the relative speed of collision. Allowing for some energy loss by radiation, a value $V \approx 1000 \text{ km sec}^{-1}$ would seem an entirely reasonable choice.

The emission is at its greatest when R takes the largest value permitted by (38), $(3M/4\pi\rho_1)^{1/3}$. The emission that can be achieved is therefore proportional to $M^{2/3}$. In considering a wholly exceptional case M should thus be set at $\sim 10^{11}\odot$ corresponding to the gaseous content of a newly formed galaxy, rather than to an old galaxy such as M31 where M is only $\sim 10^9\odot$. With $M = 10^{11}\odot$, $\rho_1 = 10^{-26} \text{ gm cm}^{-3}$, $R = (3M/4\pi\rho_1)^{1/3} \approx 1.5 \times 10^{23} \text{ cm}$. At the distance of Cygnus A— $7 \times 10^{26} \text{ cm}$, using $4 \times 10^{17} \text{ sec}$ for the reciprocal of the Hubble constant—a source of this radius has an angular diameter of $\sim 100''$. The observed diameter is about $80''$.

The time scale of the expansion R/V is thus $\sim 1.5 \times 10^{15} \text{ sec} \approx 5 \times 10^7 \text{ years}$. Inserting this time scale for t , in (11), and putting $H = 2 \times 10^{-5} \text{ gauss}$, it follows that $f = 1$ for $\nu > \sim 5 \times 10^7 \text{ c/s}$ —i.e. over essentially the whole radio band. A magnetic intensity $\sim 2 \times 10^{-5} \text{ gauss}$ after compression requires $\sim 3 \times 10^{-6} \text{ gauss}$ before compression. Once again this is rather higher than might normally be expected, but once again this is an advantage, since all factors should take favourable values in the special case of Cygnus A.

With $f = 1$, $\rho_1 = 10^{-26} \text{ gm cm}^{-3}$, $R = 1.5 \times 10^{23} \text{ cm}$, $V = 10^8 \text{ cm sec}^{-1}$, (39) gives a total emission of $\sim 10^{41} \text{ erg sec}^{-1}$. The observed radio flux corresponds to a total emission greater than this by a factor ~ 3 , if *Cygnus A radiates isotropically*. It is certain, however, that radiation will not take place isotropically for an object of the present type. The initial angle made by the lines of magnetic force with the expanding surface must affect the detailed emissivity in a considerable measure, and it is by no means unlikely that a variation of emission with line of sight by as much as a factor 3 takes place. If the Earth lies in a direction of preferential emission (39) gives closely the correct intensity, but in any case (39) is correct in order of magnitude.

It remains to consider the form of the radio frequency spectrum. The electron distribution in the ambient medium before compression is given by (14), (15) and (16). Compression across the shock front lifts the energy of each electron by ~ 20 . Hence the join of (14), (15) is lifted to $\gamma \sim 10^4$. The emitted frequency at $\gamma = 10^4$, $H = 2 \times 10^{-5} \text{ gauss}$ is about 10^{10} c/s . The radio spectrum for $\nu < 10^{10} \text{ c/s}$ is thus given essentially by the lifted form of (14). It is important in this connection to notice that, since (14) contains an appreciable fraction of the total electron energy density, the radiated energy lies mainly below 10^{10} c/s .

For $f = 1$, $\gamma < \sim 10^4$, the energy radiated by electrons between $\gamma, \gamma + d\gamma$ is proportional to $d\gamma/\gamma^{2/3}$ (in this case the electron distribution is not multiplied by $P(\gamma)$ but by γmc^2 to obtain the emission). Replacing $\gamma, d\gamma$ by $\nu, d\nu$ it is thus easily seen that the frequency spectrum is $d\nu/\nu^{5/6}$, in excellent agreement with the observed spectrum for the range $4 \times 10^8 < \nu < 10^{10} \text{ c/s}$. The observed spectrum becomes less steep at $\nu < 4 \times 10^8$, however, and this is exactly to be expected, since frequencies $< 4 \times 10^8$ are radiated by electrons at the very base of the distribution.

The problem of calculating the spectrum is then quantitatively awkward, because the flatter distribution (7) must be used in place of (8), and because energy degradation effects cannot be ignored at the base.

The lifted form of (15) must be used for $\nu > 10^{10}$. The electron distribution then has an extra factor γ^{-1} , and this steepens the spectrum to $d\nu/\nu^{4/3}$.

4. *The NGC 1275 case.*—It is of interest to compare the Cygnus A case, in which ρ_1 , H , M were favourably chosen, with a case in which these quantities take more average values, e.g. $\rho_1 = 3 \times 10^{-27} \text{ gm cm}^{-3}$, $H = 10^{-6} \text{ gauss}$, $M = 3 \times 10^9 \odot$. The value chosen for H , referring to the magnetic intensity before compression, is comparable with the halo fields within galaxies. It is hence a reasonable value for the field, say at distance 30 kpc from a galaxy within a cluster.

The expansion velocity V will again be chosen as 10^8 cm sec^{-1} , since observation suggests that a value of this order is attained in NGC 1275. In this connection it may be noted that, whereas ρ_1 , M , and possibly H also, decline as a cluster ages, there is no appreciable decline in the dynamical velocities with which galaxies may collide within the cluster.

With $N \approx 1.8 \times 10^{-3} \text{ atom cm}^{-3}$ and $H = 10^{-6} \text{ gauss}$, (13) gives the electron distribution before passage through the front,

$$\begin{aligned} &\sim 2.7 \times 10^{-7} d\gamma/\gamma^{8/3}, \quad 10^2 < \gamma < 5 \times 10^3, \\ &\sim 1.3 \times 10^{-4} d\gamma/\gamma^{11/3}, \quad \gamma \geq 5 \times 10^3. \end{aligned} \quad (40)$$

The next step is to calculate the electron distribution after passage through the front. From (37), $\rho_2 U_2 \approx 7.8 \times 10^{-11} \text{ erg cm}^{-3}$ in this case. The ratio $\rho_2 U_2 / \rho_1 U_1$, with $\rho_1 U_1 \sim 1.6 \times 10^{-12} \text{ erg cm}^{-3}$, is thus ~ 49 . Again allowing for a seven-fold increase of density, the energy of each relativistic particle is lifted by a factor ~ 7 . After passage through the front the electron distribution therefore becomes

$$\begin{aligned} &\sim 6.9 \times 10^{-6} d\gamma/\gamma^{8/3}, \quad 7 \cdot 10^2 < \gamma < 3.5 \times 10^4, \\ &\sim 2.4 \times 10^{-1} d\gamma/\gamma^{11/3}, \quad \gamma \geq 3.5 \times 10^4. \end{aligned} \quad (41)$$

The magnetic intensity after compression is $7 \times 10^{-6} \text{ gauss}$.

The maximum value of R permitted by (38) is $\sim 8 \times 10^{22} \text{ cm}$, and the volume of the expanding cloud at the stage where R takes on this value is $\sim 2 \times 10^{69} \text{ cm}^3$. The time scale R/V is thus $\sim 8 \times 10^{11} \text{ sec}$. With this time scale in (10), and with $H = 7 \times 10^{-6} \text{ gauss}$, we see that the electron energies are not seriously degraded by synchrotron radiation up to $\gamma \approx 1.2 \times 10^4$, i.e. for frequencies up to $\sim 5 \times 10^9 \text{ c/s}$. Thus to obtain the emissivity at $\nu < 5 \times 10^9 \text{ c/s}$, (41) must be multiplied by $P(\gamma)$ and $d\gamma$ must be replaced by ν , $d\nu$,

$$\sim 1.5 \times 10^{-31} \frac{d\nu}{\nu^{5/6}} \text{ erg cm}^{-3} \text{ sec}^{-1}. \quad (43)$$

At higher frequencies the electron distribution must be multiplied by γmc^2 instead of by $P(\gamma)$. This steepens the spectrum to $\sim 10^{-26} d\nu/\nu^{4/3}$, $\nu \geq 5 \times 10^9 \text{ c/s}$.

The total emissivity is $\sim 5 \times 10^{-29} \text{ erg cm}^{-3}$. Since the volume of the system $\sim 2 \times 10^{69} \text{ cm}^3$, the total emission is therefore $\sim 10^{41} \text{ erg sec}^{-1}$. It follows that the changes made in ρ_1 , H , M reduce the emission by $\sim 10^3$. The reduction is contributed roughly equally by each of these parameters.

The radio source NGC 1275 is an example of the present case, the total emission of NGC 1275 being less than Cygnus A by a factor $\sim 10^3$.

5. *Sources not associated with galaxies.*—We now take an example differing from Cygnus A, not in ρ_1 , H , M , but in V . Let $\rho_1 = 10^{-26} \text{ gm cm}^{-3}$, $H = 3 \times 10^{-6} \text{ gauss}$, $M = 10^{11} \odot$, as before, but take $V = 3 \times 10^7 \text{ cm sec}^{-1}$. Formula (39) with $f=1$ is again applicable to this case. Thus with $R \leq 1.5 \times 10^{23} \text{ cm}$ as the maximum value permitted by (38), the maximum total emission

$$\sim 3 \times 10^{42} \text{ erg sec}^{-1}.$$

The electron distribution in the ambient medium before compression is again given by (14), (15) and (16). Compression across the front is less effective than before by a factor ~ 10 , however. Thus instead of each individual electron energy being lifted by ~ 20 , the increase is now only by a factor ~ 2 . Hence the join of (14), (15) is lifted only to $\gamma \sim 10^3$. Hence the emitted frequency at $\gamma = 10^3$, $H = 2 \times 10^{-5} \text{ gauss}$ is about 10^4 c/s , the radiation spectrum now changes at $\nu \leq 10^8 \text{ c/s}$ instead of at $\nu \leq 10^{10} \text{ c/s}$, being of the form $d\nu/\nu^{5/6}$ for $\nu < \sim 10^8 \text{ c/s}$ and of the form $d\nu/\nu^{4/3}$ for $\nu > 10^8 \text{ c/s}$.

In a former paper (18) it was shown that galaxies probably form by a cooling process in which dynamical motions of order 300 km sec^{-1} are developed in the final stages. For a blob of cooled gas to remain compact, gravitation must be able to control the dynamical motions, and this requires the mass to exceed $\sim 10^{11} \odot$. If the mass $\leq \sim 10^{11} \odot$ the material simply flies apart again (except that an occasional blob may be able to hold together if the dynamical motions happen to be small in a particular locality). Here then we have a process in which the conditions assumed above may be satisfied fairly closely.

In many cases the value of ρ_1 probably falls near $3 \times 10^{-27} \text{ gm cm}^{-3}$ (this was the value obtained in (18)) rather than at $10^{-26} \text{ gm cm}^{-3}$. The effect of lowering ρ_1 is to reduce the total emission to $\sim 10^{42} \text{ erg cm}^{-3}$ and to extend the spectrum $d\nu/\nu^{4/3}$ down to the base of the radio spectrum.

The present work, taken with that of the previous paper therefore leads to a prediction of the existence of a new class of radio source. The main properties are:

- (i) M is high and V is low, the opposite to the case of NGC 1275.
- (ii) The frequency spectrum is of the form $d\nu/\nu^{4/3}$.
- (iii) There is no association with a visible galaxy.
- (iv) The total radio emission has an upper limit of about $10^{42} \text{ erg sec}^{-1}$.

The majority of the unidentified radio sources could well be of this type. It is already of great interest that Whitfield (19) finds that unidentified sources tend to possess steep frequency spectra with indices of about -1.2 .

PART III STRONG SOURCES OF GALACTIC ORIGIN

1. *Preliminary remarks.*—Exactly the same considerations as those used in Part II will be employed in the investigation of non-thermal galactic sources. The numerical results are altered, however, in an important way, because ρ_1 , H , M are all changed very markedly:

	<i>Extragalactic value</i>	<i>Galactic value</i>
ρ_1	$\sim 3 \times 10^{-27} \text{ gm cm}^{-3}$	$\sim 3 \times 10^{-24} \text{ gm cm}^{-3}$
H (before compression)	$10^{-6} - 10^{-7} \text{ gauss}$	$\sim 10^{-5} \text{ gauss}$
M	$10^9 - 10^{11} \odot$	$\odot - 10^8 \odot$

The galactic values all refer to the disk of the Galaxy rather than to the halo, for the reason that the strong galactic sources all lie near the plane of the disk.

The situation is somewhat simplified in the present case because the electron distribution has already been obtained in Part I, viz (14), (15) and (16). These formulae will be used throughout the following work.

2. *The optical emission of the Crab Nebula.*—With $\rho_1 = 3 \times 10^{-24} \text{ gm cm}^{-3}$ and with V given by the observed expansion velocity of the filamentary system of the Crab, $1.1 \times 10^8 \text{ cm sec}^{-1}$, (37) gives $\rho_2 U_2 \approx 9.3 \times 10^{-8} \text{ erg cm}^{-3}$. Again taking the main contribution as arising from the reservoir of relativistic particles with $\rho_1 U_1 \approx 1.6 \times 10^{-12} \text{ erg cm}^{-3}$, it follows that the energy of each individual particle is lifted by

$$\frac{1}{7} U_2 U_1^{-1} \approx 8.3 \times 10^3, \quad (44)$$

the factor $1/7$ being due to the straightforward compression from ρ_1 to ρ_2 .

Now the main electron energy, before passage through the shock front at surface of the expanding Crab, comes from values of γ immediately below the join of (14) and (15)—i.e. from values of γ somewhat less than 5×10^2 . After passage through the front, the main contribution therefore comes from γ values of order 3×10^6 .

It is a necessary condition (according to our rule) that the initial magnetic energy per unit volume shall be less than the energy of the relativistic particles. Taking $1.6 \times 10^{-12} \text{ erg cm}^{-3}$ for the latter, this requires $H < \sim 6 \times 10^{-6} \text{ gauss}$ before compression. Passage through the front increases H by the factor $\rho_2/\rho_1 = 7$, i.e. to a maximum of $\sim 4 \times 10^{-5} \text{ gauss}$. Reference to (3) now shows that the emitted frequency at $\gamma = 3 \times 10^6$, $H = 4 \times 10^{-5} \text{ gauss}$ is $\nu \approx 1.5 \times 10^{15} \text{ c/s}$. The synchrotron emission is thus lifted into the optical range, the bulk of the emission taking place at wave-lengths longer than 2000 Å.

The time scale of the expansion of the Crab is known to be $\sim 3 \times 10^{10} \text{ sec}$, since this is the time that has elapsed since the supernova of A.D. 1054. Equation (10) gives a time scale $t_r \sim 10^{11} \text{ sec}$ for the degradation through synchrotron radiation at $\gamma = 3 \times 10^6$, $H = 4 \times 10^{-5} \text{ gauss}$. Thus only a moderate fraction of the electron energy has been degraded by synchrotron radiation. The total energy of relativistic particles in the Crab (protons and electrons) is therefore given simply by multiplying the volume of the system by $\rho_2 U_2/7$. The rate of emission is therefore

$$0.1(\rho_2 U_2/7)(\text{Volume})t_r^{-1}, \quad (45)$$

where a factor 0.1 must be included because only some 10 per cent of the energy density is contributed by electrons.

It is possible to proceed in two ways. First, entirely conventional values will be used. On the basis that the Crab has always expanded at the present rate, the radius R must be $\sim 3 \times 10^{18} \text{ cm}$, the volume must be $\sim 10^{56} \text{ cm}^3$, and the distance 1 kpc. Accepting this distance, the observed apparent magnitude demands a white light emission rate of $\sim 2 \times 10^{36} \text{ erg cm}^{-3}$. Inserting $\rho_2 U_2 = 9.3 \times 10^{-8} \text{ erg cm}^{-3}$, $t_r = 10^{11} \text{ sec}$, in (45) yields a calculated emission rate of $1.3 \times 10^{36} \text{ erg sec}^{-1}$.

The second method of calculating leads to very interesting results, and is perhaps more likely to be correct. In the Cygnus A case, where $t_r < R/V$, the emission declines as soon as condition (38) is no longer satisfied—i.e. as soon

as the resistance of the ambient medium produces a deceleration of the expanding cloud. There is no such decline when $t_r > R/V$. Indeed the epoch of maximum emission occurs during the deceleration of the cloud, since it is not until deceleration is in progress that the energy storage in the system takes on its maximum value. The Crab Nebula being a very outstanding object, it is possible, and even likely, that this phase of deceleration has now been reached. Writing V_i for the initial expansion rate, we then require

$$\frac{1}{2}MV_i^2 \approx \left(\frac{4\pi}{3}R^3\right)\left(\rho_1 U_2\right). \quad (46)$$

With $R \approx 3 \times 10^{10} V_i$, and U_2 given by $18V_i^2/49$ in accordance with (37), this condition becomes

$$M \approx 8 \times 10^{31} \rho_1 V_i^3. \quad (47)$$

The attractive feature of these considerations is that V_i can now be set equal to the normal expansion rate of Type I supernovae, $V_i \sim 2000 \text{ km sec}^{-1}$. It has always been a remarkable feature of the Crab that its present expansion rate falls markedly below the values observed for supernovae. It is worth remarking in this connection that former discussions (4, 15, 20) do not provide this opportunity of resolving this discrepancy, since according to these discussions the gas cloud should be accelerating.

With $\rho_1 \approx 10^{-24} \text{ gm cm}^{-3}$, $V_i \approx 2 \times 10^8 \text{ cm sec}^{-1}$, (47) gives $M \approx \odot/3$, an entirely plausible value. It will be noticed that ρ_1 has been set lower than the value $3 \times 10^{-24} \text{ gm cm}^{-3}$ used previously. This ensures that U_2 remains substantially unaltered, thereby keeping the same γ values for the electron energies. This is necessary, since the radiated energy must continue to lie mainly in the optical band.

The radius R is now $\sim 6 \times 10^{18} \text{ cm}$, the volume $\sim 10^{57} \text{ cm}^3$, and the distance $\sim 2 \text{ kpc}$. Accepting this increase of distance, the observed apparent magnitude demands a white light emission rate of $\sim 10^{37} \text{ erg cm}^{-3}$. Inserting in (45) a volume 10^{57} cm^3 , and maintaining $\rho_2 U_2 \approx 9.3 \times 10^{-8} \text{ erg cm}^{-3}$, for the reason stated in the previous paragraph, the calculated emission rate is now

$$\sim 1.3 \times 10^{37} \text{ erg sec}^{-1}.$$

The cumulative effect of these results would seem to leave little doubt that the phenomenon of the Crab Nebulae is to be sought in terms of a compressive effect exerted on the electron reservoir of the Galaxy. The energy dilemma is removed, the observed intensity is explained, and no difficulty arises concerning the magnetic field with an intensity no greater than $4 \times 10^{-5} \text{ gauss}$. A simple explanation can also be offered for the difference between the Crab and the Tycho and Kepler supernovae. A similar process would be expected to operate in these cases also, but the degree to which the electron energies are lifted will be different, because ρ_1 is different in the regions where the supernovae occurred. A larger value of ρ_1 would lift the emission largely into the ultraviolet, while a smaller value would lower it into the infra-red. Moreover the Kepler and Tycho supernovae have only about 40 per cent of the age of the Crab, so that the volumes of the expanding clouds are less by a factor ~ 15 . On this score alone the emission should be reduced by a comparable factor.

Polarization measures of the Crab show that the configuration of the magnetic field may be consistent with a twisted tube of force that has become plastered onto an expanding cloud, the field initially having much the form of a force-free filament

(21). That the field is derived from an interstellar source was already proposed by Shklovsky and Ginzburg. This suggestion was rejected by Oort and Walraven (15) on the ground that compression would destroy the directivity of the field to an extent that would contradict the observed high degree of local polarization. This does not seem to be so for the systematic compression envisaged here—although it is a valid objection to the idea that the field is enhanced by small scale turbulence. It is true that some local field distortion is necessary to contain the relativistic particles, but a general modulation of the field would be sufficient for this purpose. Photographs by Baade (15, page 289 for example) show the white light zone to be dappled in a way that might be expected to arise from an undulation of the field along the envelope.

The filamentary structure of the Crab presumably arises from the compression of the normal interstellar gas at the expanding surface, and hence must be taken as marking the outer boundary of the system. It may be noted that the detailed structure of the white light zone must vary according to the direction from which it is seen, since there is never any emission along the line of sight whenever the magnetic vector points towards the observer.

3. *The magnetic case.*—The example of the Crab Nebula shows that radio sources in the Galaxy do not arise in exactly the same fashion as in extragalactic space. The enhancement of the γ -values of the electrons is so great, and the initial magnetic intensity is so high, that (3) yields frequencies far above the radio wave-band.

There remains the second possibility, not so far considered, that the main contribution to U_1 is made by the magnetic field. Since the cosmic rays always contribute $\sim 1.6 \times 10^{-12} \text{ erg cm}^{-3}$, the condition for the magnetic case to be applicable (in accordance with our rule) is

$$\frac{H^2}{8\pi} > \sim 1.6 \times 10^{-12} \text{ erg cm}^{-3}, \quad H > \sim 6 \times 10^{-6} \text{ gauss.} \quad (48)$$

The mean magnetic intensity in the Galaxy is of about this value. It is hence clear that both the case considered previously, and the magnetic case, must take place within the Galaxy. *Both cases may even occur on different portions of one and the same expanding gas cloud.* The fact that the Crab Nebula is both a radio source and an optical emitter would seem to be due to both processes occurring at different localities on the same expanding envelope. In intergalactic space, on the other hand, the condition (48) is presumably never satisfied, so that the magnetic case does not arise there.

Condition (37) continues to hold, but with the magnetic field now making the main contribution to U_2 . Thus the magnetic intensity after passage through the shock front of an expanding cloud is given by

$$H = 12(\pi\rho_1/7)^{1/2} V. \quad (49)$$

Putting $\rho_1 \approx 3 \times 10^{-24} \text{ gm cm}^{-3}$, $V = 10^8 \text{ cm sec}^{-1}$, gives $H \approx 1.4 \times 10^{-3} \text{ gauss}$. The magnetic intensity accordingly exceeds 10^{-3} gauss over the parts of the surface of the Crab where the magnetic case is applicable (a closely similar value for H is obviously obtained if the alternative values $\rho_1 \approx 10^{-24} \text{ gm cm}^{-3}$, $V = 2 \times 10^8 \text{ cm sec}^{-1}$ are used in (49)).

In the case of the radio source Cass A a portion of a rapidly expanding cloud with V perhaps as high as 3000 km sec^{-1} seems to be in collision with a more or less

stationary cloud (22). In this case ρ_1 is probably as large as $3 \times 10^{-23} \text{ gm cm}^{-3}$. Substitution in (49) yields a remarkably high magnetic intensity of $\sim 10^{-2} \text{ gauss}$.

Plainly these high magnetic intensities cannot be achieved through a one-dimensional compression from ambient density ρ_1 to ρ_2 . Such a compression would raise an initial field $\sim 10^{-5} \text{ gauss}$ to less than 10^{-4} gauss . Hence in order that the equations (32) be satisfied in accordance with our rule, the field must become highly wrapped. Because of this wrapping the value of γ to be used in (34) can still reasonably be taken as $4/3$ (if the compression had been one-dimensional the appropriate value would have been 2). Also because of the large field distortion the energies of relativistic particles probably increase only by the factor $(\rho_2/\rho_1)^{1/3}$ —rather than by ρ_2/ρ_1 , as they would for a one-dimensional gas (25). Thus the energies of the relativistic particles probably rise by no more than a factor ~ 2 in this case. The electron distribution per unit volume is therefore lifted by passage through the shock front from (14), (15) and (16) to

$$\sim 3.5 \times 10^{-8} \gamma^{-5/3} d\gamma, \quad \gamma < \sim 10^3, \quad (50)$$

$$\sim 3.5 \times 10^{-5} \gamma^{-8/3} d\gamma, \quad \sim 10^3 \leq \gamma < 10^4, \quad (51)$$

$$\sim 3.5 \times 10^{-1} \gamma^{-11/3} d\gamma, \quad \gamma \geq 10^4, \quad (52)$$

a factor 7 being also introduced to allow for the increase of the electron number density. The total electron energy density is now $\sim 1.5 \times 10^{-12} \text{ erg cm}^{-3}$, the main contribution coming from γ values somewhat below 10^3 —i.e. somewhat below the join of (50) and (51).

Where conditions are not uniform over an expanding surface, in particular where the field is highly wrapped over separate localities on the surface, some unwinding of the lines of force is to be expected. Such a process, occurring near the boundaries of the radio and optical zones, may well be responsible for the light ripples that have been reported in the Crab (15). More certainly, the writhing filaments found near Cass A would seem to be due to just such an unwrapping, taking place near the boundary of the collision zone between a mass of rapidly expanding gas and an interstellar cloud.

4. *The case of Cassiopeia A.*—If the radio emission per unit area were always the same over the surfaces of all expanding gas clouds, the radio surface brightness would always be the same, so that sources would have apparent radio magnitudes proportional to the square of their angular diameters.

Now the squares of the angular diameters of Cygnus A and Cass A are in the ratio $\sim 1:10$. The observed radio fluxes per unit frequency are, however, in the ratio $\sim 7:10$ at $\nu = 10^8 \text{ c/s}$ and in the ratio $\sim 1:2$ at $\nu = 10^{10} \text{ c/s}$. These two sources do not therefore have the same surface brightness, Cygnus A being brighter by $\sim 7:1$ at $\nu = 10^8 \text{ c/s}$, and by $\sim 5:1$ at $\nu = 10^{10} \text{ c/s}$. The reason for this difference is readily understood.

According to the work of Part II, Section 3, the energy of each relativistic particle is lifted by a factor ~ 23 at the expanding surface of Cygnus A. For galactic sources, however, the energies are lifted only by a factor ~ 2 . The ratio of the rates at which electron energy is swept per unit surface area is accordingly greater in the Cygnus A case by the factor

$$\sim 10 (V\rho_1 U_{el})_{Cass} / (V\rho_1 U_{el})_{Cygnus} \quad (53)$$

where $\rho_1 U_{el}$ is the energy density of the electron reservoir outside the expanding gas cloud. According to Part II, Section 3, $(\rho_1 U_{el})_{Cass}$ is closely the same as $\rho_1 U_{el}$

for the Galaxy—i.e. for Cass A, while the expansion velocity V is probably twice as great for Cass A. Hence (53) is a factor ~ 5 , which is just the order by which the surface brightness of Cygnus A exceeds that of Cass A.

It is implicit in this agreement that the time scale for synchrotron radiation t_r shall be less than the expansion time scale R/V . It was already seen in Part II, Section 3, that this is so for Cygnus A. The condition that it shall also be so in Cass A, even down to frequencies as low as 10^8 c/s, places a requirement on the magnetic intensity. Taking $R/V \sim 3 \times 10^{10}$ sec for Cass A, and using (11) at $\nu = 10^8$ c/s, shows that if $t_r < R/V$ then $H > \sim 2 \times 10^{-2}$ gauss. This was precisely the order of the field obtained in the previous section for the case of Cass A.

The radio spectrum obtained in Part II, Section 3, for Cygnus A was of the form $d\nu/\nu^{5.6}$. This should apply also for Cass A, as indeed it does.

Finally, a direct computation of the total radio emission rate can readily be made. The surface area of Cass A is somewhat uncertain, because the surface is probably not a simple sphere, but a value $\sim 5 \times 10^{38}$ cm² must be correct in order of magnitude. At an expansion velocity ~ 3000 km sec⁻¹ the volume swept out is thus $\sim 10^{47}$ cm³ per sec. The electron energy $\sim 3 \times 10^{-13}$ erg cm⁻³ (this includes the factor ~ 2 by which the individual electron energies are lifted), so that the rate of sweeping of electron energy $\sim 3 \times 10^{34}$ erg sec⁻¹, and for $t_r < R/V$ this gives the total emission rate—in excellent agreement with observations.

5. *The radio emission of the Crab Nebula.*—The Crab Nebula and Cass A possess approximately the same angular diameter. If conditions at their surfaces were the same they would therefore appear as sources of equal intensity. The observed radio fluxes are in fact in the ratio $\sim 1:1$ at $\nu = 10^{10}$ c/s, but whereas the spectrum of Cass A is of the form $d\nu/\nu^{0.8}$ for $\nu < 10^{10}$ c/s the spectrum of the Crab is $d\nu/\nu^{0.33}$. Thus at $\nu = 10^8$ c/s the ratio of the observed fluxes is $\sim 1:10$.

The clear implication is that, while in Cass A the magnetic intensity is large enough for the synchrotron time scale t_r to be $< R/V$ for frequencies $\nu > \sim 10^8$ c/s, in the Crab $t_r < R/V$ only for $\nu > \sim 10^{10}$ c/s. This requires the magnetic intensity to be greater in Cass A by about 5, a result already obtained in Section 3 from a consideration of equation (49).

For $\nu < 10^{10}$ c/s, the frequency spectrum of the Crab is therefore given by first multiplying (50) by $P(\gamma)$ and then by the usual procedure of replacing $\gamma, d\gamma$ by $\nu, d\nu$ in accordance with (3). The result is a spectrum $d\nu/\nu^{1.3}$ in noteworthy agreement with observation.

Accepting the conventional value of 1 kpc for the distance, the surface area of the Crab is $\sim 10^{38}$ cm²—about five times less than the surface of Cass A. Since the velocity of expansion of the Crab is also less than that of Cass A by a factor ~ 2 , the rate of sweeping of electron energy is thus greater in Cass A by ~ 10 . A further factor of two arises in the total emission rate because of the less efficient radiation in the Crab—on account of the lower magnetic intensity. (The energy contained in the spectrum $(10^{10}/\nu)^{1.3} d\nu$, $10^8 \leq \nu \leq 10^{10}$ c/s, is less than the energy contained in $(10^{10}/\nu)^{0.33} d\nu$, $10^8 \leq \nu \leq 10^{10}$ c/s, by about 2.) Thus the total emission rate for the Crab should be less than the rate $\sim 3 \times 10^{34}$ erg sec⁻¹ calculated above for Cass A by a factor ~ 20 —i.e. $\sim 1.5 \times 10^{33}$ erg sec⁻¹. This result is too small by about 5, a difference of importance.

A number of suggestions can be made for resolving this discrepancy. The simplest is to say that the Crab is a non-isotropic emitter (this is almost certainly the case) and that the Earth lies in a strongly preferential direction. This possibility

is made plausible by the circumstance that the line of sight is almost perpendicular to the long axis of the Crab, which in turn points nearly along the spiral arm.

6. *The IC 443 Case.*—The effect of reducing the velocity of expansion V is to lower the magnetic intensity. Thus for $V \approx 100 \text{ km sec}^{-1}$, $\rho_1 \approx 10^{-24} \text{ gm cm}^{-3}$ the value of H given by (49) is $\sim 10^{-4} \text{ gauss}$. Large, slowly expanding clouds, such as IC 443 and the Cygnus Loop, may be expected to possess fields of this order.

The emissivity in such cases is given by multiplying (50), (51) by $P(\gamma)$ and by writing in terms of ν , $d\nu$

$$\begin{aligned} &\sim 5 \times 10^{-33} \frac{d\nu}{\nu^{1/3}}, & \nu < \sim 4 \times 10^8 \text{ c/s,} \\ &\sim 10^{-28} \frac{d\nu}{\nu^{5/6}}, & \nu \geq \sim 4 \times 10^8 \text{ c/s,} \end{aligned} \quad (54)$$

the units being $\text{erg cm}^{-3} \text{ sec}^{-1}$. The emission rate per unit volume for the frequency range $4 \times 10^7 \leq \nu \leq 4 \times 10^9$ is thus $\sim 10^{-26} \text{ erg cm}^{-3} \text{ sec}^{-1}$. For an expanding spherical shell of radius 15 pc and thickness 1.5 pc the volume is $\sim 10^{59} \text{ cm}^3$, yielding a total emission (for the same frequency range) of $\sim 10^{33} \text{ erg sec}^{-1}$. Such a cloud because of its greater volume is therefore capable of emitting at a rate that approaches the Crab Nebula. This result is consistent with the observed intensities from the non-thermal galactic sources of large angular diameter—on the basis that brighter sources are distant about 1-2 kpc.

7. *Remarks on the shock front condition.*—The above results have been obtained from an interesting, and perhaps unconventional, use of the Rankine-Hugoniot relations. Reference to (37) shows that the energy density behind the shock depends on the speed V of the expanding cloud and on the density ρ_1 of the ambient medium into which the cloud is moving. By making ρ_1 , V large this energy density can therefore be made essentially as large as we please. Under suitable conditions the energy storage behind the front takes place, not in ordinary material (density ρ_2), but in an assembly of relativistic particles. The energies of the latter particles can then be lifted essentially in any degree simply by increasing ρ_1 , V .

In the absence of a thorough analysis of the physical processes taking place within the shock front, the present treatment must remain unproved. Yet the considerable successes achieved in explaining a wide range of phenomena give a strong reason for accepting the implications of this process. One cannot help wondering whether a similar effect might not arise even where the high speed particles are non-relativistic—in the case for example where the material ahead of the shock front consists of a high-density gas at temperature $\sim 10^4 \text{ deg. K}$ mixed with a low-density gas at temperature $\sim 10^6 \text{ deg. K}$. With the low temperature component making the main momentum contribution, and the high temperature component the main energy contribution, a situation might well exist whereby the temperature of the hot component was considerably enhanced, perhaps even to values $\sim 10^8 \text{ deg. K}$ that would be of interest in the thermonuclear field. A lack of collisional equilibrium between the two components of the assembly is of course implicit in these remarks.

Lastly, we may mention that the present treatment of the case where the magnetic field supplies the dominant energy term differs considerably from that given by de Hoffman and Teller (24, see also Helfer, 25). The difference lies in the admission of detailed irregularities. Thus the Teller-de Hoffman

treatment assumes that uniform conditions are maintained over the shock front. The examples of Cass A and of the filamentary structure of the Crab Nebula would seem to argue against uniformity.

St. John's College,
Cambridge;
1959 July.

References

- (1) Schwinger, J., *Phys. Rev.*, **75**, 1912 (1949).
- (2) Burbidge, G. R., *Ap. J.*, **123**, 178 (1956).
- (3) McDonald, F. B., *Nuovo Cim. Supp.* **8** Ser. 10, 500 (1958).
- (4) Burbidge, G. R., *Ap. J.*, **127**, 48 (1958).
- (5) Brenner, A. E. and Williams, R. W., *Phys. Rev.*, **106**, 1020 (1957).
- (6) Mott, N. F. and Massey, H. S. W., *Theory of Atomic Collisions*, Oxford.
- (7) Baldwin, J. E., *I.A.U. Symposium No. IV on Radio Astronomy*, page 233, Cambridge (1957).
- (8) Peters, B., *Nuovo Cim. Supp.* **8** Ser. 10, 556 (1958).
- (9) Brown, R. H., and Hazard, C., *M.N.*, **113**, 123 (1953).
- (10) Brown, R. H., *Symposium on Radio Astronomy, Paris* (1958).
- (11) Mills, B. Y., *Aust. J. Phys.*, **8**, 368 (1955).
- (12) Burbidge, G. R., *Ap. J.*, **124**, 416 (1956).
- (13) Burbidge, G. R. and Burbidge, E. M., *Ap. J.*, **125**, 1 (1957).
- (14) Burbidge, G. R., *Symposium on Radio Astronomy, Paris* (1958).
- (15) Oort, J. H. and Walraven, T., *B.A.N.*, **12**, 285 (1956).
- (16) Buneman, O., *private communication*.
- (17) Parker, E. N., *private communication*.
- (18) Hoyle, F., *11th Solvay Conference*, 66 (1958).
- (19) Whitfield, G. R., *M.N.*, **117**, 680 (1957).
- (20) Woltjer, L., *B.A.N.*, **13**, 301 (1956-7).
- (21) Gold, T. and Hoyle, F., *M.N.*, **120**, 89 (1960).
- (22) Baade, W. and Minkowski, R., *Ap. J.*, **119**, 206 (1954).
- (23) Spitzer, L., *Physics of Fully Ionized Gases*, Interscience, page 13.
- (24) de Hoffman, F. and Teller, E., *Phys. Rev.*, **80**, 692 (1950).
- (25) Helfer, H. L., *Ap. J.*, **117**, 177 (1953).

ON THE DIMENSIONS, SPATIAL DENSITY, AND POWER OF THE EXTRAGALACTIC RADIO SOURCES

H. E. C. Tunmer

(Communicated by F. Graham Smith)

(Received 1959 August 11)

Summary

Although the majority of the discrete radio sources are unidentified, it is believed that they are very distant extragalactic objects. They may be galaxies with few visible stars. This paper examines physical conditions in large gas clouds, and shows that if these constitute the major class of radio sources a lower limit may be placed on their radio powers. If a large proportion of the mass is condensed into stars the conditions for gravitational stability, which form a part of the present argument, will not apply; however it appears that even under these circumstances the radio power must exceed 10^{38} w. ster $^{-1}$ (c/s) $^{-1}$ at 80 Mc/s.

Introduction.—It has been shown (Ryle 1958) that the majority of radio stars, apart from those concentrated towards the galactic plane, must in all probability lie at great distances from the Galaxy. This result has the most important implications in cosmological theory, and further consideration should be given to the limits which may be placed both on the average spatial density and the radio luminosity of these extragalactic objects.

Basing his argument on the number of radio sources falling within given ranges of flux density, on their isotropic distribution, and on the observed limit of their maximum integrated emission, Ryle was able to show that most of the extragalactic objects had a radio luminosity P greater than 10^{23} w. (c/s) $^{-1}$ ster $^{-1}$ at 80 Mc/s and a space density ρ less than 10^{-20} pc $^{-3}$. An extension of his arguments was based on measured angular diameters of the brighter sources, and on the failure to identify most of them with objects; this argument suggested that P was greater than 3×10^{25} w. (c/s) $^{-1}$ ster $^{-1}$ and ρ was less than 10^{-25} pc $^{-3}$. This further argument depended, however, on the assumption that extragalactic radio sources were likely to have physical dimensions or an optical brightness as great as those of normal galaxies, and although this is justified to some extent by the most recent identifications (Dewhurst 1959), it is desirable to examine this assumption further.

The radio emission from Cygnus A apparently comes from two regions on either side of the visible galaxy associated with it (Jennison and Das Gupta 1956). These regions themselves are optically dark. It is possible that the association of radio sources with galaxies may be fortuitous and that the interaction of colliding gas clouds of smaller dimensions could account for a major class of radio sources with a high spatial density and a low luminosity. Such clouds would not necessarily contain any stars and might belong to a completely new class of astronomical objects. In this paper, therefore, we shall consider radio sources which are simply bodies of gas. The question of supplying sufficient energy

to account for the radio emission provides a basis for this discussion, and this factor, taken in conjunction with the requirement for gravitational stability, will be found to reinforce the previous arguments.

The relation between the size and luminosity of an extragalactic radio source.—For a typical extragalactic radio source we will use the relation (Ryle 1958) between P in watts (c/s) $^{-1}$ ster $^{-1}$ at 80 Mc/s and ρ in pc $^{-3}$:

$$\frac{1}{3}\rho P^{3/2} = K \times 10^{14}$$

where K is found observationally to lie between limits of 2 and 4. Now it is observed that very few of these sources have angular diameters greater than 2' arc, so that if we assign a radius R (in cm) to a source we can obtain the relation

$$P^{1/2}R^{-1} \geq 3.6 \times 10^{-11}. \quad (1)$$

We may now represent possible types of source on a graph of $\log P$ against $\log R$ as in Fig. 1; the above condition shows that combinations of P and R representing real sources must lie in the area below and to the left of the line A in this graph.

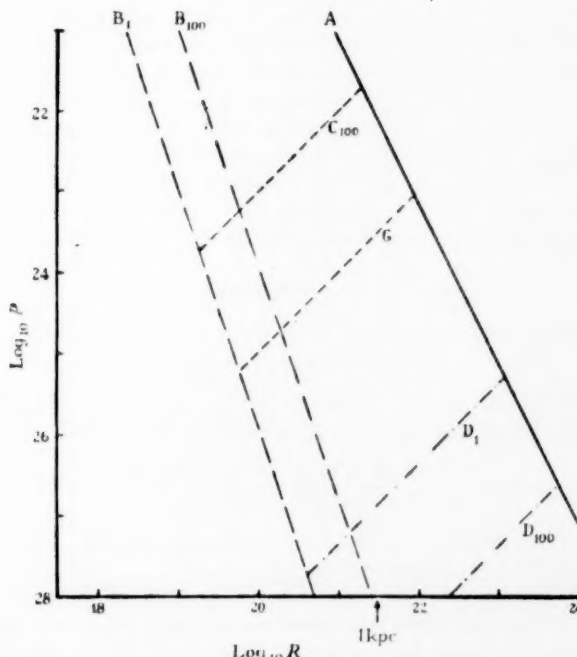


FIG. 1.—The limits on the power P (in watts (c/s) $^{-1}$ ster $^{-1}$) and size R (in cms) which may be placed on radio sources.

The energy contained in extragalactic sources.—It is generally accepted that the radio emission is the synchrotron radiation from relativistic electrons in a magnetic field. The energy of the electrons in any given source may be calculated provided the field is known, but the total energy will include the energy of the

field itself and the energy of the other fast particles which must be present. It will appear that the total energy must be so high that the balance between magnetic energy and particle energy must be such as to give a minimum total energy; otherwise the supply of sufficient total energy will be impossible. The precise balance depends on the spectrum of the electron energy, but for observed spectra it is near equipartition.

In integrating the total energy of a source, it is necessary to consider the lower limit e_0 of energy of the electrons. This is taken throughout at 10^7 eV which is just sufficient for the electrons to be counted as relativistic and therefore contributing to the radiation. By excluding electrons of energy less than e_0 we are excluding those which do not contribute to the synchrotron radiation and are estimating a minimum energy in the electrons.

Since the radio emission varies on the average as γ^{-1} (Whitfield 1957) we infer that the number of electrons in unit energy interval varies with energy e as e^{-3} , and we obtain for the total electron energy

$$\int_{e_0}^{\infty} Ke^{-3}e \, de = K/e_0$$

where $Ke^{-3}de$ is the number of electrons of energy between e and $e+de$. The energy of all fast particles will lie between this value and about one hundred times larger according to the relation of the electrons to the total cosmic-ray flux. We will denote this factor by Q . That Q is of the order of 20 is suggested by a consideration of the detailed relationship between cosmic rays and electrons (Tunmer 1959). For weak sources like the Galaxy a factor of 30 fits the observations. Values much higher than these involve very severe difficulties in the supply of energy, as will be seen later.

Synchrotron emission from an electron flux Ke^{-3} gives a power P at 80 Mc/s where

$$4\pi P = 1.43 \times 10^{-18} KH^2 \text{ watts (c/s)}^{-1}.$$

Hence the total particle energy $QK/e_0 = 6.25 \times 10^4 QK$ is

$$5.47 \times 10^{23} PQH^{-2} \text{ ergs.}$$

The total magnetic energy is $H^2 R^3/6$. If we set this equal to the total particle energy we have the following relations between H , P , R and the total energy E :

$$H = 1.34 \times 10^6 Q^{1/4} P^{1/4} R^{-3/4} \text{ gauss,} \quad (2)$$

$$E = 6 \times 10^{11} Q^{1/2} P^{1/2} R^{3/2} \text{ ergs.} \quad (3)$$

These relations have been plotted as contour lines in Fig. 2, a graph of $\log P$ against $\log R$ for various values of E and H .

An upper limit to H is provided by consideration of the observed smooth continuation of the radio spectrum down to 20 Mc/s or lower. The electrons responsible for this must have energies of at least 10^7 eV, and their critical frequency ν_c must be below $20/3$ Mc/s.

Since $\nu_c = 4.25 \times 10^6 H(e/mc^2)^2$ it may be deduced that $H < 4 \times 10^{-3}$ gauss. We can use the expression (2) above for H to show that possible combinations of P and R lie to the right of the lines B, depending on the value of Q (Fig. 1).

The source of the energy.—From the line B on Fig. 1 and the energy contour lines on Fig. 2, we can see that extragalactic sources, which according to Ryle must have $P > 10^{23} \text{ w. (c/s)}^{-1} \text{ ster}^{-1}$, require energy of at least 10^{52} ergs. It is

apparent from Table I that this could only be supplied by the translational energy of gas clouds with masses approaching those of galaxies.

TABLE I
The magnitudes of various possible sources of energy

(1)	10^{48} ergs:	the gravitational energy of the Sun in the galaxy ($10^{11} M_{\odot}$)
(2)	10^{50} ergs:	the nuclear energy released by 1 per cent M_{\odot} of hydrogen turning into helium, e.g. in a supernova.
(3)	10^{52} ergs:	the kinetic energy of a gas cloud of $10^4 M_{\odot}$ moving at 300 km/sec, the escape velocity at the Sun's orbit. (This is the same as its gravitational potential.)
(4)	10^{58} ergs:	the kinetic energy of the gas in a galaxy ($10^9 M_{\odot}$) moving at 1000 km/sec.
(5)	10^{60} ergs:	the gravitational energy of the galaxy as a whole.

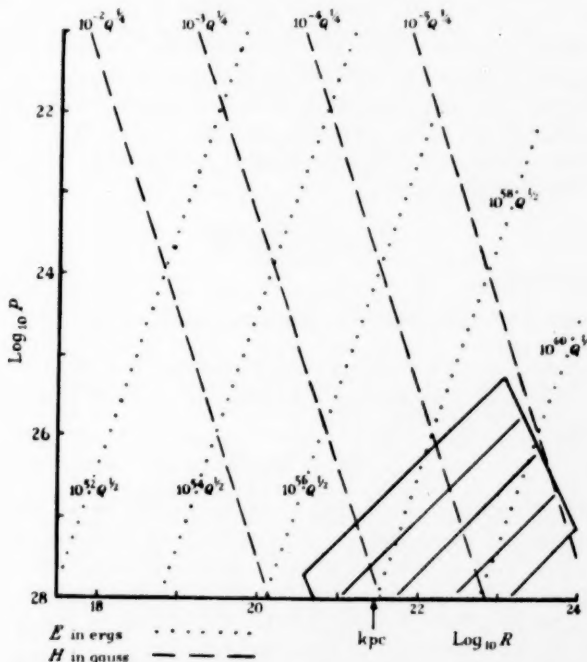


FIG. 2.—The minimum energy E and the magnetic field H which could obtain in sources of power P (in watts $(c/s)^{-1} \text{ ster}^{-1}$) and size R (in cms). Q is the factor by which the total energy in relativistic particles exceeds the energy in the relativistic electrons alone.

The kinetic energy may be converted into a magnetic field which will grow both by its compression between the two bodies and by its stretching by the irregular motions of the gas. Subsequently particles may be accelerated by the irregularities in the field. On this picture it is possible that Parker's Mach 1 principle (Parker 1958) is applicable, in which case the energy in the particles approaches that in the magnetic field and the equilibrium is maintained. The condition for minimum total energy is then satisfied.

Gravitational stability.—The total energy E in the particles and magnetic field acts as a disruptive pressure which must be contained by the gravitational potential of the whole body. This is obviously true in the case of an isolated body of gas. In the case of colliding bodies, their kinetic energy is converted into fast particles and magnetic fields of E only so long as the collision continues. But the gas clouds will start to disperse as soon as the value of E approaches that of the gravitational potential. The total energy E therefore cannot exceed the gravitational potential of the whole mass; consequently the mass must exceed the mass M_g where:

$$\gamma \frac{M_g^2}{R} = E$$

where γ is the gravitational constant. From the equation for E (3) we can show that

$$M_g = 3.0 \times 10^9 (QPR^5)^{1/4}. \quad (4)$$

Spectral index.—An upper limit for the mass of the clouds forming a typical radio source is determined by consideration of the spectral index. It is so steep that the electrons must be losing energy more quickly by synchrotron radiation than by bremsstrahlung. For this to be true the number density of hydrogen atoms may not exceed $10^9 H^2$ (Tunmer 1959). The total mass of gas must therefore be less than M_H where

$$M_H = \frac{4\pi}{3} R^3 m_1 10^9 H^2$$

or, using equation (2),

$$M_H = 2.1 \times 10^{-14}, \quad E = 12.6 \times 10^{-3} Q^{1/2} P^{1/2} R. \quad (5)$$

This upper limit is not too low for the release of kinetic energy in the collision of two gas clouds to be the source of E provided that the velocity of collision V is large enough. It is given by

$$\frac{1}{2} M_H V^2 q = E$$

where q is the efficiency of conversion of the kinetic energy to magnetic fields and fast particles. Consequently the velocity of collision must exceed $100 q^{-1/2}$ km/sec, which is certainly possible unless q is very small.

The upper limit M_H and the lower limit M_g are only consistent if $M_H \geq M_g$. This is only true for values of P and R below the lines C on Fig. 1 along which $M_H = M_g$ for the extreme values of $Q = 1$ and $Q = 100$.

The optical visibility of the radio sources.—Since very few radio sources have been identified optically, their optical luminosities must be small. They are at the same time quite massive. In this section, we shall estimate the free-free emission to be expected from the minimum mass, M_g , of hydrogen and show under what conditions it would escape detection in photographic surveys.

The energy of the collision is sufficient to ionize the hydrogen so that its temperature is at least 10^4 K. On the other hand, the power of the collision is not in general large enough to maintain the total optical radiation if the temperature much exceeds 10^6 K. Since the power emitted in unit frequency interval at $\lambda = 5500$ Å is almost independent of temperature between these two values, we may assume a temperature of 10^4 K. The power emitted by a cloud of gas of

density N and radius R at 5500 Å is $1.68 \times 10^{-10} N^2 R^3$ ergs/sec $^{-1}$ (c/s) $^{-1}$ ster $^{-1}$. We invoke the gravitational stability condition (4) which may be rewritten as

$$N^2 R^3 > 1.86 \times 10^{65} P^{1/2} Q^{1/2} R^{-1/2} \quad (6)$$

and hence shows that the power emitted is greater than

$$3.13 \times 10^{25} P^{1/2} Q^{1/2} R^{-1/2} \text{ ergs sec}^{-1} (\text{c/s})^{-1} \text{ ster}^{-1}.$$

Using a distance determined by the radio luminosity P and the flux S , we can put a lower limit on the optical flux: it is

$$3.13 \times 10^{25} \frac{Q^{1/2} S}{P^{1/2} R^{1/2}} \text{ ergs sec}^{-1} (\text{c/s})^{-1} \text{ m}^{-2}.$$

This can be converted to photovisual magnitude in the manner used by Woltjer (1958). The Sun's m_{pr} is -26.94 , its area is 2.89×10^6 square seconds of arc, and its surface emits 9.36×10^{-5} erg cm $^{-2}$ sec $^{-1}$ (c/s) $^{-1}$ at 5500 Å. The Sun's flux at the Earth is therefore 2.02×10^{-9} erg sec $^{-1}$ cm $^{-2}$ (c/s) $^{-1}$.

The radio source must therefore be brighter than m_{pr} where

$$m_{pr} = -26.94 - \frac{5}{2} \log \frac{3.13 \times 10^{21} Q^{1/2} S}{2.02 \times 10^{-9} P^{1/2} R^{1/2}} = -102.4 - \frac{5}{2} \log S + \frac{5}{4} \log \frac{PR}{Q}. \quad (7)$$

Few radio sources having a flux density S equal to or less than 10^{-24} have been identified with optical objects. We may conclude then that for these sources, $m_{pr} > +18.0$. This condition corresponds to the requirement that

$$\log \frac{PR}{Q} > 48.3. \quad (8)$$

Points satisfying it lie below the lines D on Fig. 1.

Discussion.—We have seen that various arguments limit the range of values of radio power P and size R which can represent typical radio sources.

(i) The observed number-intensity relationship and the observed limits of angular diameter place radio sources below and to the left of line A.

(ii) The condition for minimum total energy led to expressions for that energy and the magnetic field as plotted on Fig. 2. The observed smoothness of the spectrum even at low frequencies led to an upper limit for the magnetic field. Radio sources therefore must lie to right of the lines B_0 or B_{100} , depending on the distribution of energy between the relativistic electrons and all other fast particles.

(iii) Gravitational stability, together with the condition for efficient rate of loss of energy by the electrons, places the radio sources below the lines C.

(iv) The requirement of low optical visibility places radio sources below the lines D.

Radio sources must therefore lie in the area of the P - R diagram between the lines A and B and below D on Fig. 1. This area is shaded in Fig. 2. We can see that the minimum power within this area at the intersection of D and A is 2×10^{25} watts ster $^{-1}$ (c/s) $^{-1}$ or approximately 1 per cent of the power of Cygnus A. The minimum energy at the intersection of B and D is, from Fig. 2, $4 \times 10^{36} Q^{1/2}$ ergs.

If more accurate measurements show that the angular diameter limit is less than 2' arc, the line A will be shifted to the left and its intersection with D will be at even higher values of P . If the fast particle energy is not mostly in the electrons, i.e. $Q > 1$, the limiting line D which is applicable is lower. Again this possibility increases the minimum value of P . At each stage in our discussion the extreme

values have been taken, i.e. the minimum stored energy and the minimum mass which could maintain gravitational stability. It is therefore most probable that the lower limit of P which we have derived is a very conservative estimate.

We have assumed throughout this paper that it is the mass of gas alone which maintains gravitational stability, and so it is possible to put a lower limit on it (M_g). This argument fails however if a mass of condensed material, for example stars greater than M_g , is allowed. Then the criterion of gravitational stability is that

$$\frac{\gamma M_{\text{gas}} \times M_{\text{condensed matter}}}{R} > E \quad (9)$$

and it is not possible to put a lower limit on the mass of gas. On the other hand, if the mass of condensed matter is in stars with normal luminosities, the sources are simply galaxies. Then, from expression (9), the known ratios of the mass of gas to stars and the mass-luminosity ratios for different classes of galaxies, the optical luminosity may be estimated. This gives a minimum power of 5×10^{25} watts ster $^{-1}$ (c/s) $^{-1}$.

It is possible that sources are short-lived and their temperatures are very high indeed, e.g. 10^8 K. The free-free emission which above a million degrees varies at $T^{-1/2}$ at $\lambda = 5500$ Å, will be less and the limits D_0 and D_{100} must be raised towards lower values of P . The limits C_0 and C_{100} will remain, however.

Conclusion.—The power of radio sources must be at least of the order of 1 per cent of the power of Cygnus A. This is true whether they are purely gaseous or normal galaxies. They could be less powerful only if they were massive associations of under-luminous stars. Even with this exception in mind, it is reasonable to assume that $P > 2 \times 10^{25}$ and hence that the observed number-intensity relationship should be sensitive to cosmological effects.

*Mullard Radio Astronomy Observatory,
Cavendish Laboratory,
Cambridge:
1959 August.*

References

- D. W. Dewhurst, 1960 (in preparation).
- R. C. Jennison and M. K. Das Gupta, 1956. *Phil. Mag. Ser. 8*, **1**, 65.
- E. N. Parker, 1958. *Phys. Rev.*, **109**, 1328.
- M. Ryle, 1958. *Proc. Roy. Soc. A.*, **248**, 289.
- H. E. C. Tunmer, 1959. *M.N.*, **119**, 184.
- G. Whitfield, 1957. *M.N.*, **117**, 680.
- L. Woltjer, 1958. *B.A.N.*, **14**, 39.

GRAVITATION AND THE PRINCIPLE OF STATIONARY ACTION

C. Gilbert

(Received 1959 September 16)*

Summary

A quadratic action principle is used to derive equations for pure gravitational fields. Matter is described by solutions of the field equations which are free from singularities and have a non-vanishing action density. A cosmological model is determined by this type of "matter-field", but the discrete nature of matter in the universe is taken into account by replacing parts of the matter-field by mass particles of equal action and by free-space solutions of the field equations. Inertial systems are defined by the matter-field and the inertial mass of a particle is defined from the form of its action. The inertial mass is not constant, but varies as $(\text{epoch})^{1/2}$.

The properties of the model are shown to agree with results found by Dirac for a cosmological model. Also the equations of motion of free particles in a local field are shown to be approximately the same as the Newtonian equations of motion under an inverse square law of attraction with the gravitational power of matter proportional to $(\text{epoch})^{-1/2}$. For small angular velocities there are paths which are equiangular spirals, and it is shown how these paths can give rise to spiral arms in a galaxy.

A brief discussion is given of the relation of the model to the Einstein-de Sitter universe, and of certain resemblances to E. A. Milne's kinematic model.

1. *Introduction.*—The gravitational field equations adopted by Einstein for free-space were

$$G_{ij} = 0, \quad (1)$$

where G_{ij} is the Ricci tensor of a Riemannian space-time. It is well-known that these equations may be derived from a principle of stationary action, with an action density $G\sqrt{-g}$, where G is the scalar curvature and g is the determinant $|g_{ij}|$ formed from the components of the fundamental tensor g_{ij} . In consequence of the equations (1) the action density is identically zero, so that these equations cannot be used to describe the field in a region containing matter, unless the material particles generating the field are situated at singular events. When matter can occur at non-singular events, we shall call the field a *matter-field*. In order to describe such a field in Einstein's theory one has to introduce additional terms on the right-hand side of equation (1), which include the energy-momentum tensor. Since matter is composed of charged particles this tensor will in general include the energy of the electromagnetic field. The field equations then imply the principles of the conservation of mass and the conservation of charge.

If instead of deriving field equations from the linear action principle, one derives them from the quadratic action principle

$$\delta \int G^2 \sqrt{-g} dV^4 = 0, \quad (2)$$

where dV^4 is the element of coordinate 4-volume, one finds that matter-fields can be determined from the equations without the use of an energy-momentum

* Received in original form 1959 January 5

tensor. This is because, instead of the condition $G=0$, of the linear action principle, the field equations then give the condition

$$\Delta G=0, \quad (3)$$

where Δ is the operator $g^{ij}(\quad)_{ij}$, the comma denoting covariant differentiation, and solutions of the equations (3) exist for which $G \neq 0$. The action does not therefore necessarily vanish, and the field of matter can be determined from solutions of the field equations which are free from singularities.

The field equations used in this paper are derived from the variational principle (2). They determine pure gravitational fields, and the theory is not linked with any specific theory of electricity, although it is possible that it may be associated with either the unified field theory of H. Weyl (1), or that of C. Lanczos (2). The matter field of a cosmological model is determined from solutions of these field equations. The matter is assumed to exist in the form of mass particles, without random motions, and having a uniform average density throughout space. The particles are assumed to be of finite size and the action of a particle in any time-interval is assumed to be equal to the action of that part of the matter-field which it replaces in the same time-interval. Each particle generates a local gravitational field which joins onto the matter-field at a 3-space where certain boundary conditions are satisfied.

We shall make use of the postulates and principles stated below.

- A. The geometry of space-time is Riemannian.
- B. The field equations are derived from the principle of stationary action (2).
- C. The cosmological principle.
- D. The principle of equivalence in a restricted form.
- E. Mach's principle.

F. On the small-scale the action is discontinuous, and an elementary particle is a world-tube in free-space, with a non-singular action density in the interior of the tube.

G. The action density is invariant under transformations to conformal space-times.

(The transformations are equivalent to the gauge transformations in Weyl's generalized geometry (1). In the following work frequent use will be made of the gauge in which the action in any space-time volume is proportional to the invariant volume. In the case of the large-scale, or the average field, this will be called the *natural gauge*, and in the case of a local centrally symmetric field it will be called the *local gauge*. When the average field is defined by the fundamental tensor g_{ij} alone, proper intervals will be said to be measured in the *geodetic gauge*.)

H. When the invariant interval in the natural gauge is separated into a cosmic time interval and an orthogonal space interval, the world-tube of an elementary particle has a time-section of constant radius.

I. The proper period of monochromatic light emitted by a particle, which is at rest relative to the mean motion of the matter in its immediate neighbourhood, is constant in the natural gauge.

J. The path of a free particle is a geodesic of the quadratic form for the geodetic gauge.

In the following discussion it will be assumed that the line element for the model is written in the form of equation (30), where x^a are spatial coordinates of a co-moving coordinate system, and t is cosmic time.

A solution of the field equations giving a matter-field for a cosmological model is obtained in Section 3. On account of the observed discrete nature of matter in the universe this solution is assumed to give the average field for a model in which matter has been smoothed out uniformly throughout space, and on the small-scale the action is assumed to be discontinuous (postulate F). The average field is therefore assumed to describe the large-scale properties of a model in which matter exists in the form of world-tubes separated by free-space solutions of the field equations. We consider one world-tube and join the associated free-space field onto the average field. The free-space field is defined by a Schwarzschild line element with the cosmological constant $\Lambda=0$, but more information is obtained from the boundary conditions by assuming this field to be the limiting case of fields with $\Lambda \neq 0$.

Boundary conditions play an essential part in the theory and the gauge transformations were first introduced in order to make certain solutions satisfy these conditions. From Weyl's generalization of Riemannian geometry it is known that these transformations leave the field equations unchanged. The meaning of the boundary conditions, which are derived in Section 2, may be understood by considering the effect of replacing a world-tube of matter in the average field, bounded by the world-lines $x^a = \text{constant}$, by the world-tube of an elementary particle and its associated centrally symmetric field. In so far as the principle of stationary action is concerned the impact of the change on the exterior average field comes through the 3-dimensional surface integral for small arbitrary variations of the field variables on the surface. The question arises as to whether the substitution of the centrally symmetric field can be made, without affecting the surface integral, if certain conditions are satisfied at the surface? It is found that this is indeed the case, when the average field has zero spatial curvature, provided the additional variables given by the gauge transformations are introduced.

The significance of the gauge transformations is also apparent from a different point of view. On account of the discontinuity of the action at a 3-space separating different regions of space-time, some, or all, of the components of the fundamental tensors and their first derivatives may be discontinuous at the 3-space. There is therefore no *a priori* reason why the Riemannian geometry of these different regions should be based on the same standards of interval measurement. (In the case when the fundamental tensors and their first derivatives are continuous it is assumed that standards may be compared by parallel transport). By introducing the gauge transformations the geometry of the whole of space-time may be described in terms of one of these standards of interval measurement. From this point of view postulate G is a natural consequence of postulate F.

Postulate J may be considered to be a consequence of both D and E. Since mass particles do not occur as singularities of the field, the usual method of derivation of the path of a free particle cannot be used (3). It is possible that the equations of the free paths could be derived from the field equations by a suitable method, but without such a method at hand we assume the form of the equations and justify the assumption by use of the principles D and E. At any space-time event in the average field a transformation of the coordinates can be made such that the first derivatives of the metric tensor are zero in the neighbourhood of the event. Then by an appeal to the principle of equivalence, the general equations of the paths in the field may be derived as a natural generalization of these equations

in the special theory of relativity. The principle of equivalence is not used in this manner to determine the equations of the free paths in the local field (this is the restriction on the use of the principle), because then the influence of all the other masses in the universe on the motion of a free particle would be neglected. Instead Mach's principle is taken into account by making the paths continuous at the boundary with the paths in the average field. This is achieved by assuming that the paths are geodesics of the quadratic form determined by the geodetic gauge of the average field.

In Section 5 inertial systems are defined and the concept of inertial mass is derived from the form of the action of a mass particle. The inertial mass of a particle is found to be proportional to $T^{1/2}$, where T is the measure of the epoch in the inertial system, and a free particle is shown to have constant momentum. Also in Section 7 it is shown that the equations of motion in the neighbourhood of an attracting mass have approximately the Newtonian form, with the gravitational power of matter proportional to $T^{-1/2}$. The paths given by this law of force were calculated long ago by J. H. Jeans (4), who found that certain paths were equiangular spirals. These paths are assumed to be described by matter which is continually detached from the rim of a rotating nucleus of a galaxy, so as to form spiral arms, in the manner suggested by E. A. Milne (5, 6). The equation of a spiral arm is obtained in very nearly the same form as that found by Milne.

Postulates H and I are based on the assumption that the natural gauge gives a fundamental system of measurement in atomic physics. It appeared necessary to make this assumption in order to get agreement with Dirac's principle (7) for measurements made in an inertial system. In the models of relativistic cosmology the unit of measurement of the distance coordinate is undefined, but in the present case, on account of H, we are able to define the unit in terms of the radius of an elementary particle. The constant t_0 which appears throughout the work makes the measures of proper intervals and of intervals of coordinate time in the different gauges, equal to the values they would have in the natural gauge at epoch t_0 . The description of the model in terms of atomic units is, however, independent of t_0 , the constant being completely absorbed in the measures of the atomic quantities.

The main conclusions are:

- (1) A cosmological model is determined by solutions of the field equations derived from the quadratic action principle, which are free from singularities.
- (2) Inertial systems are determined by all the masses in the universe, in accordance with Mach's principle, and in these systems the gravitational power of matter is proportional to $T^{-1/2}$.
- (3) The value of Hubble's constant is $\frac{1}{2}T^{-1}$.
- (4) The properties of the model are in agreement with results derived from Dirac's principle.
- (5) The paths of free particles in a local gravitational field are geodesics of a metric which is conformal to the Schwarzschild metric. These paths do not differ appreciably from the geodesic paths in the latter field for the cases of astronomical interest in the solar system but, in the galaxy, matter with small angular velocity will spiral away from the nucleus.
- (6) The theory gives support to Milne's gravitational theory of the formation of spiral arms in a galaxy.

Notation.—Latin suffixes take the values 1, 2, 3, 4 and Greek suffixes the values 1, 2, 3, with summation for a repeated suffix in each case, except that when explicitly stated Greek suffixes have the values 2, 3, 4. The time coordinate is x^4 and spatial coordinates are x^a . When spatial polar coordinates are used x^1 is the distance coordinate.

2. *The field equations and boundary conditions.*—In Weyl's theory (1) the metrical structure of space-time is characterized by a quadratic form

$$ds^2 = g_{ij} dx^i dx^j \quad (4)$$

and a linear form

$$dl/l = \kappa_i dx^i, \quad (5)$$

where dl is the change of length of a displacement which is carried by parallel transport from x^i to an infinitely near event $x^i + dx^i$. The g_{ij} and κ_i are general functions of the coordinates, and the forms (4) and (5) are said to define a gauge-system, which is invariant under transformations of the coordinates. The metrical structure of a domain is also invariant under gauge transformations, which are made by replacing g_{ij} and κ_i by the quantities $\chi^2 g_{ij}$, $\kappa_i + (1/\chi) \partial \chi / \partial x^i$, where χ is a scalar function of the coordinates.

When the κ_i have the form of a gradient 4-vector

$$\kappa_i = -\partial \sigma / \partial x^i = -\sigma_i, \quad (6)$$

where σ is a scalar function of the coordinates, the Weyl space is Riemannian. It is then possible, by a change of gauge, to make the linear form vanish everywhere and to transform the quadratic form into

$$d\tilde{s}^2 = \tilde{g}_{ij} dx^i dx^j, \quad (7)$$

where

$$\tilde{g}_{ij} = e^{2\sigma} g_{ij}. \quad (8)$$

The gauge will then be said to be geodetic.

We write G_{ij} , G and G_{ij} , G for the Ricci tensors and curvatures of (4) and (7) respectively, and we assume that G is proportional to $e^{-2\sigma}$. Then

$$G = (G + 6\sigma_i^i + 6\sigma^i \sigma_i) e^{-2\sigma} = 4\Lambda e^{-2\sigma}, \quad (9)$$

where Λ is a constant, $\sigma^i = g^{ij} \sigma_j$ and $\sigma_i^i = \frac{1}{\sqrt{-g}} \frac{\partial}{\partial x^i} (\sigma^j \sqrt{-g})$.

The action \mathcal{A} of the gravitational field, in a region \mathcal{R} of the space-time (7), will be defined by

$$\mathcal{A} = \frac{C}{8\Lambda} \int G^2 \sqrt{-\tilde{g}} dV^4. \quad (10)$$

The integral is taken throughout \mathcal{R} , C is a constant giving \mathcal{A} the dimensions of action, $\tilde{g} = |\tilde{g}_{ij}|$ and $dV^4 = dx^1 dx^2 dx^3 dx^4$. We find from (8), (9) and (10) that \mathcal{A} is proportional to the invariant volume when the quadratic form is (4). The system of measurement will then be called the natural gauge, or the local gauge.

The principle of stationary action

$$\delta \mathcal{A} = \frac{C}{8\Lambda} \delta \int G^2 \sqrt{-\tilde{g}} dV^4 = 0, \quad (11)$$

for small arbitrary variations δg_{ij} , $\delta(\partial g_{ij} / \partial x^k)$, $\delta \sigma_i$, $\delta \sigma$ will be used to derive field equations. When the field in a region \mathcal{R} bounded by a V_3 is considered without reference to external conditions, it will be assumed that the small variations are

zero on V_3 . On the other hand, when the fields in different regions $\mathcal{R}_1, \mathcal{R}_2$ have a common boundary V_3 , this assumption will not be made and the boundary conditions will be deduced from the integrals over V_3 .

The variation of the action $\delta\mathcal{A}$ may be written as the sum of an integral I_1 throughout \mathcal{R} and an integral I_2 over V_3 . These integrals may be readily deduced from expressions given by Eddington (8). If V_3 has the equation $x^1 = \text{constant}$, we find

$$I_1 = C \int [\{ - (G^{ij} - \frac{1}{2}g^{ij}G) + 6(-\sigma^i\sigma^j + \frac{1}{2}g^{ij}\sigma_k\sigma^k) - \Lambda g^{ij} \} \delta g_{ij} - 12\sigma_i^i \delta\sigma] \sqrt{-g} dV^4, \quad (12)$$

$$I_2 = C \int \left[g^{ij} \sqrt{-g} \delta \left(\frac{\partial \mathcal{L}}{\partial g_{ij}} \right) + 6\delta(\sigma^1 \sqrt{-g}) + 12\sigma^1 \sqrt{-g} \delta\sigma \right] dS_1, \quad (13)$$

where

$$dS_1 = dx^2 dx^3 dx^4, \quad g_1^{ij} = \frac{\partial}{\partial x^1} (g^{ij} \sqrt{-g})$$

and \mathcal{L} is the generalized Lagrangian formed from the Riemann-Christoffel symbols $\{ij, k\}$,

$$\mathcal{L} = g^{ij} \sqrt{-g} [\{il, m\} \{jm, l\} - \{ij, l\} \{lm, m\}]. \quad (14)$$

When use is made of the symmetric properties of δg_{ij} and $\delta(\partial g_{ij}/\partial x^k)$ with respect to interchange of the suffixes i and j , we find from (13) and (14)

$$I_2 = C \int \left[\left(g^{ij}g^{1k} - \frac{1}{2}g^{ik}g^{1j} - \frac{1}{2}g^{il}g^{jk} \right) \delta \left(\frac{\partial g_{ij}}{\partial x^k} \right) + \left\{ \frac{1}{4} (2g^{ln}g^{il}g^{jm} + 2g^{ln}g^{jl}g^{im} - 2g^{ln}g^{il}g^{jm} - g^{lm}g^{il}g^{jn} - g^{lm}g^{jl}g^{in}) \frac{\partial g_{lm}}{\partial x^n} \right. \right. \\ \left. \left. - 3\sigma^j g^{il} - 3\sigma^l g^{ij} + 3\sigma^1 g^{ij} \right) \delta g_{ij} + 6g^{il} \delta\sigma_i + 12\sigma^1 \delta\sigma \right] \sqrt{-g} dS_1. \quad (15)$$

Since $\delta g_{ij}, \delta\sigma$ are arbitrary, their coefficients in the integrand of (12) must be zero. We thus obtain the field equations, which may be written in the form

$$G_{ij} + 6\sigma_i\sigma_j = \Lambda g_{ij} \quad (16)$$

$$\sigma_i^i = 0. \quad (17)$$

These equations can also be derived from results obtained by H. A. Buchdahl (9).

We now consider the boundary conditions at V_3 when the fields in \mathcal{R}_1 and \mathcal{R}_2 have fundamental tensors $g_{ij}^{(1)}, g_{ij}^{(2)}$ and 4-vectors $-\sigma_i^{(1)}, -\sigma_i^{(2)}$. We assume that the fields are centrally symmetric, that $\sigma^{(1)}$ and $\sigma^{(2)}$ are functions of x^4 only, and that V_3 is the hypersurface $x^1 = a$, where a is a constant and spatial polar coordinates are used. Then $g_{ia}^{(1)} = g_{ia}^{(2)} = 0$, ($i \neq x, x = 2, 3$), $\sigma_\beta^{(1)} = \sigma_\beta^{(2)} = 0$, ($\beta = 1, 2, 3$), and in the variational principle the variations of these components, and their derivatives may be set equal to zero. Let us assume for the moment that suitable boundary conditions have been found which enable the fields to be joined at $x^1 = a$ in such a manner that the principle of stationary action is fulfilled for arbitrary small variations of the field quantities. At $x^1 = a$ relations then exist between the field quantities for \mathcal{R}_1 and those for \mathcal{R}_2 and in consequence some, or all, of the arbitrary small variations of the field quantities for \mathcal{R}_1 can

be expressed linearly in terms of arbitrary small variations of the field quantities in \mathcal{R}_2 . Conversely in order to determine the boundary conditions we make an assumption concerning the linear dependence of the arbitrary small variations of the field quantities. We investigate the simple assumption that the arbitrary small variations of the non-vanishing quantities for the two fields satisfy the relations

$$\delta\sigma^{(1)} = \delta\sigma^{(2)}, \quad \delta\sigma_4^{(1)} = \delta\sigma_4^{(2)}, \quad (18)$$

$$\delta g_{ij}^{(1)} = \delta g_{ij}^{(2)}, \quad \delta(\partial g_{ij}^{(1)}/\partial x^k) = \delta(\partial g_{ij}^{(2)}/\partial x^k), \quad (i=j), \quad (19)$$

$$\delta g_{41}^{(1)} = \delta g_{41}^{(2)}, \quad \delta(\partial g_{41}^{(1)}/\partial x^k) = \delta(\partial g_{41}^{(2)}/\partial x^k). \quad (20)$$

From the principle of stationary action (11) we find that equations of the forms (16) and (17) must be satisfied by each of the fields, and that in addition

$$I_2^{(1)} = I_2^{(2)}, \quad (21)$$

where $I_2^{(1)}, I_2^{(2)}$ are integrals of the form (13) for each of the fields. All the small variations in (21) can be expressed in terms of arbitrary variations

$$\delta g_{ij}^{(1)}, \quad \delta(\partial g_{ij}^{(1)}/\partial x^k), \quad \delta\sigma^{(1)}, \quad \delta\sigma_4^{(1)}$$

by use of (18), (19) and (20), and the coefficient of each of these variations in the integrand must therefore vanish. This gives the boundary conditions at V_3 , which may be stated in the form that the following expressions must be continuous at $x^1 = a$:

$$\sqrt{-g} g^{41} \quad \text{and} \quad \sqrt{-g} \sigma^1, \quad (22)$$

$$\sqrt{-g} (g^{ij} g^{k1} - \frac{1}{2} g^{ik} g^{j1} - \frac{1}{2} g^{jk} g^{i1}), \quad (23)$$

$$\begin{aligned} \frac{1}{4} \sqrt{-g} \left[(2g^{ln} g^{mj} g^{i1} + 2g^{ln} g^{mj} g^{j1} - 2g^{li} g^{mj} g^{n1} - g^{lm} g^{nj} g^{i1} - g^{lm} g^{ni} g^{j1}) \frac{\partial g_{lm}}{\partial x^n} \right. \\ \left. - 12\sigma^j g^{i1} - 12\sigma^i g^{j1} + 12\sigma^1 g^{ij} \right], \end{aligned} \quad (24)$$

with $i=j$, or $i=4, j=1$ in (23) and (24).

In order to satisfy (22) we take $g_{41}^{(1)} = g_{41}^{(2)} = 0$ at $x^1 = a$. Then we find from (23) that the values of $\sqrt{-g} g^{11} g^{za}$, ($z = 2, 3, 4$, not summed) are continuous at $x^1 = a$. Hence we have

$$[g_{ij}^{(1)}] = [g_{ij}^{(2)}] e^{2\omega}, \quad (i=j) \quad (25)$$

where ω is in general a function of x^2, x^3, x^4 and the bracket signifies that the values of the quantities are calculated at $x^1 = a$. Also from (24) we find when $i=j$, and $i=4, j=1$ respectively that

$$g^{za} \frac{\partial g_{za}}{\partial x^1}, \quad (z = 2, 3, 4, \text{ not summed}) \quad (26)$$

and

$$g^{11} \frac{\partial g_{11}}{\partial x^4} + g^{22} \frac{\partial g_{22}}{\partial x^4} + g^{33} \frac{\partial g_{33}}{\partial x^4} - g^{44} \frac{\partial g_{44}}{\partial x^4} + 12\sigma_4, \quad (27)$$

are continuous at $x^1 = a$.

If we write

$$\gamma_{ij} = e^{b(\sigma-b)} g_{ij}, \quad (28)$$

where b is an arbitrary constant, the conditions (25), (26) and (27) are satisfied, provided that

$$\gamma_{ij}, \frac{\partial \gamma_{ij}}{\partial x^1}, \frac{\partial \gamma_{ab}}{\partial x^1}, (i=j, a=\beta=2, 3, 4) \quad (29)$$

are continuous at $x^1 = a$.

When σ is discontinuous at $x^1 = a$, the metrics for \mathcal{R}_1 and \mathcal{R}_2 with fundamental tensors $g_{ij}^{(1)}$, $g_{ij}^{(2)}$ give measures of proper intervals between any two events in the hypersurface $x^1 = a$, which are in the ratio $\exp\{3(\sigma^{(1)} - \sigma^{(2)}) - 3(b^{(1)} - b^{(2)})\}$ to 1. In order to describe the geometry of the whole of V_4 with one system of measurement, the gauge must be changed in at least one of the regions \mathcal{R}_1 and \mathcal{R}_2 .

3. *The solution for an expanding universe.*—We shall now find solutions of the field equations (16) and (17) when (4) has the form of the line element for a cosmological model. It has been shown by H. P. Robertson (10) and A. G. Walker (11), from general considerations based on the hypotheses of homogeneity and isotropy, that this line element has the form

$$ds^2 = c^2 dt^2 - R^2 h_{\alpha\beta} dx^\alpha dx^\beta, \quad (30)$$

where c is a constant, R is a function of t only, and $h_{\alpha\beta}$ is the fundamental tensor of a 3-space of constant curvature $k = -1, 0$, or $+1$. Then the lines of parameter t are geodesics giving the world-lines of fundamental observers, who are at rest relative to the mean motion of matter in their neighbourhood, and light paths are the null geodesics.

From the equations (16) we find

$$\frac{\ddot{R}}{R} + \frac{2(\dot{R}^2 + kc^2)}{R^2} = \Lambda c^2, \quad (31)$$

$$3\frac{\dot{R}}{R} + 6\dot{\sigma}^2 = \Lambda c^2, \quad (32)$$

where the dot denotes differentiation with respect to t . From (31) we find

$$\dot{R}^2 = -kc^2 + A^2/R^4 + \frac{1}{3}\Lambda R^2 c^2, \quad (33)$$

where A is a constant of integration, and from (32) and (33) we find

$$\dot{\sigma} = \pm A/R^3. \quad (34)$$

This value of $\dot{\sigma}$ satisfies equation (17), and the solution of the field equations may therefore be found by integrating (33) and (34) to obtain R and σ as functions of t . It will, however, be more convenient at present to use a dimensionless coordinate σ instead of the time coordinate t . Then writing $R(t) = R'(\sigma)$, the metric (30) becomes

$$ds^2 = c_0^2 R'^6 d\sigma^2 - R'^2 h_{\alpha\beta} dx^\alpha dx^\beta, \quad (35)$$

where $c_0 = c/A$ is a constant having the dimensions of a length.

Also from (33) and (34)

$$\left(\frac{dR'}{d\sigma}\right)^2 = -kc_0^2 R'^6 + R'^2 \pm \alpha^2 R'^8, \quad (36)$$

where

$$\alpha^2 = |\Lambda| c_0^2/3, \quad (37)$$

and the upper and lower signs in the last term of (36) correspond to positive and negative values of Λ respectively.

In the case $k=0$, we find the following solutions:

$$(i) \quad \Lambda > 0, \quad R'^{-3} = \alpha \sinh 3(d - \sigma), \quad (38)$$

$$(ii) \quad \Lambda < 0, \quad R'^{-3} = \alpha \cosh 3(d - \sigma), \quad (39)$$

$$(iii) \quad \Lambda = 0, \quad R' = e^{\sigma - d'}, \quad (40)$$

where d, d' are arbitrary constants. Case (iii) may be considered to be the limiting case of (i), or (ii), when $\alpha \rightarrow 0$ and $d \rightarrow \infty$ so that

$$\lim_{\alpha \rightarrow 0, d \rightarrow \infty} (e^{3d}\alpha/2) = e^{3d'}. \quad (41)$$

If we write

$$e^{3d'} = t_0^{-1}, \quad e^\sigma = (t/t_0)^{1/3}, \quad (42)$$

the metric (35) becomes

$$ds^2 = c^2 dt^2 - t^{2/3} k_{\alpha\beta} dx^\alpha dx^\beta, \quad (43)$$

where $c = c_0/3$ and $k_{\alpha\beta}$ is the fundamental tensor of the 3-space with $k=0$. Then writing

$$T = \frac{3}{4} t^{4/3} t_0^{-1/3}, \quad T_0 = \frac{3}{4} t_0, \quad (44)$$

the metric for the geodetic gauge is

$$ds^2 = c^2 dT^2 - t_0^{2/3} \left(\frac{T}{T_0} \right) k_{\alpha\beta} dx^\alpha dx^\beta. \quad (45)$$

4. *The mass particle in an expanding universe.*—When the quadratic form (4) has a centrally symmetric form with g_{ij} independent of x^i , it is found that equations (16) and (17) have solutions with $\sigma_4 = \text{constant}$. We consider only the case $\sigma_4 = 0$ which gives the Schwarzschild exterior solution of Einstein's equations for free-space. Taking spatial polar coordinates $x^1 = \rho$, $x^2 = \theta$, $x^3 = \phi$, and a time coordinate $x^4 = \tau$, the metric can be written

$$ds'^2 = c^2 e^\beta d\tau^2 - e^\beta d\rho^2 - \rho^2 d\theta^2 - \rho^2 \sin^2 \theta d\phi^2, \quad (46)$$

where

$$e^\beta = 1 - \frac{2\Gamma m}{c^2 \rho} - \frac{\Lambda'}{3} \rho^2. \quad (47)$$

In this solution Λ' has been written for Λ in equation (16), and Γ, m are constants. In Einstein's theory Γ is the gravitational constant and m the gravitational mass, but we shall use these terms to describe different quantities later on.

We shall now show that, when $k=0$, the field of the mass particle can be joined onto the field of the expanding universe so as to satisfy the boundary conditions (29). Let the 3-space with fundamental tensor $k_{\alpha\beta}$ be described in terms of polar coordinates (r, θ, ϕ) , and let $b=0$ in (28). Then γ_{ij} can be taken to be the fundamental tensor of a quadratic form

$$ds'^2 = c^2 dt'^2 - S(t')^2 (dr^2 + r^2 d\theta^2 + r^2 \sin^2 \theta d\phi^2), \quad (48)$$

where

$$c_0 e^{3\sigma} R'(\sigma)^3 d\sigma = c dt', \quad e^{3\sigma} R'(\sigma) = S(t'). \quad (49)$$

From (49) we find for both the cases (i) and (ii) given by (38) and (39), that

$$\frac{c_0^2}{c^2} \left(\frac{dS(t')}{dt'} \right)^2 = \frac{8\alpha e^{3d}}{S(t')} + \alpha^2 e^{-6d} S(t')^2. \quad (50)$$

On the other hand γ_{ij} for the local field is the fundamental tensor of (46), since for this field $\sigma = \text{constant}$.

The conditions (29) which must be satisfied by γ_{ij} are included in the conditions derived by S. O'Brien and J. L. Synge (12). It has been shown (13) that the latter conditions can be satisfied at a 3-space $r=a$, by taking

$$\tau = \tau(t', r), \quad \rho = S(t')r, \quad (51)$$

provided that

$$\left(\frac{dS(t')}{dt'} \right)^2 = \frac{2\Gamma m}{a^3 S(t')} + \frac{\Lambda' c^2}{3} S(t')^2. \quad (52)$$

Comparing (50) and (52) we find that the conditions (29) are satisfied at $r=a$, provided that

$$\alpha e^{3d} = \frac{\Gamma m c_0^3}{4a^3 c^2}, \quad \alpha^2 e^{-6d} = \frac{\Lambda' c_0^2}{3}. \quad (53)$$

Λ' is therefore positive, and from (37) and (53) we deduce

$$e^{6d} = \frac{|\Lambda|}{\Lambda'}, \quad \frac{\Gamma m}{a^3} = \frac{4c^2 |\Lambda|}{c_0 \sqrt{3\Lambda'}}. \quad (54)$$

In the limiting case $\Lambda=0$, $\Lambda'=0$ we find from (41), (42) and (54) that

$$\text{Limit}_{\Lambda=0, \Lambda'=0} \frac{c_0 |\Lambda|}{\sqrt{3\Lambda'}} = \frac{2}{t_0}, \quad (55)$$

$$\frac{\Gamma m}{a^3} = \frac{8}{9t_0}. \quad (56)$$

In this case we also find from (40), (42) and (49) that we can write

$$t' = t^2/2t_0 \quad (57)$$

and hence the quadratic form (48) becomes

$$ds'^2 = c^2 dt'^2 - \left(\frac{4}{t_0}\right)^{2/3} t'^{4/3} k_{ab} dx^a dx^b. \quad (58)$$

This metric gives measures of intervals in the local gauge, and is similar to the metric of an Einstein-de Sitter universe (14) but the description in the geodetic gauge will be shown to be more significant, and this will lead to different properties of the model.

5. *Inertial systems*.—E. Mach held the view that the inertia of matter is due to the presence of other matter, and that the inertial frames are determined by all the masses in the universe (15). These ideas of Mach are incorporated in a cosmological model by the following steps:

(i) The matter-field solution of Section 3 is assumed to give the average field of a cosmological model consisting of mass particles, and an inertial system is defined to be a system of reference at a given event for which spatial and temporal coordinates are natural coordinates for the average field in the geodetic gauge.

(ii) Mass particles and their associated Schwarzschild fields replace the average field in regions of space-time, in the manner described in Section 4, and the action of a particle is equal to the action of that part of the average field which it replaces.

(iii) The inertial mass of a particle is defined by making the action of a particle in a local inertial system similar to action in mechanics.

We consider the limiting case $\Lambda=0$, $\Lambda'=0$ for which the average field in the geodetic gauge is defined by (45). Then at an event having coordinates (T, x^a) we can define local coordinates

$$\xi^a = t_0^{1/3} \left(\frac{T}{T_0}\right)^{1/2} x^a \quad (59)$$

such that the metric locally has the form

$$d\bar{s}^2 = c^2 dT^2 - (d\xi^1 + d\xi^2 + d\xi^3)^2. \quad (60)$$

Then the metric (60) will define the local inertial system at the event*.

In the general formula (10) for the action \mathcal{A} , we can choose any value of C which will give \mathcal{A} the form of action in mechanics, but the same value of C must be used in different regions $\mathcal{R}_1, \mathcal{R}_2$ in order that the boundary conditions shall be applicable. We find it convenient to take the value

$$C = \frac{c^3}{4\pi\Gamma} \frac{\Lambda}{\Lambda'}, \quad (61)$$

Then in the limiting case $\Lambda = 0, \Lambda' = 0$ we find that there is a non-vanishing action density for the average field. Calculating the action in the region between the hypersurfaces $x^1 = a, T = T_1, T = T_2$, we find in this limiting case from (9), (10), (43) and (44)

$$\mathcal{A} = \frac{2}{3} c^4 a^3 t_0 \underset{\Lambda=0, \Lambda'=0}{\text{Limit}} \left(\frac{\Lambda^2}{\Gamma \Lambda'} \right) \int_{T_1}^{T_2} \left(\frac{T}{T_0} \right)^{1/2} dT. \quad (62)$$

Using (55), (56) and remembering that $c = c_0/3$, we find

$$\mathcal{A} = \int_{T_1}^{T_2} m \left(\frac{T}{T_0} \right)^{1/2} c^2 dT. \quad (63)$$

Since dT is the interval of proper cotime in the local inertial system, the equation (63) shows that \mathcal{A} has the form of action in mechanics if the inertial mass of the matter in the 3-space is

$$m_i = m(T/T_0)^{1/2}. \quad (64)$$

When the average field in the region is replaced by a mass particle and its associated Schwarzschild field, the action of the latter field is zero. This is because the action is equal to the invariant volume occupied by the field multiplied by the factor $\underset{\Lambda=0, \Lambda'=0}{\text{Limit}} (2C\Lambda')$, which vanishes on account of (61). Hence

all the action (63) is equal to the action of the particle and m_i is identified with the inertial mass of the particle.

By the postulate J the equations of the free paths in the field are given by

$$\delta \int d\bar{s} = 0. \quad (65)$$

From the metric (45) we find that these equations give

$$\frac{dx^\alpha}{dT} = \frac{T_0}{t_0^{1/3}} \frac{v^\alpha}{T} \left(1 - \frac{t_0^{2/3} T}{c^2 T_0} k_{\alpha\beta} \frac{dx^\alpha}{dT} \frac{dx^\beta}{dT} \right)^{1/2}, \quad (66)$$

where v^α are arbitrary constants.

From (59), (64) and (66) we can write

$$\frac{m_i \mathbf{V}}{\sqrt{(1 - V^2/c^2)}} = \mathbf{p}, \quad (67)$$

where \mathbf{p} is a constant 3-vector and \mathbf{V} is the velocity 3-vector at the event $x^\alpha = 0$, having components $d\xi^\alpha/dT$ and magnitude V .

* The coordinates T, ξ^a are not natural coordinates according to the usual definition (8, p. 80), but the difference is unimportant for the following work. A transformation of the time coordinate $T = T_1 + T'/c - (\xi^1 + \xi^2 + \xi^3)/4c^2 T_1$ is required in addition to (59), in order to make the first derivatives of \tilde{g}_{14} zero at the event $T = T_1, \xi^a = 0$, and also to make the velocity of light unity.

Equation (67) expresses the conservation of linear momentum according to the special theory of relativity, but on account of the variation of m_i with T it is easily seen that the velocity of a free particle decreases as T increases. On the other hand, the energy E of the particle given by the special relativity formula

$$\frac{m_i c^2}{\sqrt{(1 - V^2/c^2)}} = E, \quad (68)$$

is found to increase with T on account of this variation.

In the neighbourhood of a fundamental particle of inertial mass m_i , a free particle will be acted on by a gravitational force in an inertial system. The equations of the paths in the local field are derived in Section 7 where it is shown (equation (105)) that, for sufficiently small values of ξ , there is a Newtonian attractive force on the particle of intensity

$$\frac{\Gamma m}{\xi^2} \left(\frac{T_0}{T} \right)^{1/2}.$$

In Newtonian theory it is assumed that gravitational mass m_g and inertial mass are equal. In order to preserve the equality $m_g = m_i$ we shall therefore write the intensity of the force in the form $\gamma m_i/\xi^2$, where the gravitational power of matter is

$$\gamma = \Gamma \left(\frac{T_0}{T} \right) = \frac{2}{3} \frac{a^3}{m T}. \quad (69)$$

γ rather than Γ is the measure at any epoch of the Newtonian constant of gravitation.

Also since inertial mass m_i is enclosed in a spherical surface of radius $t_0^{1/3}(T/T_0)^{1/2}a$ at epoch T , we find that the mean density of matter in the universe is

$$\omega = \frac{3m_i}{4\pi t_0^3 a^3} \left(\frac{T_0}{T} \right)^{3/2} = \frac{9m}{16\pi a^3 T}. \quad (70)$$

6. *Dirac's principle*.—The cosmological theory of Dirac (7) was based on the principle that "any two of the very large dimensionless numbers occurring in nature are connected by a simple mathematical relation in which the coefficients are of the order of magnitude unity". Since the values of the gravitational constant, the mean density of matter in the universe and Hubble's constant, when made dimensionless by the use of constants of atomic theory, were found to give very large numbers of the same order as the reciprocal of the very large number t formed from the age of the universe and an atomic unit of time, Dirac concluded that the first three quantities were approximately equal to t^{-1} . In order to describe a cosmological model by the equations of the general theory of relativity he then changed the units of time and distance so that the gravitational "constant" was an absolute constant and the velocity of light was unchanged. It was later pointed out by H. Bondi (16), that the latter procedure was not justified, because the change of units would make the value of the electronic charge vary with the time, and this would be contrary to the principle of the conservation of charge which is inherent in the general theory of relativity. Nevertheless it would appear necessary to take into account the results derived from Dirac's principle in constructing a cosmological model. Theories in which the gravitational power of matter varies inversely as the epoch have also been proposed by P. Jordan (17) and R. H. Dicke (18).

We shall show that the results derived from Dirac's principle are obtained from measurements in an inertial system, in consequence of postulate H, when appropriate units of the time and distance coordinates are chosen. Let these units be chosen so that a is the radius in the natural gauge of an elementary particle of inertial mass m_i , and

$$c = 4/3 \cdot a. \quad (71)$$

Then, in the geodetic gauge of the inertial system, we can define atomic units of length and time by

$$\delta = a \left(\frac{T}{T_0} \right)^{1/4}, \quad \epsilon = \frac{a}{c} \left(\frac{T}{T_0} \right)^{1/4}. \quad (72)$$

Also from (44), (71) and (72) a dimensionless measure of time in the inertial system is given by

$$T/\epsilon = c/a \cdot T^{3/4} T_0^{1/4} = t. \quad (73)$$

Then from (64), (69), (70), (71), (72) and (73) we find

$$\gamma = \frac{\delta^3}{m_i \epsilon^2} \cdot \frac{1}{2t}, \quad (74)$$

$$\omega = \frac{m_i}{\delta^3} \frac{3}{4\pi t}. \quad (75)$$

On account of postulate I we calculate Hubble's constant from the metric (43) for the natural gauge. We find in the usual manner (19) the value $\frac{1}{3}t^{-1}$. Since coordinate time in the natural gauge is by (73) equal to the dimensionless quantity T/ϵ , the value of Hubble's constant H in the inertial system is

$$H = \frac{1}{3}(\epsilon t)^{-1}. \quad (76)$$

At epoch $t=1$ proper distance in the natural gauge is equal to coordinate distance, and consequently the average field of the model is a complete matter-field, in the sense that there are no free-space regions. The description of the model in terms of discrete masses will therefore only hold for $t > 1$. We then find that the Schwarzschild field is free from singularities. The condition for this is that $2\Gamma m/c^2 \rho_0 < 1$, where ρ_0 is the radius of an elementary particle in the local gauge. Since $\rho_0 = (T/T_0)^{1/2} \delta$, we find from (56) and (44) that

$$\frac{2\Gamma m}{c^2 \rho_0} = \frac{1}{t} < 1. \quad (77)$$

Hence the free space regions are free from singularities.

If we write γ^*, ω^*, H^* for the values of γ, ω, H when they are made dimensionless by the use of the quantities m_i, δ, ϵ we find from (74), (75) and (76)

$$\gamma^* = \frac{1}{2t}, \quad \omega^* = \frac{3}{4\pi t}, \quad H^* = \frac{1}{3t}. \quad (78)$$

Since t is the epoch T divided by the unit of time ϵ , these results agree with the deductions from Dirac's principle (7), if m_i, δ and ϵ are assumed to be quantities occurring in atomic theory.

From (72), (74) and (76) we find

$$\delta = \left(\frac{2}{3} \frac{\gamma m_i}{c H} \right)^{1/2}, \quad (79)$$

and since the quantity on the right-hand side of (79) has the dimensions of length, we can use the values of the quantities in c.g.s. units to calculate the value of δ . Assuming that m_i is the neutron mass, and that $H = 75$ km/sec/megaparsec, we find that δ is approximately 10^{-12} cms, which is of the same order of magnitude as the nuclear radius. This result justifies the assumption that m_i, δ, ϵ are the measures of quantities occurring in atomic theory.

7. *Spiral orbits in a local gravitational field.*—The local field of a mass M has the form

$$ds'^2 = c^2 \left(1 - \frac{2\Gamma M}{c^2 \rho} \right) d\tau^2 - \left(1 - \frac{2\Gamma M}{c^2 \rho} \right)^{-1} d\rho^2 - \rho^2 d\theta^2 - \rho^2 \sin^2 \theta d\phi^2. \quad (80)$$

This field will be joined onto the average field in the local gauge defined by (58), at a 3-space $r = b$, by the use of boundary conditions (29). These boundary conditions are satisfied by the method described in Section (4).

We make the transformation

$$\tau = \tau(t', r), \quad \rho = \left(\frac{4}{t_0} \right)^{1/3} t'^{2/3} r, \quad (81)$$

where

$$c^2 \left(1 - \frac{2\Gamma M}{c^2 \rho} \right)^2 \frac{\partial \tau}{\partial t'} \frac{\partial \tau}{\partial r} = \frac{\partial \rho}{\partial t'} \frac{\partial \rho}{\partial r}, \quad (82)$$

so that the metric (80) has the form

$$ds'^2 = c^2 e^{\psi_1} dt'^2 - e^{\psi_2} dr^2 - (4/t_0)^{2/3} t'^{4/3} r^2 (d\theta^2 + \sin^2 \theta d\phi^2), \quad (83)$$

where ψ_1, ψ_2 are functions of t', r . When (82) is solved for τ , subject to the boundary conditions at $r = b$, the functions ψ_1, ψ_2 can be calculated from expressions involving $\partial \tau / \partial t'$, $\partial \tau / \partial r$.

We find from the boundary conditions that

$$\frac{\Gamma M}{b^3} = \frac{8}{9t_0}, \quad (84)$$

which corresponds to the condition (56). Also when ψ_1 and ψ_2 are expressed in terms of the variables T, r and the constants T_0, t_0, b , we find, after a lengthy but straightforward calculation, that

$$e^{\psi_1} = t_0^{2/3} \left(\frac{T}{T_0} \right)^2 \left\{ 1 + \frac{N}{T} \left(\frac{b}{r} - \frac{r^2}{b^2} \right) \right\}, \quad (85)$$

$$e^{\psi_2} = 1 + \frac{N}{T} \left(\frac{3}{2} - \frac{b}{r} - \frac{r^2}{2b^2} \right), \quad (86)$$

where

$$N = \frac{3}{2} \frac{\Gamma M t_0^{2/3}}{c^2 b}. \quad (87)$$

T is defined by (44) and terms of higher order in N/T are neglected. Since $N/T = 2\Gamma M/c^2 \rho_1$, where ρ_1 is the radius of the boundary in the local gauge, the neglected terms will be $\ll 1$.

We shall now determine the free paths in the local field. The metric in the local gauge is given by (44), (57), (83), (85) and (86), but the free paths are

geodesics in the geodetic gauge, and the metric is then given by the conformal space-time which is continuous with (45) at $r=b$. We find

$$ds^2 = e^r dT^2 - e^\lambda dr^2 - e^\mu (d\theta^2 + \sin^2 \theta d\phi^2), \quad (88)$$

where

$$e^\lambda = \frac{1}{2} T t_0^{-1/2} \left\{ 1 + \frac{N}{T} \left(\frac{b}{r} - \frac{r^2}{b^2} \right) \right\}, \quad (89)$$

$$e^\mu = \frac{1}{2} T t_0^{-1/2} r^2, \quad (90)$$

$$e^r = c^2 \left\{ 1 + \frac{N}{T} \left(\frac{3}{2} - \frac{b}{r} - \frac{r^2}{2b^2} \right) \right\}. \quad (91)$$

The Christoffel symbols for the metric (88) were calculated from general formulae (19), and the equations of the geodesics were then found to be

$$\begin{aligned} \frac{d^2 r}{d\tilde{s}^2} + \frac{1}{2} \lambda' \left(\frac{dr}{d\tilde{s}} \right)^2 + \lambda \frac{dr}{d\tilde{s}} \frac{dT}{d\tilde{s}} - \frac{1}{2} e^{\mu-\lambda} \mu' \sin^2 \theta \left(\frac{d\phi}{d\tilde{s}} \right)^2 \\ - \frac{1}{2} e^{\mu-\lambda} \mu' \left(\frac{d\theta}{d\tilde{s}} \right)^2 + \frac{1}{2} e^{\nu-\lambda} \nu' \left(\frac{dT}{d\tilde{s}} \right)^2 = 0, \end{aligned} \quad (92)$$

$$\frac{d^2 \theta}{d\tilde{s}^2} + \mu' \frac{dr}{d\tilde{s}} \frac{d\theta}{d\tilde{s}} - \sin \theta \cos \theta \left(\frac{d\phi}{d\tilde{s}} \right)^2 + \dot{\mu} \frac{d\theta}{d\tilde{s}} \frac{dT}{d\tilde{s}} = 0, \quad (93)$$

$$\frac{d^2 \phi}{d\tilde{s}^2} + \mu' \frac{dr}{d\tilde{s}} \frac{d\phi}{d\tilde{s}} + 2 \cot \theta \frac{d\theta}{d\tilde{s}} \frac{d\phi}{d\tilde{s}} + \dot{\mu} \frac{d\phi}{d\tilde{s}} \frac{dT}{d\tilde{s}} = 0, \quad (94)$$

$$e^r \left(\frac{dT}{d\tilde{s}} \right)^2 - e^\lambda \left(\frac{dr}{d\tilde{s}} \right)^2 - e^\mu \left(\frac{d\theta}{d\tilde{s}} \right)^2 - e^\nu \sin^2 \theta \left(\frac{d\phi}{d\tilde{s}} \right)^2 = 1. \quad (95)$$

Considering paths which satisfy the initial conditions $\theta = \pi/2$, $d\theta/d\tilde{s} = 0$, we find from (93) that $d^2\theta/d\tilde{s}^2 = 0$. These paths will therefore always lie in the plane $\theta = \pi/2$. In this case we find from (94)

$$Tr^2 \frac{d\phi}{d\tilde{s}} = ha^2/c, \quad (96)$$

where h is a constant of integration. Then from (92) and (95) we find

$$\frac{d^2 r}{d\tilde{s}^2} + \left\{ \frac{1}{2} \lambda' \left(\frac{dr}{dT} \right)^2 + \lambda \frac{dr}{dT} + \frac{1}{2} e^{\nu-\lambda} \nu' \right\} \left(\frac{dT}{d\tilde{s}} \right)^2 - \frac{e^{\mu-\lambda} \mu' h^2 a^4}{2c^2 T^2 r^4} = 0, \quad (97)$$

$$\left(\frac{dT}{d\tilde{s}} \right)^2 = \left(1 + \frac{e^\mu h^2 a^4}{c^2 T^2 r^4} \right) \left(e^r - e^\lambda \left(\frac{dr}{dT} \right)^2 \right)^{-1}. \quad (98)$$

We obtain an approximate form of the equations by writing

$$T \frac{d}{dT} = \frac{d}{dq}, \quad \eta = \frac{r}{a}, \quad (99)$$

and expressing the terms in powers of T^{-1} . Equating to zero the coefficients of the lowest powers of T^{-1} in (96) and (97), we find

$$\eta^2 \frac{d\phi}{dq} = h, \quad (100)$$

$$\frac{d^2 \eta}{dq^2} - \frac{1}{2} \eta + \frac{1}{2} \frac{n}{\eta^2} - \frac{h^2}{\eta^3} = 0, \quad (101)$$

where

$$n = M/m. \quad (102)$$

In deriving these results use has been made of equations (56), (84), (87), (96), (97) and (98). When η is small compared with the other terms in (101), these are the Newtonian equations of motion under a central force $-n/2\eta^2$, and the paths are therefore conics. The solution in the more general case has been discussed by Jeans (4).

If we use proper cotime T and proper distance

$$\xi = t_0^{1/3} \left(\frac{T}{T_0} \right)^{1/2} r = T^{1/2} \eta d, \quad (103)$$

where $d = 2at_0^{-1/6}/\sqrt{3}$, the equations (100) and (101) transform into

$$\xi^2 \frac{d\phi}{dT} = H, \quad (104)$$

$$\frac{d^2\xi}{dT^2} - \frac{1}{4} \frac{\xi}{T^2} + \frac{\mathcal{M}}{\xi^2} - \frac{H^2}{\xi^3} = 0. \quad (105)$$

The constant $H = hd^2$ and \mathcal{M} is given by

$$\mathcal{M} = \frac{nd^3}{2T^{1/2}} = \Gamma M \left(\frac{T_0}{T} \right)^{1/2} = \gamma M_i, \quad (106)$$

where M_i is the inertial mass of the attracting body and γ is given by (69). For small values of ξ the term $-\xi/4T^2$ in (105) is negligibly small and then the equations of motion are the same as the Newtonian equations of motion under a central attraction \mathcal{M}/ξ^2 , where $\mathcal{M} \propto T^{-1/2}$. The nature of the orbits in this case have also been discussed by Jeans (4). In particular there are orbits given by equations (100) and (101) for which $\eta = \text{constant}$, and these give the equiangular spirals

$$\xi = \xi_0 e^{\phi \tan \epsilon_0}, \quad (107)$$

where ξ_0, ϵ_0 are constants and

$$\tan \epsilon_0 = - \frac{1}{\phi \mathcal{M}} \frac{d\mathcal{M}}{dT} = \frac{1}{2\phi T}. \quad (108)$$

The angle ϵ_0 measures the inclination of the spiral at any point to the circle through the point, whose centre is at the attracting mass. From (108) we see that this angle will only be appreciable when ϕ is extremely small, of order T^{-1} , or less.

When $r \ll b$ terms of the next higher order in N/T have to be retained in forming the equations (100) and (101). These terms come from the approximate expressions for e^{λ} and e^{ν} given by (89) and (91), the contributions from the new terms of the higher order approximations for e^{λ} and e^{ν} being negligibly small in comparison. From the equations the calculated values of the centennial advance of the perihelion of Mercury and the gravitational deflection of light by the Sun agree with the results of Einstein's theory. Also the calculated value of the gravitational shift of the spectral lines, for light emitted by atoms at the surface of a star, is found, from (88) and (91), in conjunction with postulate I, to be in agreement with the result for the latter theory.

The theory of the structure of a spiral nebula can be developed from the equations (100) and (101) along the lines proposed by E. A. Milne (5, 6). We assume that the nucleus of the nebula has a constant radius x_1 in the natural gauge. This assumption is made because of its similarity to the postulate H

for an elementary particle, although a closer resemblance to Milne's results would be obtained by assuming the radius to be constant in the local gauge (cf. Section 8). At epoch T_1 let $\eta = \eta_1$ for events on the boundary of the nucleus, so that using (43) and (44), we find

$$\chi_1 = T_0^{1/4} T_1^{1/4} \eta_1 d. \quad (109)$$

Then at epoch T the radius of the nucleus in the geodetic gauge of the inertial system is

$$\xi_1 = T^{1/4} T_1^{1/4} \eta_1 d. \quad (110)$$

We assume that the nucleus is rotating with constant angular velocity, and that matter is continually detached from a point $(\xi_1, \pi/2, \phi_1)$, with fixed angular coordinates, on the rim of the nucleus. We assume that each portion of matter detached describes a circular orbit $\eta = \eta_1$ where the value of η_1 depends on the epoch T_1 at which it became detached. At epoch T this matter has coordinates $(\xi, \pi/2, \phi)$, where

$$\xi = T^{1/2} \eta_1 d. \quad (111)$$

Also from the equations of motion (100) and (101), we find

$$\phi - \phi_1 = \frac{h}{\eta_1^2} \log \left(\frac{T}{T_1} \right), \quad (112)$$

$$\frac{h^2}{\eta_1^4} = \frac{1}{2} \frac{n}{\eta_1^3} - \frac{1}{2}. \quad (113)$$

Eliminating h, η_1, T_1 from equations (110)–(113) and using (106), we find the equation of the spiral arm at epoch T in the form

$$\phi - \phi_1 = 4 \left(\frac{\gamma M_i T^2}{\xi^3} - \frac{1}{2} \right)^{1/2} \log \left(\frac{\xi}{\xi_1} \right). \quad (114)$$

This may be compared with the corresponding equation found by Milne, (5, 6) which in our notation becomes

$$\phi - \phi_1 = \left(\frac{\gamma M_i T^2}{\xi^3} \right)^{1/2} \log \left(\frac{\xi}{\xi_1} \right). \quad (115)$$

In the kinematic treatment, however, γ is proportional to T and M_i is a constant. At distances from the nucleus which are small compared with the distance $\xi = T^{1/2} b a^{-1} d$, which is the radius of the sphere of influence of the local field, we find $\gamma M_i T^2 \xi^{-3} \gg \frac{1}{2}$. Consequently Milne's general conclusions regarding his equation for a spiral arm will apply also to the equation (114).

8. *Discussion.*—We have seen in Section 4 that in the local gauge the average field has the same metric as an Einstein-de Sitter universe. Also from (44), (57) and (63) we find that if proper intervals are defined by the metric (58), the action \mathcal{A} will have the same form as action in mechanics if m is defined to be the inertial mass of a particle. The question therefore arises as to whether the system of measurement which corresponds to measurements in the physical universe should be defined by the local gauge rather than the geodetic gauge. This also raises the question of the validity of postulate J, because then from the principle of equivalence we should be led to make the assumption that free paths are

geodesics of the metric (58). There would then be no essential difference between the properties of this model and the Einstein-de Sitter universe. There are at least two reasons against making this interpretation. One is that it does not appear to admit of a satisfactory derivation of Dirac's results, and the other that it does not incorporate Mach's principle into the theory.

We consider the second reason from the point of view of Newtonian cosmology (16). It was shown by E. A. Milne (20) that there is an exact correspondence between the Einstein-de Sitter universe and a Newtonian universe described in Euclidean space, with distance coordinate ρ and Newtonian time t' defined by (51) and (57) respectively. The position vector of a point in this space may be written

$$\rho = \left(\frac{4}{t_0} \right)^{1/3} t'^{2/3} \mathbf{r}, \quad (116)$$

where \mathbf{r} is the position vector of the corresponding point in the subspace $du^2 = k_{ab} dx^a dx^b$ of the space-time with metric (58). The Newtonian model satisfies the principle of relativity for transformations to any of the fundamental observers $\mathbf{r} = \text{constant}$. In Milne's description with Newtonian time t' , these fundamental observers were relatively accelerated, but if Newtonian time is defined differently by

$$T = 3t_0^{1/3}t'^{2/3}/2^{4/3} \quad (117)$$

they have uniform relative velocities

$$\mathbf{v} = \frac{\mathbf{p}}{T}. \quad (118)$$

Now consider the motion of a free particle relative to a local fundamental observer, the relative velocity being small compared with the velocity of light. If we use postulate J and the integrals (66) of the geodesic equations, we find that the local velocity of the particle is $d\rho/dT \approx \mathbf{v}$ where \mathbf{v} is the constant vector with components v^a . In the given frame of reference the particle accelerates from one fundamental observer to another, but it always has approximately the velocity \mathbf{v} relative to the frame of reference of a fundamental observer in its immediate neighbourhood. We can picture the motion as consisting of a uniform velocity relative to a uniformly expanding space. The frames of reference are thus a generalization, for an expanding space, of the Newtonian concept of inertial frames. On the other hand, if we postulate that the paths are geodesics of the metric (58) we find that the local velocity of the particle is $d\rho/dT \approx \mathbf{v} T_0^{1/2}/T^{1/2}$. The particle then comes to rest relative to the expanding space as T tends to infinity. The former postulate rather than the latter is therefore more in accordance with Mach's principle.

The description of the model in terms of measurements made in the geodetic gauge therefore seems preferable to the other alternative. The fact that the inertial mass of a body increases with the epoch, does not imply the creation of particles, since the masses of elementary particles also vary with the epoch in the same manner.

The description of the model in Euclidean space with distance coordinate ρ and Newtonian time T brings out certain resemblances to Milne's kinematic model. The velocity-distance relation (118) is the same as that found by Milne

for his system of fundamental observers. Also from the equations (100) and (101) we readily deduce

$$\rho^2 \frac{d\phi}{dT} = H'T, \quad (119)$$

$$\frac{d^2\rho}{dT^2} - \rho \left(\frac{d\phi}{dT} \right)^2 = - \frac{\rho - 2T}{2T^2} \frac{d\rho}{dT} - \frac{\Gamma M}{\rho^2} \left(\frac{T}{T_0} \right), \quad (120)$$

where $H' = a^2 t_0^{2/3} h / T_0^2$. These equations resemble the equations of motion obtained by Milne for a particle in the neighbourhood of an attracting mass (5). A slight difference occurs in the first term on the right-hand side of equation (120), where we have $-\rho/2T^2$, whereas Milne's equation has $-\rho/T^2$. The difference can be traced to the occurrence of the term $-\frac{1}{2}\eta$ in equation (101), and arises from an essential difference in treatment of the problem. In the present theory the gravitational field of the mass M merges into the background field of the universe, whereas in Milne's theory the gravitational field of the condensation is superposed on the field of his substratum. It is on account of the close resemblance of equations (119) and (120) to Milne's equations that the equation of a spiral arm can be obtained in very nearly the form (115) if $\rho = \text{constant}$ at the boundary of the nucleus.

The nature of the field in the interior of an elementary particle, or a nebular nucleus, has been left undetermined. This problem may require a more complex field theory than has been used here, but the following property of the fields should be mentioned, as indicating that the matter-fields of Section 3 may be significant for the description of fields in the interior of matter. Using the notation of equations (19) and (20), we find from (30), (33) and (46) by the method of Section 4, that

$$\Lambda g_{ij}^{(1)} = \Lambda' g_{ij}^{(2)} \quad (121)$$

at an expanding boundary

$$r = \left(\frac{\Lambda'}{\Lambda} \right)^{1/6} \left(\frac{2\Gamma m}{A^2} \right)^{1/3} R. \quad (122)$$

If in the equation (10) defining \mathcal{A} we had omitted the factor Λ^{-1} , we should have arrived at the boundary conditions (29) by taking $\Lambda \delta g_{ij}^{(1)} = \Lambda' \delta g_{ij}^{(2)}$ etc. in equations (19) and (20). It seems possible that these conditions on the small variations may therefore be related to the continuity relations (121) at the boundary of the particle, whereas the derived conditions (29) express the continuity relations with the average field.

*Kings College,
Newcastle-upon-Tyne:
1959 September 15.*

References

- (1) H. Weyl, *Space-Time-Matter*, Methuen, 1922.
- (2) C. Lanczos, *Rev. Mod. Phys.*, **29**, 337, 1957.
- (3) L. Infeld and A. Schild, *Rev. Mod. Phys.*, **21**, 408, 1949.
- (4) J. H. Jeans, *M.N.*, **85**, 2, 1924.
- (5) E. A. Milne, *Kinematic Relativity*, O.U.P., 1948.
- (6) E. A. Milne, *M.N.*, **106**, 180, 1946.
- (7) P. A. M. Dirac, *Proc. Roy. Soc. A*, **165**, 199, 1938.

- (8) A. S. Eddington, *The Mathematical Theory of Relativity*, 2nd Edn., C.U.P. p. 210, 1930.
- (9) H. A. Buchdahl, *Quart. Journ. Maths.*, **19**, 150, 1948.
- (10) H. P. Robertson, *Astrophys. J.*, **82**, 284, 1935.
- (11) A. G. Walker, *Proc. London Math. Soc.* (2), **42**, 90, 1937.
- (12) S. O'Brien and J. L. Synge, Comm. of the Dublin Inst. for Advanced Studies, A. No. 9, 1952.
- (13) C. Gilbert, *M.N.*, **116**, 678, 1956.
- (14) A. Einstein and W. de Sitter, *Proc. Nat. Acad. of Sciences*, **18**, 213, 1932.
- (15) E. Mach, *The Science of Mechanics*, 6th Edn., 1904.
- (16) H. Bondi, *Cosmology*, C.U.P. 1950.
- (17) P. Jordan, *Schwerkraft und Weltall*, Braunschweig, 1952.
- (18) R. H. Dicke, *Rev. Mod. Phys.*, **29**, 363, 1957.
- (19) R. C. Tolman, *Relativity, Thermodynamics and Cosmology*, Oxford, 1934.
- (20) E. A. Milne, *Quart. Journ. of Maths.*, **5**, 64, 1934.

NOTICE TO AUTHORS

Presentation of Papers at Meeting

At some meetings of the Society the background and conclusions of selected papers are presented and then discussed. In order to assist the Secretaries in the selection of papers for such meetings, authors are asked to let the Society know, when submitting papers, whether they would be willing to give an account of their paper, if requested.

The attention of authors resident abroad is drawn to the fact that the Society welcomes information about their work. The Secretaries would be happy to consider having such work described at a meeting, in accordance with the author's wishes, either by a Secretary or other Fellow.

Publication of Papers

1. *General*.—It is the aim of the Society to be of the greatest possible service in disseminating astronomical results and ideas to the scientific community with the utmost possible speed. Contributors are accordingly urged to give the most careful consideration to the presentation of their work, for attention to detail will assuredly result in a substantial saving of time.

It is the practice of the Society to seek a referee's opinion on nearly every paper submitted for publication in *Monthly Notices*; experience has shown that frequently the comments of referees have enabled authors to improve the presentation of their work and so increase its scientific value.

2. *Communication*.—Papers must be communicated to the Society by a Fellow. They should be accompanied by a summary at the beginning of the paper conveying briefly the content of the paper, and drawing attention to important new information and to the main conclusions. The summary should be intelligible in itself, without reference to the paper, to a reader with some knowledge of the subject; it should not normally exceed 200 words in length. Authors are requested to submit MSS. in duplicate. These should be typed using double spacing and leaving a margin of not less than one inch on the left-hand side. Corrections to the MSS. should be made in the text and not in the margin. By Council decision, MSS. of accepted papers are retained by the Society for one year after publication; unless their return is then requested by the author they are destroyed.

3. *Presentation*.—Authors are allowed considerable latitude, but they are requested to follow the general style and arrangement of *Monthly Notices*. References to literature should be given either in the traditional form of a numbered list at the end of the paper, or as prescribed in *Notes on the Preparation of Papers to be Communicated to the Royal Society*.

4. *Notation*.—For technical astronomical terms, authors should conform closely to the recommendations of Commission 3 of the International Astronomical Union (*Trans. I.A.U.*; Vol. VI, p. 345, 1938). Council has decided to adopt the I.A.U. 3-letter abbreviations for constellations where contraction is desirable (Vol. IV, p. 221, 1932). In general matters, authors should follow the recommendations in *Symbols, Signs and Abbreviations* (London: Royal Society, 1951) except where these conflict with I.A.U. practice.

5. *Diagrams*.—These should be designed to appear upright on the page, drawn about twice the size required in print and prepared for direct photographic reproduction except for the lettering, which should be inserted in pencil. Legends should be given in the manuscript indicating where in the text the figure should appear. Blocks are retained by the Society for 10 years; unless the author requires them before the end of this period they are then destroyed. Rough copies or prints of the diagrams should accompany each manuscript.

6. *Tables*.—These should be arranged so that they can be printed upright on the page.

7. *Proofs*.—Authors are liable for costs of alteration exceeding 5 per cent of composition. It is therefore in their own and the Society's interests to seek the maximum conciseness and simplification of symbols and equations consistent with clarity.

CONTENTS

	PAGE
R. F. Griffin and R. O. Redman, Photoelectric measurements of the $\lambda 4200\text{ \AA}$ CN band and the G band in G8-K5 spectra	287
B. R. Leaton and B. E. J. Pagel, Preliminary list of radial velocities for 33 stars nearer than 20 parsecs	317
M. J. Seaton, H I, He I and He II intensities in planetary nebulae	326
F. Hoyle, Radio-source problems	338
H. E. C. Tunmer, On the dimensions, spatial density and power of the extra-galactic radio sources	360
C. Gilbert, Gravitation and the principle of stationary action	386

